January 2019

Manganese Catalysis In The Activation Of Si-H And B-H Bonds And Synthesis Of Degradable Poly(silylether)s From Renewable Resources

Srikanth Vijjamarri

MANGANESE CATALYSIS IN THE ACTIVATION OF SI-H AND B-H BONDS AND SYNTHESIS OF DEGRADABLE POLY(SILYLETHER)S FROM RENEWABLE RESOURCES

by

Srikanth Vijjamarri
Bachelor of Science, Osmania University, Hyderabad, India, 2009
Master of Science, Osmania University, Hyderabad, India, 2011

A Dissertation

Submitted to the Graduate School

of the

University of North Dakota

in partial fulfillment of the requirements

for the degree of

Doctor of Philosophy

Grand Forks, North Dakota

December

2019

This dissertation, submitted by Srikanth Vijjamarri in partial fulfillment of the requirements for the degree of Doctor of Philosophy from the University of North Dakota, has been read by the Faculty Advisory Committee under whom the work has been done, and is hereby approved.

Dr. Guodong Du (Chairperson)

Dr. Harmon Abrahamson

Dr. Lothar Stahl

Dr. Julia Zhao

Dr. Yun Ji

This dissertation meets the standards for appearance, conforms to the style and format requirements of the Graduate School at the University of North Dakota, and is hereby approved.

Chris Nelson
Associate Dean of the School of Graduate Studies

12/10/19
Date

PERMISSION

Title MANGANESE CATALYSIS IN THE ACTIVATION OF SI-H AND B-H BONDS AND SYNTHESIS OF DEGRADABLE POLY(SILYLETHER)S FROM RENEWABLE RESOURCES

Department Chemistry

Degree Doctor of Philosophy

In presenting this dissertation in partial fulfillment of the requirements for a graduate degree from the University of North Dakota, I agree that the library of this University shall make it freely available for inspection. I further agree that permission for extensive copying for scholarly purposes may be granted by the professor who supervised my dissertation work or, in his absence, by the chairperson of the department or the dean of the Graduate School. It is understood that any copying or publication or other use of this dissertation or part thereof for financial gain shall not be allowed without my written permission. It is also understood that due recognition shall be given to me and to the University of North Dakota in any scholarly use which may be made of any material in my dissertation.

Srikanth Vijjamarri
December 1st, 2019

TABLE OF CONTENTS

LIST OF FIGURES

LIST OF TABLES

LIST OF SCHEMES

Scheme Page

LIST OF ABBREVIATIONS

Å	Angstrom
BPA	Bisphenol-A
BHMF	2,5-bis(hydroxymethyl)furan
$BF_3.OEt_2$	Boron trifluoride diethyl etherate
^{t}Bu	tertiary-butyl
C	Carbon
C_6D_6	Benzene-d_6
$CDCl_3$	Chloroform-d_3
CD_3CN	Acetonitrile-d_3
Conv	Conversion
Cp	Cyclopentadienyl
Cy	Cyclohexyl
D	Deuterium
Đ	Poly dispersity index
DBpin	Deuterated pinacolborane
DCM	Dichloromethane
DFF	2,5-Diformylfuran
Et	Ethyl
Et_3SiH	Triethylsilane
EtOAc	Ethyl acetate
EtOH	Ethanol
$(EtO)_3SiH$	Triethoxysilane
FDCA	2,5-Furandicarboxylic acid
FTIR	Fourier transform infrared spectroscopy
GC	Gas chromatography

GPC	Gel permeation chromatography
H	Hydrogen
HBcat	Catecholborane
HBpin	Pinacolborane
HMDS	Hexamethyldisilazane
HMF	Hydroxymethylfurfural
HPLC	High performance liquid chromatography
KIE	Kinetic Isotopic Effect
L_n	Salen ligand
LC	Liquid chromatography
Me	Methyl
MeOH	Methanol
Mes	Mesitylene
mmol	Millimoles
Mn	Manganese
MnN	Manganese nitrido
M_n	Number average molecular weight
M_w	Weight average molecular weight
N	Nitrogen
N_2	Nitrogen gas (inert atmosphere)
Naph	Naphthyl
NMR	Nuclear magnetic resonance
O	Oxygen
OBMF	5,5'-[oxybis(methylene)]di(2-furaldehyde)
ORTEP	Oak ridge thermal-ellipsoid plot
PDI	Polydispersity index
PE	Polyethylene
Ph	Phenyl

$PhMeSiH_2$	Phenylmethylsilane
$PhSiH_3$	Phenylsilane
Ph_2SiH_2	Diphenylsilane
$PhCH_2OH$	Benzyl alcohol
Ph_3SiH	Triphenylsilane
Pr	Propyl
PSE	Poly(silylether)
^{i}Pr	Isopropyl
RI	Refraction index
Ru	Ruthenium
Salcy	Salicylidene
Salen	*N*,*N*-bis(salicylidene)-1,2-diaminoalkane
Si	Silicon
SEC	Size-exclusion chromatography
$^{t}BuMe_2SiH$	Tertiarybutylmethylsilane
$T_{-5\%}$	5 % weight loss at a particular temperature
$T_{-50\%}$	50 % weight loss at a particular temperature
T_g	Glass transition temperature
TBS	*Tert*-Butyldimethylsilyl
THF	Tetrahydrofuran
TMS	Tetramethylsilane
TLC	Thin-layer chromatography
TOF	Turnover frequency
TON	Turnover number
UV	Ultraviolet

ACKNOWLEDGEMENTS

I would like to express my sincere gratitude to my advisor, Dr. Guodong Du for his continuous support of my Ph.D. research, for his patience, motivation, and immense knowledge. His guidance helped me in all the time of research and writing of this thesis.

I would like to thank my graduate committee members, Dr. Harmon Abrahamson, Dr. Lothar Stahl, Dr. Kathryn Thomasson, and Dr. Yun Ji, for their insightful advice, support, and encouragement at the University of North Dakota.

I thank my previous lab mates Dr. Vamshi K Krishna and Dr. Shi Bian for their help and encouragement during my initial days in our laboratory and for all the good times at UND. I also would like to thank our previous undergraduate and current graduate students for being cooperative.

I would also like to thank Dr. Edward Kolodka and Dr. Alena Kubatova and her group members for allowing us to use their analytical instruments for my research work. I also would like to thank Dr. Julie Abrahamson, Dr. Alexi Novikov, and Mr. Michael Whitney for their guidance and mentorship as an instructor and for teaching me professional skills during my time as a TA. I thank the chemistry department staff for their great support and encouragement.

I also need to thank our collaborators at North Dakota State University for providing us chemical substrates for my research work.

I thank UND Chemistry Department, Graduate School, ND EPSCoR, for all the financial support they provided.

I also thank ACS Red River Valley, UND Graduate school, UND Provost, UND Chemistry Department, SOFA, and CGSA for all the needful travel awards they provided.

I thank all co-graduate students and my friends with whom I have shared my time during my graduate student life at Grand Forks.

Finally, I thank my loving and caring family who supported my education endeavors every step of the way. This includes my mother (amma) and father (nanna), Sulochana and Laxman, my brothers, Anil Kumar (anna), and Ajay Kumar (china), and my ever-supportive wife Swathi. Without all of you being there at every step of this journey, this truly would have been an impossible undertaking. Thank you all.

‘‘Dedicated to my parents, wife, brothers, and to all my teachers’’

ABSTRACT

In recent years, significant efforts have been made regarding the development and synthesis of degradable and thermally stable polymers from renewable feedstock due to the sustainability concerns caused by petroleum-based chemicals and materials. The present dissertation describes the synthesis, structural studies, degradation, and thermal stabilities of various poly(silylether)s prepared from biomass-based chemicals.

An air-stable manganese salen nitrido complex [$Mn^{V}N$(salen-3,5-tBu_2)] (Mn-1) was found to be an effective catalyst for the synthesis of poly(silylether)s via dehydrogenative coupling and hydrosilylation reactions. The catalytic activity of the manganese catalyst was initially examined in the protection of hydroxyl and carboxylic groups of alcohols and carboxylic acids with hydrosilanes via dehydrogenative coupling reactions. Under an inert atmosphere, hydroxyl and carboxylic acid functional groups were successfully protected to generate silyl ethers and silyl esters, respectively. A wide variety of functional groups such as chloro, nitro, methoxy, carbonyl, and carbon–carbon multiple bonds were tolerated in the reaction.

Thereafter, the Mn-1 complex was employed as the catalyst to synthesize a series of poly(silylether)s via step-growth polymerization from diol, dicarbonyl, and hydroxy carbonyl substrates including aliphatic and aromatic backbones. Due to the notable dual activity (dehydrogenative coupling and hydrosilylation) of the manganese complex, unsymmetrical substrates with alcohol and carbonyl functional groups produced poly(silylether)s with multiple silicon connectivity in the polymer backbone. Driven by concern for the environmental sustainability, we then directed our studies to synthesize hydrolytically degradable and thermally

stable poly(silylether)s from renewable feedstock, such as 1,4:3,6-dianhydrohexitols (isosorbide and isomannide), 5-hydroxymethylfurfural and its derivatives 2,5-bis(hydroxymethyl)furan, 2,5-diformylfuran, and 5,5′-[oxybis(methylene)]di(2-furaldehyde). Thermal analysis demonstrated that isosorbide and isomannide based poly(silylether)s displayed high thermal stability with thermal decomposition temperatures ($T_{-50\%}$) up to 510 °C and glass transition temperatures up to 120 °C. Structure-property analysis suggested that steric hindrance of substrates plays a vital role in determining the thermal properties of these polymers.

In consideration of the high catalytic activity of **Mn-1** in Si-H bond activation, the same catalytic system was employed to activate the B-H bond in hydroboration of carbonyl compounds. The reactions were performed at room temperature with using 0.02-0.2 mol % of catalyst and proceeded rapidly (>99 % conversion in <5 min). Several synthetically important functional groups were successfully tolerated and achieved chemoselective hydroboration of aldehydes over ketones. Impressively, TOF of these reactions was observed as 5700 h^{-1} under these conditions. Mechanistic investigations indicate that a reduced manganese species, Mn-H, acts as the active catalyst.

CHAPTER 1

GENERAL INTRODUCTION

Polymers have gained a unique position in human life due to their vast number of industrial and academic applications.[1,2,3] During the initial development of human society, the use of naturally available polymers became more sophisticated, illustrated by the development of several technologies such as textile manufacturing, wood processing, and paper production. The chemical transformation and modification of natural polymers for the synthesis of thermoplastic materials such as vulcanized natural rubber and cellulose acetate was the beginning of the commercial polymerization era. Later, various synthetic polymers, including poly(vinylchloride), polystyrene, nylons, polyesters, were successfully synthesized from fossil fuel based sources.[4] These synthetic polymers have completely changed the lifestyle of humankind and modern society as they are present in almost every commercialized industry including packaging, paints and coatings, building and construction, thermal and electrical appliances, aerospace, and automotive.[5]

The majority of today's polymer products are based on non-renewable fossil fuel sources. Approximately 80% of the feedstock is based on crude oil, 10% is other fossil raw materials like coal and natural gas, and 10 % is renewable resources.[6,7] However, environmental pollution by petroleum based synthetic polymers has assumed dangerous proportions because most of those polymers are not readily degradable, which makes them accumulate in the environment.[89] Besides, depletion of petroleum resources is one of the unavoidable concerns to utilize them for polymer synthesis.[10]

Driven by these concerns about the future fossil fuel feedstock availability and environmental issues, as well as the need for sustainable society, renewable and bio-based sources have become the major potential alternatives to replace fossil fuel sources as they can be replenished over a relatively short timescale and they are essentially highly abundant.[11] In the process, a large number of natural macromolecules and renewable monomers, including sugars, vegetable oils, hydroxy and amino acids, and biopolymers such as cellulose, hemicellulose, chitin, starch, lignin, and protein-based derivatives, have emerged in the preparation of various polymers.[12,13]

Carbohydrates which encompass cellulose, hemicellulose, and sucrose and starch, are one of the most important and abundant biomasses represent nearly 75% of the annual renewable biomass production (Figure 1).[14,15] Surprisingly, humans use are a minor fraction (approximately 4%) of this amount; the rest decays and recycles along natural pathways. However, one of the major disadvantages of directly employing these highly abundant bio-based chemicals is their limited thermal stability caused by the presence of multiple functional groups, such as hydroxyl functionalities. Therefore, simplified and bi-functional biomass-based building blocks such as furanic derivatives and 1,4:3,6-dianhydrohexitols (isohexides) are more attractive than the parent carbohydrate molecules for polymer synthesis.[16,17]

Hexoses are one of the highly abundant and hydroxyl groups containing monosaccharide in nature. These days, the catalytic transformation of hexoses into value-added chemicals such as furanic derivatives and isohexides are of great interest.[18] These monomers can be utilized as starting materials for the synthesis of numerous polymers as well as for the replacement of petroleum-based chemicals.

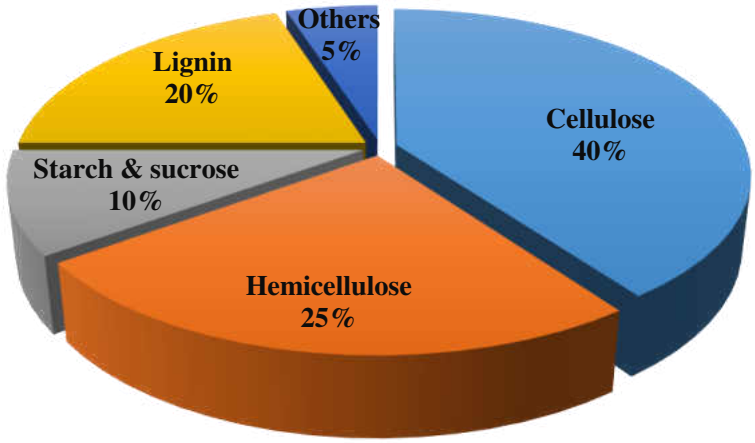

Figure 1**.** Distribution of types of natural products in biomass.[19,20]

1.1 Furanic monomers

Notably, furan derivatives obtained from carbohydrates which include both C5 and C6 sugars have a large potential as a starting material for the synthesis of new materials via further functionalization at hydroxyl, aldehyde, and carboxylic acid functional groups and, in turn, used in polymer applications.[21,22] Hydroxymethylfurfural (HMF) (**1**), has been determined to be as a highly interested and versatile chemical platform derived from carbohydrate source due to the diverse functionalizations it can undergo to produce various value-added chemicals and monomers before subsequent polymerization.[23,24,25] The general pathway of HMF production consists of three major steps, 1. Acid-catalyzed hydrolysis to produce glucose from cellulose, 2. A Lewis acid-mediated isomerization of glucose to fructose, 3. A Brønsted acid facilitated dehydration of fructose to generate HMF (Figure 2).[26,27,28,29] Furthermore, many scientific investigations have demonstrated that HMF can be produced directly from raw biomass.

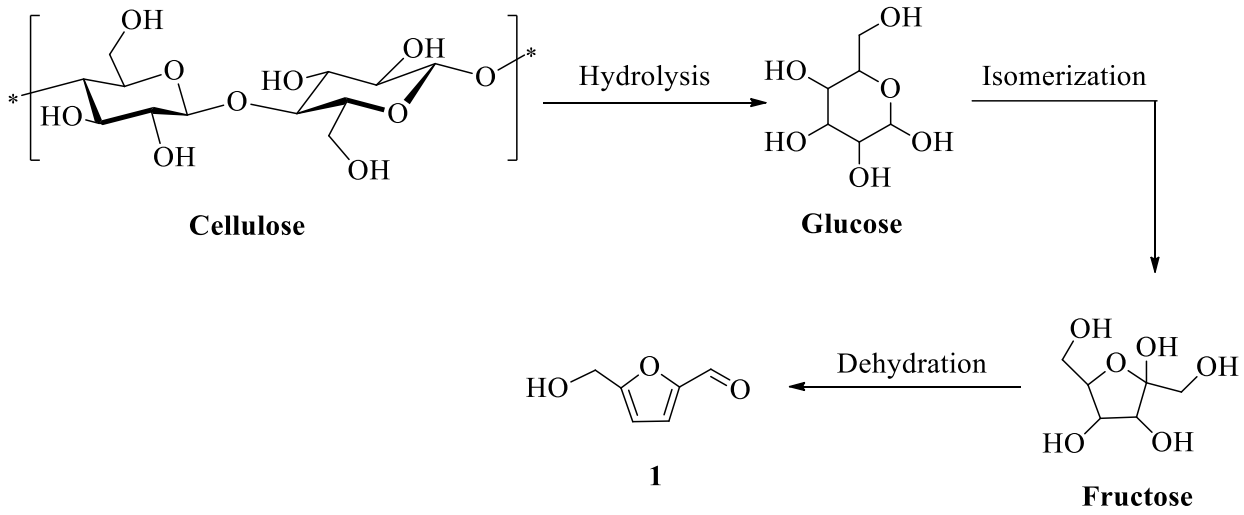

Figure 2. A general reaction scheme to produce HMF from cellulose

Some of the selected derivatives and further functionalized chemicals of HMF are listed in Figure 3. 2,5-Furandicarboxylic acid (FDCA) (**2**) is an emerging high-value chemical platform which is a highly prominent substitute for terephthalate in plastic production.[30] 2,5-dimethylfuran (**3**), hydroxymethylfuroic acid (**4**), 2,5-bis(hydroxymethyl)furan (BHMF) (**5**), 2,5-diformylfuran (DFF) (**6**), and 5,5'-[oxybis(methylene)]di(2-furaldehyde) (OBMF) (7), are other examples of HMF-derived chemicals with mono and di-functional groups for use in polymers or as intermediates to higher value.[31] Caprolactone (**8**) is commonly used as a monomer in synthesis of polyesters via ring-opening polymerizations and a precursor to synthesize caprolactam (**9**), which is a building block of Nylon 6, a high-performance polymer used in the synthesis of high strength fibers and mechanical parts.[32,33] Levulinic acid (**10**) and succinic acid (**11**) are the other prominent chemical precursors for the production of polyesters and polyamides.[34,35]

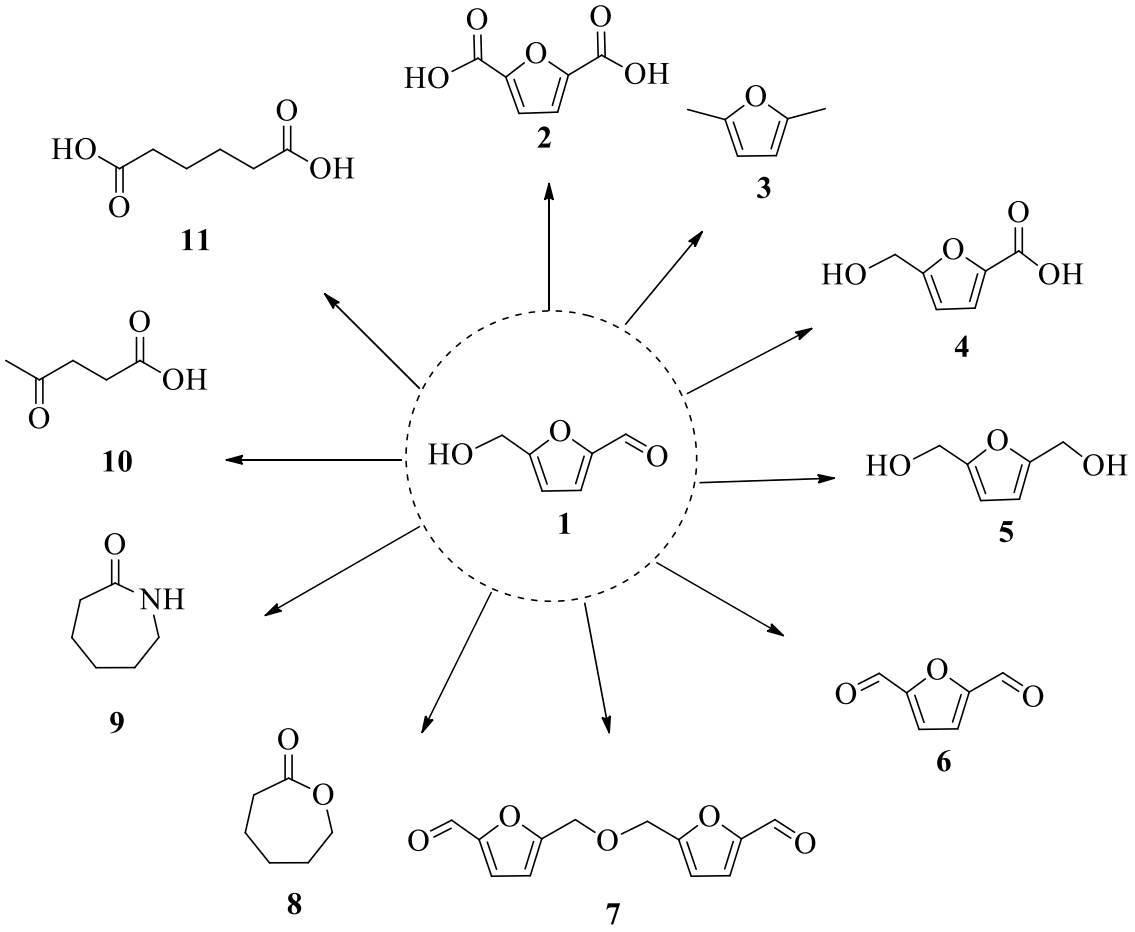

Figure 3. Structure of 5-hydroxymethylfurfural and possible derivatives

1.2 Isohexides

Isohexides are also known as 1,4:3,6 dianhydrohexitols, are a group of secondary and rigid diols, and have been used as a monomer in step-growth type polymerization reactions for the synthesis of different polymeric systems.[36] The structure of the isohexide molecule is composed of two fused tetrahydrofuran rings and two secondary hydroxyl groups located either inside or outside at the C2 and C5 positions (Figure 4). The angle between the two rings is approximately 120°. Interestingly, due to the intrinsic rigidity of the structures, isohexides are capable of increasing the thermal stabilities and glass transition temperatures when they are incorporated into the polymer backbone by replacing linear and more flexible diols. Furthermore, the combined

biocompatibility and degradability, the presence of chirality, and capability to increase thermal properties makes isohexides as unique and attractive building blocks for a variety of step-growth polymers, such as polyamides, polyurethanes, and poly(ester amides) and also for the synthesis of poly(ethylene terephthalate), poly(butylene terephthalate), and polyesters.[37,38,39,40]

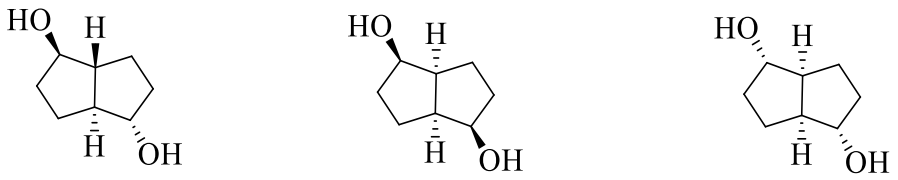

Isosorbide (12) **Isomannide (13)** **Isoidide (14)**

Figure 4. Isomers of isohexides and their structures

There are three major isohexides reported; isosorbide **(12)**, isomannide**(13)**, isoidide **(14)**. The preparation of isohexides from carbohydrate sources such as cellulose, starch, sucrose, and glucose comprise multistep organic transformations including hydrolysis, depolymerization, hydrogenation, and dehydration (Figure 5). The initial acidic or enzymatic depolymerization of the carbohydrate source results in the formation of monosaccharides (D-fructose, D-glucose). Further hydrogenation followed by dehydration of the resultant hexitols (D-glucitol, D-mannitol) and sugar alcohols yields isohexides. According to the literature, isosorbide is the only monomer, that has been produced on an industrial-scale and is the most commonly employed substrate with moderate reactivity among the three available isomers.[41,42] Whereas isomannide is less studied due to its lesser reactivity and the difficulties to synthesize from its parent carbohydrate source. On the other hand, isoidide is the most highly reactive isomer, however, it is derived from a monosaccharide called L-idose which rarely exists in nature and it is difficult to synthesize from biomass.[43] Alternatively, isoidide can be synthesized from isosorbide via a multistep organic

transformation (acetylation, Mitsunobu inversion, and hydrolysis).[44,45] However, an efficient and economical pathway for isoidide synthesis has not yet been reported.

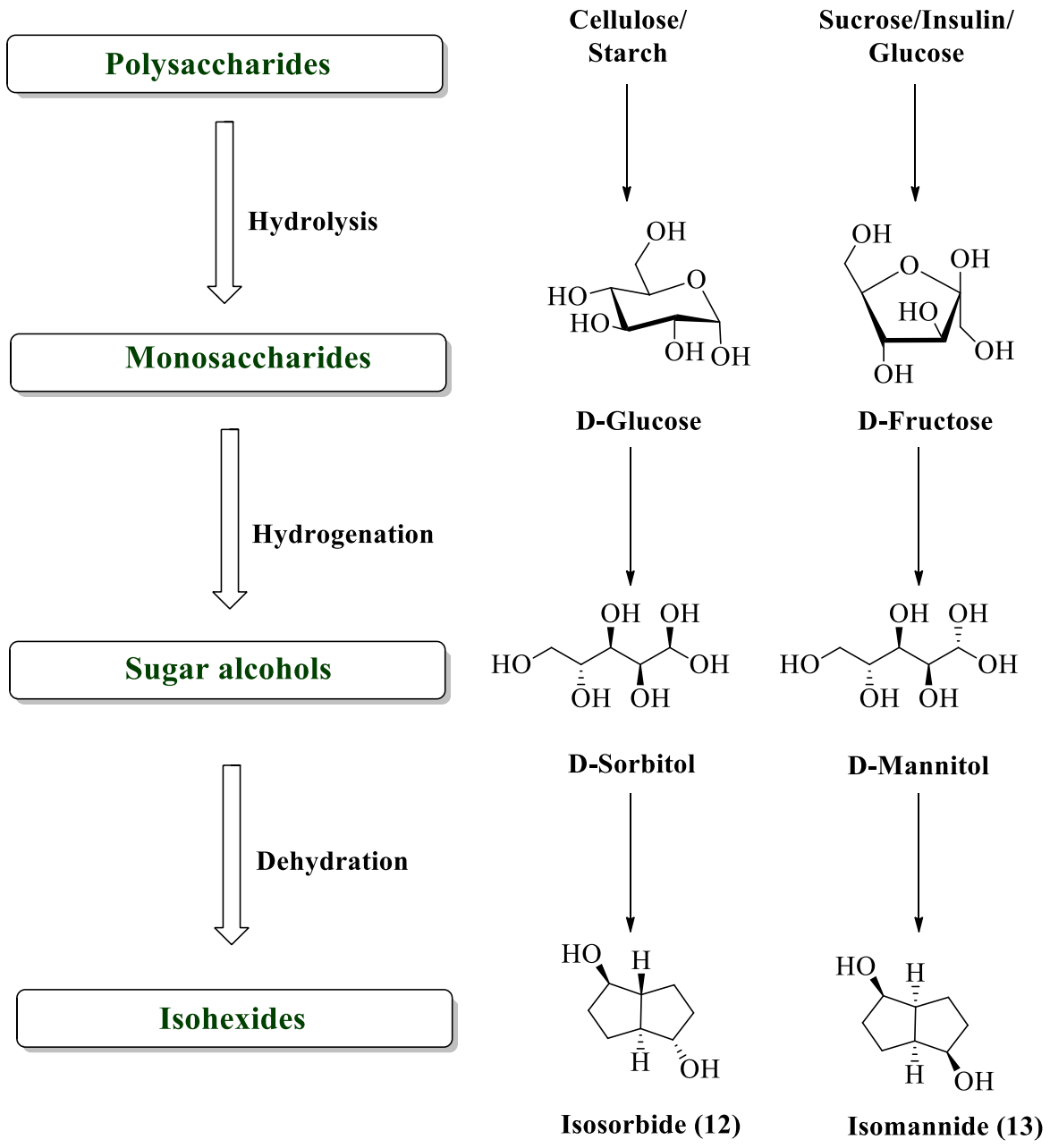

Figure 5. Schematic synthetic pathway of isohexides production from carbohydrates

1.3 Silyl ethers and poly(silylether)s

Silicon-containing chemicals and materials have been great interest both in the laboratory and in industrial research due to a wide range of applications as silica-based mesoporous materials, surface coatings, silicon rubbers, adhesives, paper coatings, silane coupling agents, and in particular materials as precursors of polymers. Popularly known silicon precursors are disilanes, oligosilanes, siloxanes, silanols, and silyl ethers. Among the several, silyl ethers have been gaining significant interests due to their resistance to oxidation, their low viscosity, their good thermal stability, and their ease of synthesis at mild reaction conditions. Silyl ethers are also called as alkoxysilanes as their structure contains a silicon atom covalently bonded with alkoxy functional groups (silyl ether bond; Si-O-C).[46]

1.3.1 General methods to synthesize silyl ethers

1.3.1A. Hydrosilylation

Catalytic hydrosilylation of carbonyl compounds is a well-known and widely used method to synthesize silyl ethers.[47] This method is one of the major approaches for reduction of a variety of unsaturated organic functional groups including C=O, C=C, C=N, N=N, C≡N, and C≡C (Figure 6). Among these, the reduction of carbonyl compounds is a process of high significance as it further allows for the synthesis of alcohols with various substrate moieties, which are widely used in various fields of synthetic chemistry. Hydrosilanes have been employed as reducing agents to reduce carbonyls, as they produce no considerable by-products, which makes it a unique and highly recognized reduction process.

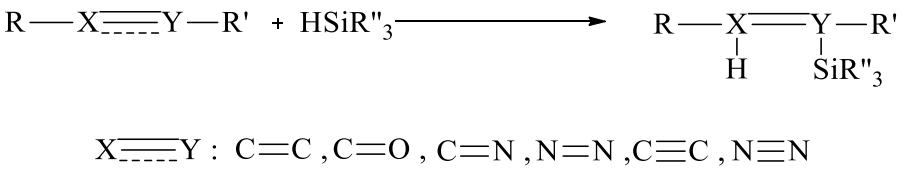

Figure 6. Hydrosilylation of unsaturated organic substrates

Several transition metal-based catalysts for hydrosilylation of carbonyls (ruthenium, rhodium, platinum, iridium, rhodium, molybdenum, iron, copper, silver, and, gold) have been successfully implemented and reported. Interestingly, most of the rhodium and ruthenium metal-based hydrosilylation catalytic systems are well described and documented in the literature. One half-sandwich ruthenium complex, $[CpRu(PR_3)(NCMe)_2]$ (R=^{i}Pr) (**15**) was found to catalyze hydrosilylation of carbonyl substrates under mild conditions. The proposed mechanism of complex **15** is similar to the classical Ojima type mechanism.[48,49] Initially, it forms a cationic complex (**16**) $[CpRu(PR_3)(NCMe)(\eta^2\text{-}HSiR''_3)]^+$ after one of the nitriles groups coordinated to the metal atom dissociates and addition of Si–H across the metal center (Scheme 3). Substitution of the carbonyl substrate with the remaining nitrile group on the metal center yields the $[CpRu(PR_3)(O{=}CR'_2)(\eta^2\text{-}HSiR''_3)]^+$ (**17**). Silyl transfer from (**17**) to the coordinated carbonyl substrate yields $[CpRu(PR_3)(H)(CR'_2(SiR''_3)]^+$ complex (**18**), which further undergoes a hydride ion transfer from the metal center and releases the silyl ether $R''_3SiO\text{-}CHR'_2$ via regeneration of the catalyst (**16**) by reacting with hydrosilane.

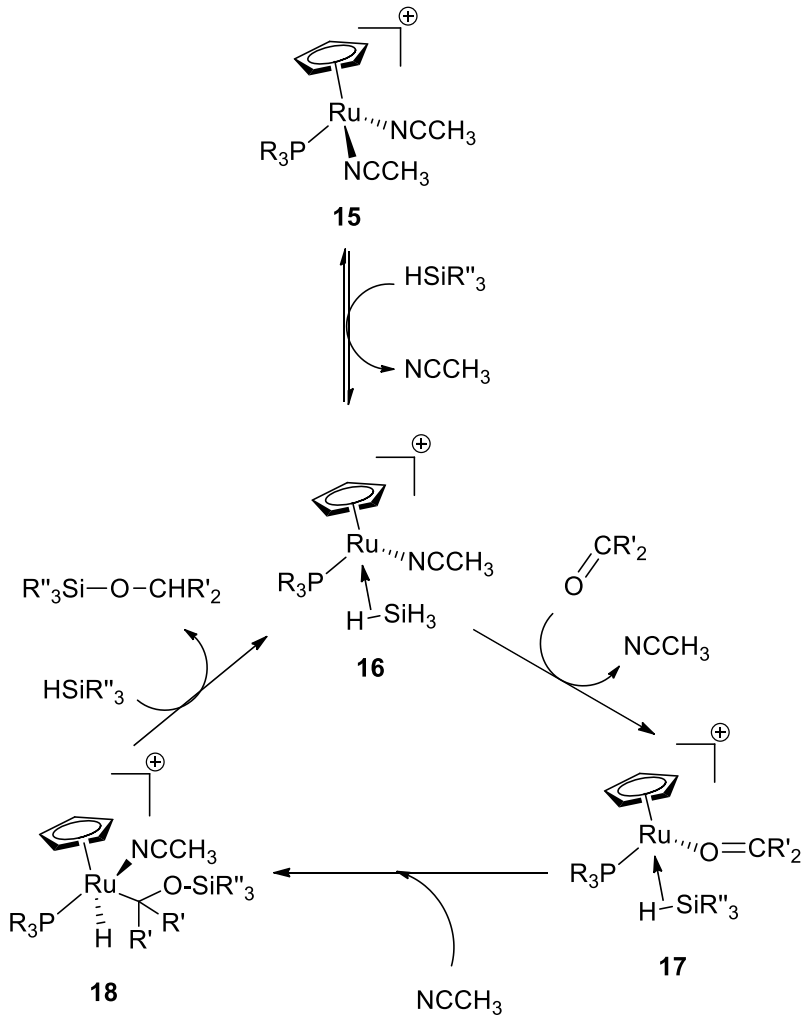

Scheme 1. The proposed Ojima type mechanism of hydrosilylation of carbonyls mediated by $[CpRu(PR_3)(NCMe)_2]^+$

1.3.1B. Protection of hydroxyl functional groups

One of the primary uses of silyl ethers is protecting alcohol functional groups in organic synthesis, which has gained great interest in recent years not only because of their importance but also for their significant role in the multifunctional synthesis of target molecules. Silyl ether synthesis from hydroxyl-functional substrates such as alcohols or phenols can be carried out by treatment with silylating reagents such as silyl triflates, cholorsilanes, and hexamethyldisilazane in the presence of a base and, sometimes, a silyl transfer agent.[50,51] However, employing

silyltriflates and cholorsilanes have drawbacks such as the production of unwanted by-products and their removal. In recent years, hydrosilanes have emerged as a prominent, green, and halogen-free alternative to the former silylating reagents since they produce hydrogen as the only byproduct. Several transition metal complexes have been successfully employed as the catalysts for dehydrogenative coupling of alcohols or phenols with hydrosilanes.

1.4. Poly(silylether)s

Considering the environmental effects of non-degradable polymers and utilization of renewable resources, degradable polymers have been synthesized from the biomass-based source.[52,53,54] Specifically, hydrolytically degradable polymers have been designed and developed towards a wide variety of biomedical applications including drug delivery systems, scaffolds for tissue engineering, and orthopedic implants.[55] Several degradable polymers with various moieties have been discovered and the resulting polymeric materials altered to achieve a broad range of mechanical properties as well as degradation profiles. Among the many, aliphatic polyesters, such as poly(lactic acid) and poly(caprolactone), have received vital attention as tunable polymers that degrade on the order of years under general physiological conditions. On the other hand, poly(anhydrides) and poly(ortho esters) bearing labile functionalities can generate materials that can degrade on the order of minutes to days.

Poly(silylether)s are an important class of silicon-based polymers with unique and significant properties, for instance, low T_g, good thermal stability, biocompatibility, and high gas permeability.[56,57,58] Catalytic systems based on palladium[59], platinum,[60] rhodium,[61,62,63] iridium[64,65] iron,[66] and cesium[67] have been developed. The general ways to synthesize PSEs are; 1. Dehydrogenative coupling reactions of alcohols with hydrosilanes catalyzed by metal complexes (Scheme 2), 2. Metal catalyzed hydrosilylation of dicarbonyls, 3. Uncatalyzed melt-condensation

of aryl- or diaryl diols with diphenoxysilanes, 4. Metal free or quaternary ammonium salts catalyzed reactions [68,69,70,71,72]

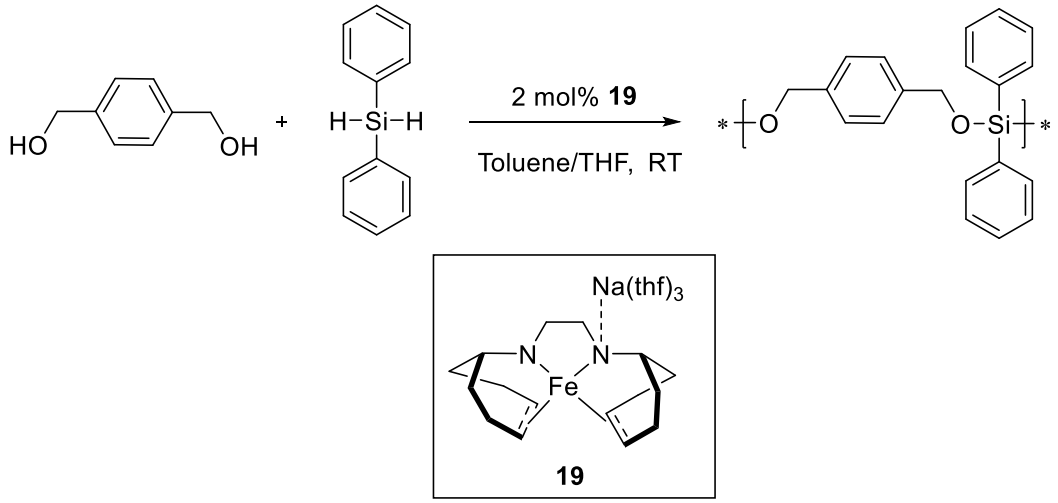

Scheme 2. Dehydrogenative coupling of 1,4 benzenedimethanol with diphenylsilane catalyzed by 19.

The presence of a labile Si-O-C (silyl ether) linkage makes them a promising degradable material under hydrolytic conditions. Hydrolysis of PSEs mostly produces nontoxic silyl ethers, silanols, and alcohols as the final products. A poly(silylether) (**21**) (M_n 23000 g/mol) synthesized by Hartwig and coworkers from a undecenoic acid derived bifunctional monomer (**20**) was completely degraded to furnish the respective alcohol products (**22**) under both acidic and basic hydrolytic conditions (Figure 7).[67] The degradation and molecular weights of the polymer were analyzed and confirmed by using nuclear magnetic resonance (NMR) spectroscopy and gel permeation chromatography (GPC). Besides, Voit and coworkers have reported a silyl ether thiol-ene polymer system (**25**) containing labile Si-O-C linkages in the polymer backbone by using silyl ether containing thiol (**23**) and alkene (**24**) monomers. The Si-O-C linkages in polymer backbone were successfully broken to generate the respective thiol alcohol (**26**) and Si-O containing byproducts such as silanols under hydrolytic conditions (Figure 8).[56]

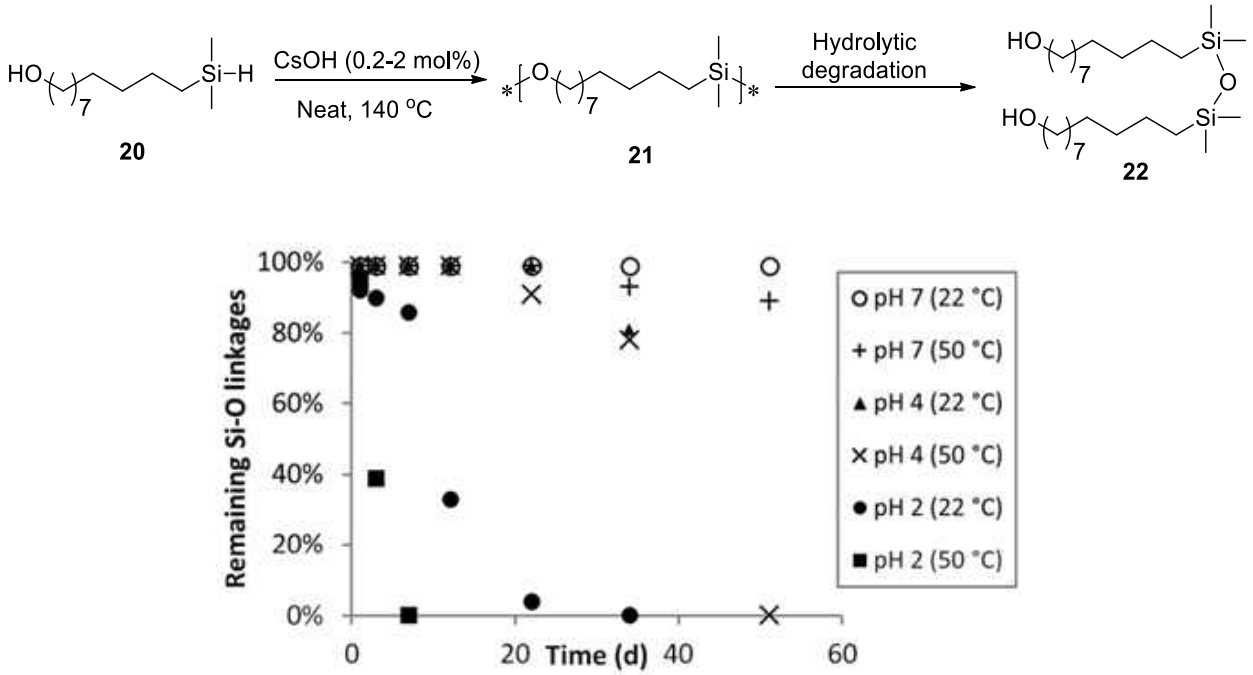

Figure 7. Degradation of polymer **21** via hydrolysis under acidic and basic medium [67]

Significantly, the majority of the reported PSEs have exhibited high thermal stabilities ($T_{-5\%}$ 300-430 °C, $T_{-50\%}$ 350-470 °C) depending on the molecular weights and backbone structures of polymers. Interestingly, these polymers can exhibit low or high glass transition temperatures depending on the rigidity of the incorporated molecules' structures of the polymer backbones.

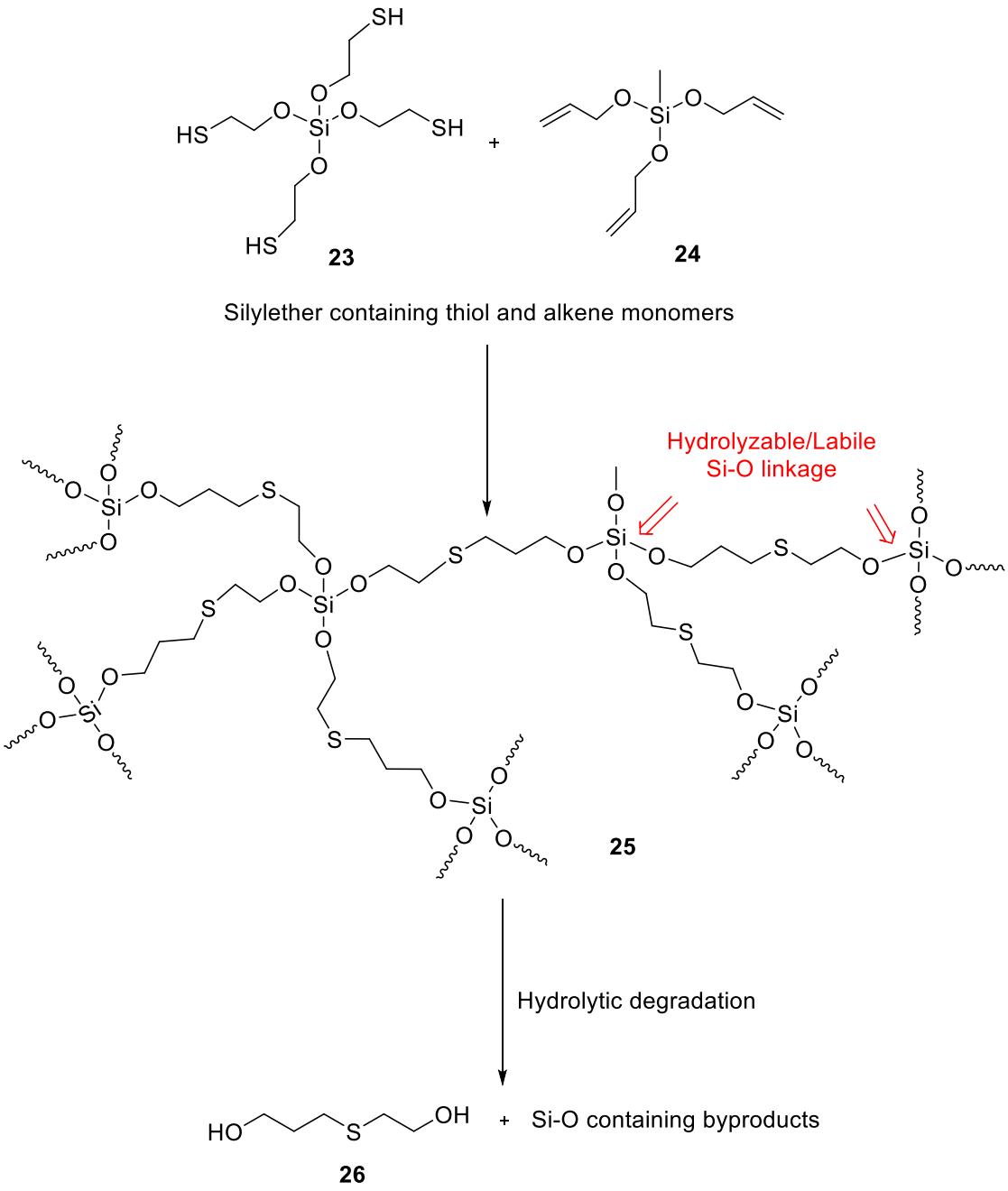

Figure 8. Schematic of the network structure and degradation products of a silyl ether thiol ene polymer [56]

1.5. Manganese catalysis in epoxidation and Si-H bond activation

Earth-abundant transition metal based catalysis for the synthesis of fine chemicals and polymers has become intensified due to the high abundance and inexpensive nature of metal atoms. Among the several transition metal catalytic systems reported, manganese based catalysis has significant attention due to its unique characteristics.[73,74] For instance, along with high abundance, manganese is relatively nontoxic, an essential element for biological systems, biocompatible, and environmentally benign element.[75] In addition, it can form compounds with coordination number up to 7 and has great potential redox activity due to the wide range of possible oxidation states (-3 to +7).[76] Manganese catalysis in oxidation reactions such as olefin epoxidation and activation of C-H bonds including carbon-oxygen (C–O) and carbon-halogen (C–F) bond formation, has been extensively established and reported.[77,78]

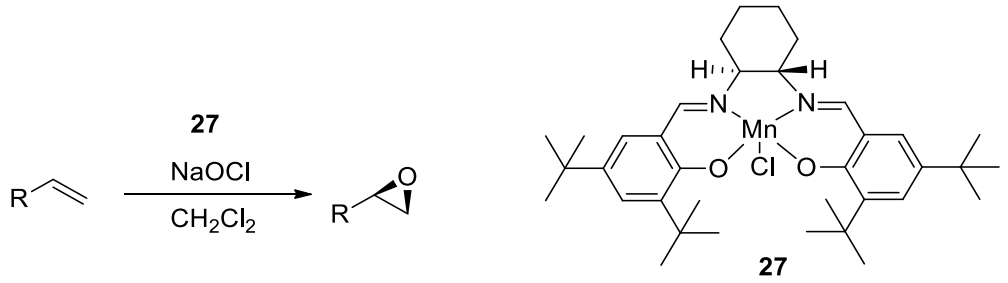

Figure 9. Epoxidation of alkene catalyzed by a manganese(III) (salan) complex

In recent years, manganese based hydrosilylation of carbonyl compounds has been generating as an environmentally benign process for the manufacture of silicon based chemicals and materials. Manganese diiminopyridine complexes and acyl manganese species were reported for hydrosilylation of carbonyls (Figures 10 & 11). In addition, several other manganese complexes have been reported for the hydrosilylation of carbonyl groups of amides.[79,80]

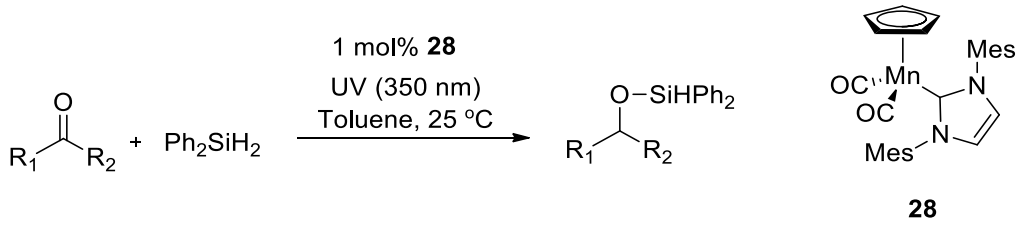

Figure 10. A manganese carbene catalyzed hydrosilylation of ketones

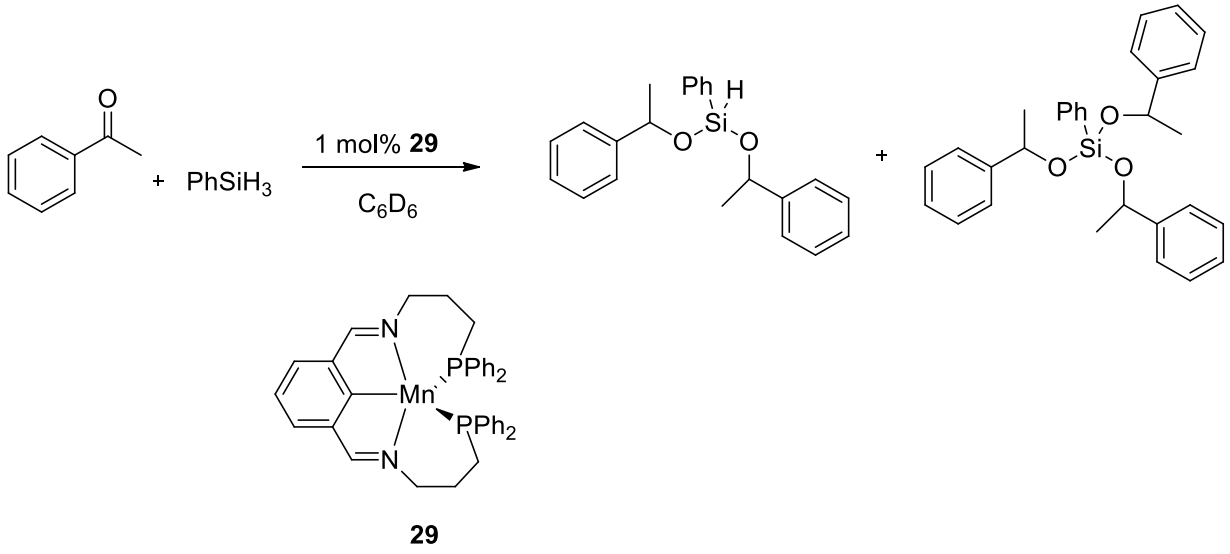

Figure 11. Hydrosilylation of carbonyls with a manganese bis(imino)pyridine complex

In 2013, a high valent manganese(V) (salan) nitride (**Mn-1**) (Figure 12) was reported as an efficient catalyst for hydrosilylation of carbonyl compounds.[81] **Mn-1** is an air-stable complex and can be synthesized easily at regular laboratory conditions.[82] In consideration of high activity of **Mn-1** in carbonyl hydrosilylation reactions and our interests in high-valent metal catalyzed reactions led us to explore the catalytic activity of **Mn-1** in activation of Si-H and B-H bonds and synthesis of degradable polymers.

1.5. Objectives of the dissertation

The primary objective of this dissertation was manganese catalysis in the synthesis of degradable and thermally stable poly(silylether)s from renewable resources via dehydrogenative coupling and hydrosilylation reactions. One of the other objectives of this thesis includes manganese catalyzed activation of B-H bonds for chemoselective hydroboration of aldehydes and ketones under mild reaction conditions. In this thesis, we mainly focused on a Mn^{V} catalyst that is isoelectronic with other transition element based catalytic systems, Mo^{IV}, Re^{V}, and Ru^{VI}, containing a diamagnetic d^2 electron configuration. [MnN(salen-3,5-^{t}Bu$_2$)] (**Mn-1**) is chosen as a model complex because it is easily prepared and able to soluble in general organic solvents.

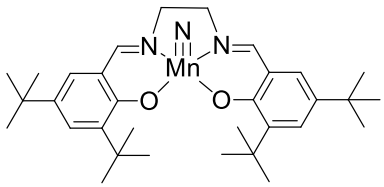

Mn-1

Figure 12. Structure of [MnN(salen-3,5-^{t}Bu$_2$)] (**Mn-1**)

1.6. Structure of the dissertation

This dissertation includes six chapters.

Chapter 1 *Introduction to my research work.* The chapter is about the general importance renewable resources, classes of monomers can be derived from biomass, type of monomers used in this disserration and their synthesis from biomass source.

Chapter 2 *Dehydrogenative coupling reactions catalyzed by a manganese complex*. In this chapter, synthesis of silyl ethers and silyl esters from alcohols and carboxylic acids with hydrosilanes is discussed.

Chapter 3 *Poly(silylether)s synthesis*. In this chapter, salen manganese complex was successfully employed as the catalyst for the synthesis of poly(silylether)s from various non-bio-based monomers which includes symmetrical diols (1,4-benzenedimethanol, 1,4-benzenediol, 4,4′-biphenol, 1,4-cyclohexanediol, 1,4-cyclohexanedimethanol, and 1,6-hexanediol), symmetrical dicarbonyls (1,4-cyclohexanedione, benzene-1,4-dicarboxaldehyde, and 1,6-hexanedial), and unsymmetrical substrates (p-hydroxybenzyl alcohol, 3(4-hydroxyphenyl)-1-propanol, and p-hydroxybenzaldehyde).

Chapter 4 *Synthesis of poly(silylether)s from furan-based monomers*. In this chapter, biomass based, 5-(hydroxymethyl)furfural and its derivatives such as 2,5-bis(hydroxymethyl)furan, 2,5-furandicarboxaldehyde, and 5,5'-[Oxybis(methylene)]di(2-furaldehyde) were successfully utilized to synthesize hydrolytically degradable PSEs. Thermal analysis and glass transition temperature analysis were also studied.

Chapter 5 *Synthesis of poly(silylether)s from isohexides*. In this chapter, isosorbide and isomannide based PSEs were prepared via step-growth polymewrization process using a manganese complex. PSEs detailed thermal analysis, glass transition temperature analysis, and degradtion properties under neutral, acidic, and basic conditions were studied.

Chapter 6 *Manganese catalysis in hydroboration of carbonyls*. In this chapter, carbonyls were reduced to their respective 1° and 2° alcohols via hydroborations process at mild reaction conditions. A tentative plausible mechanism is also discussed.

CHAPTER 2

DEHYDROGENATIVE COUPLING OF ALCOHOLS AND CARBOXYLIC ACIDS WITH HYDROSILANES CATALYZED BY A SALEN MN(V) COMPLEX

2.1. Introduction

The Si-O bond containing compounds such as silylethers and silylesters are important chemicals with an assortment of applications. For example, silylethers are commonly employed for protecting hydroxyl groups in multi-step syntheses,[83,84] and serve as precursors to silicone polymers.[85] They are also valuable for surface modifications, constructing organic-inorganic hybrids, functionalizing silica materials, and tethering organometallic catalysts.[86,87,88,89,90] Silyl esters are useful for protecting carboxylic acid groups[83] and poly(silylester)s are an interesting class of degradable materials with tunable degradation profile.[91,92] The standard method for the synthesis of silylethers and silylesters is treating alcohol and carboxylic acid substrates with chlorosilanes, in which the HCl byproduct is neutralized with a stoichiometric amount of bases such as imidazole and diisopropylethylamine.[93,94,95] Moreover, the corrosiveness and hydrolytic sensitivity of chlorosilanes make it inconvenient for handling and storage. For tertiary and hindered alcohols, use of more expensive silyl triflate reagents is required.[96] Hexamethyldisilazane (HMDS) has also been utilized for silylether synthesis, but it usually takes longer reaction times and the ammonia byproduct needs to be removed continuously.[97,98]

Dehydrogenative coupling of alcohols and carboxylic acids with hydrosilanes has emerged as an alternative for the synthesis of silylether and silylesters. Compared to chlorosilanes, hydrosilanes are generally less prone to hydrolysis and easier to handle. The dehydrogenative coupling reaction

is a single step process with high atom economy, generating hydrogen gas as the only byproduct. Due to these attractive features, a number of catalysts have been reported for the dehydrogenative coupling of alcohols and hydrosilanes. They are typically complexes of various transition metals,[99,100,101,102,103,104] while metal-free systems such as N-heterocyclic carbenes[105] and Lewis acid $B(C_6F_5)_3$[106,107] have also been developed for the process. In comparison, only a few catalytic systems are available for the dehydrogenative coupling of carboxylic acids and hydrosilanes.[108,109,110,111,112]

Recent concerns about sustainability have led to significant efforts towards the development of catalytic systems derived from inexpensive, biocompatible, and abundant metals.[113,114] Taking this into consideration, manganese is of particular interest, since its global reserve is one of the largest among transition metals and it is an essential element for biological systems. Traditionally manganese complexes have been extensively investigated in oxidation reactions, and their applications in other types of transformations are only being explored more recently.[115] During the course of our study with high valent transition metal catalysts for hydrosilylations,[81,116,117] we observed that hydroxyl groups reacted with hydrosilanes in the presence of a Mn(V) complex, [MnN(salen-3,5-^{t}Bu$_2$)] (**Mn-1**) that is readily available and easily prepared[82,118 ,119] Herein we report our study on the dehydrogenative coupling of alcohols and carboxylic acids with hydrosilanes catalyzed by manganese complex **Mn-1**.

2.2. Results and discussion

2.2.1. Dehydrogenative coupling of alcohols and silanes: Screening

In the initial experiments, we examined the dehydrogenative coupling reaction by taking benzyl alcohol as a template substrate. Various hydrosilanes were examined under different conditions in the presence of 0.5 mol % (vs alcohol) of **Mn-1**, and the selected results are presented

in Table 1. Primary $PhSiH_3$, secondary Ph_2SiH_2, and tertiary $(EtO)_3SiH$ hydrosilanes reacted readily with $PhCH_2OH$ to produce the corresponding silylethers, with $(EtO)_3SiH$ being the fastest among them (Entries 3 *vs* 9, 8 *vs* 10).

According to the product analysis of the crude reaction mixture, mono alkoxysilane $Ph_2SiH(OCH_2Ph)$ was produced when one equivalent of Ph_2SiH_2 was employed, with a small amount of dialkoxysilane $Ph_2Si(OCH_2Ph)_2$ (Entry 3). When the ratio of alcohol:Ph_2SiH_2 is 2:1, dialkoxysilane $Ph_2Si(OCH_2Ph)_2$ was produced as the predominant product (Entry 2). In this case the time profile of the reaction monitored by ^{1}H NMR spectroscopy shows a rapid consumption of Ph_2SiH_2 and buildup of $Ph_2SiH(OCH_2Ph)$, followed by a slower disappearance of $Ph_2SiH(OCH_2Ph)$ (Figure 13). Similar to the Mn-catalyzed hydrosilylation of carbonyl compounds,[81] the coupling reaction could be carried out at room temperature with extended reaction time (Entry 11). Running reaction under inert nitrogen atmosphere could shorten the reaction time (Entry 1 *vs.* 1, entry 9 *vs.* 10), though the effect seems to be less substantial than in hydrosilylation. Thus, later reactions were performed without exclusion of air for convenience. On the other hand, tertiary alkyl silanes such as $PhMe_2SiH$, Et_3SiH, and $^tBuMe_2SiH$ showed no reactivity, while Ph_3SiH showed reasonable conversion with prolonged reaction time (72 h), likely due to their electronic and steric characters (entries 4–7). In a control experiment, no reaction between $PhCH_2OH$ and $(EtO)_3SiH$ was observed after 12 h without adding the catalyst (Entry 12).

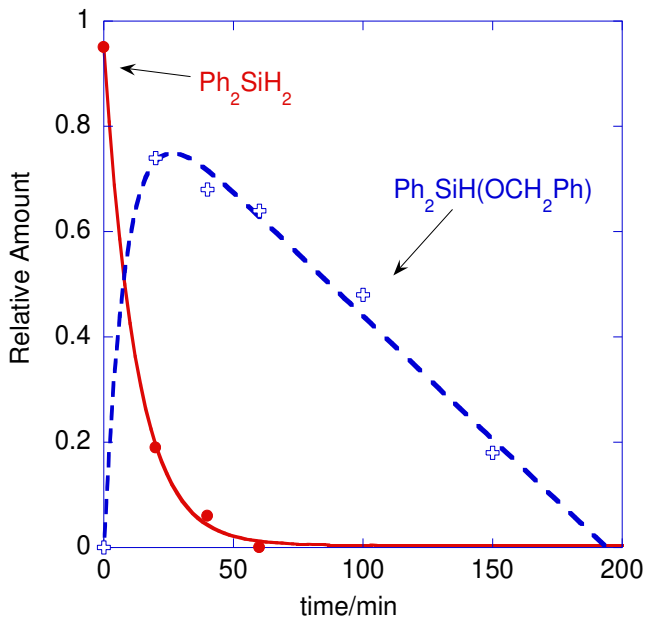

Figure 13. Time profile for the reaction of benzyl alcohol with Ph_2SiH_2 (one equiv.)

Table 1. Dehydrogenative coupling of benzyl alcohol with hydrosilanes[a]

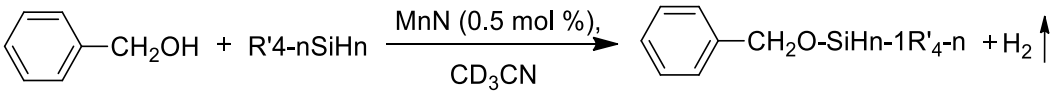

Entry	Silane	BnOH:silane	Products	*T*(°C)	*t* (h)	Conversion (%)[b]
1[e]	Ph_2SiH_2	2:1	$(PhCH_2O)_2$-$SiPh_2$	80	2.5	89
2[c]	Ph_2SiH_2	2:1	$(PhCH_2O)_2$-$SiPh_2$	80	3	85
3	Ph_2SiH_2	1:1	$PhCH_2O$-$SiHPh_2$[d]	80	1	90
4[c]	$PhMe_2SiH$	1:1	N.R	80	72	-
5	$^tBuMe_2SiH$	1:1	N.R	80	24	-
6	$(Et)_3SiH$	1:1	N.R	80	24	-
7	$(Ph)_3SiH$	1:1	$PhCH_2O$-$Si(Ph)_3$	80	72	57
8	$PhSiH_3$	1:1	$(PhCH_2O)_2$-$SiHPh$[e]	80	1.5	90
9[c]	$(EtO)_3SiH$	1:1	$PhCH_2O$-$Si(OEt)_3$	80	0.67	98

10	$(EtO)_3SiH$	1:1	$PhCH_2O$-$Si(OEt)_3$	80	1	94
11	$(EtO)_3SiH$	1:1	$PhCH_2O$-$Si(OEt)_3$	RT	7	90
12[f]	$(EtO)_3SiH$	1:1	N.R	80	12	-

[a]Reaction conditions: substrate (0.7-0.8 mmol), silanes (one or two equivalents), $PhSiMe_3$ (10 mol%, as internal standard), and **Mn-1** (0.5 mol%). [b]Determined by ^1H NMR on the basis of consumption of Ph_2CH_2OH or silane. [c]Reaction was performed under N_2. [d]Dialkoxy silyl ether was observed as a minor product. [e]Mono and trialkoxy silyl ethers were observed as minor products. [f]Catalyst was not used.

2.2.2. Alcohol substrate scope

Having established the activity of **Mn-1** in the dehydrogenative coupling reactions, we moved on to a variety of alcohol substrates including primary, secondary, tertiary, cyclic and phenolic alcohols (Table 2). Under specified reaction conditions, all types of alcohols resulted in the corresponding silylethers with >90% conversions and slightly lower isolated yields. Unlike primary alcohols, the dehydrogenative coupling of secondary and tertiary alcohols with Ph_2SiH_2 afforded monoalkoxysilanes as the primary product, even when excess alcohols were used (Entries 2-4). This observation indicates that the last Si-H bond was more challenging to couple with a bulky alcohol because of the steric crowding. For example, when 2 equivalents of a tertiary alcohol ^tBuOH was allowed to react with Ph_2SiH_2, only half the amount of alcohol was consumed, even after prolonged reaction time (6 h). Addition of another equivalent of Ph_2SiH_2 led to the complete conversion of ^tBuOH within 2.5 h and the monoalkoxysilane was the predominant product detected (Table 2, Entry 3). Similarly, reaction of a secondary alcohol, cyclohexanol, with Ph_2SiH_2 resulted in the monoalkoxysilane as the main product with 95% conversion in 1 h (Table 2, Entry 4).

Table 2. Mn complex **1** catalyzed dehydrogenative coupling of various alcohols with silanes[a]

Entry	Silane[b]	Products	t (h)	Conversion(%)[c]
1	Ph_2SiH_2 (0.5)	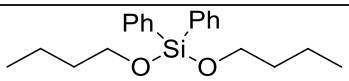	7.5	95 (81)
2	Ph_2SiH_2 (1.0)	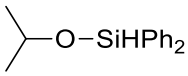	1.5	96 (67)
3	Ph_2SiH_2 (1.0)	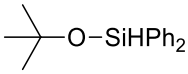	8.5	97 (79)
4	Ph_2SiH_2 (1.0)	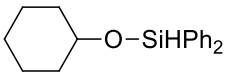	1	95 (63)
5	Ph_2SiH_2 (0.5)	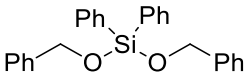	3	85 (50)
6[d]	Ph_2SiH_2 (0.5)	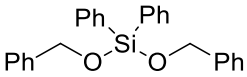	2.7	95 (81.2)
7	$(EtO)_3SiH$ (1.0)	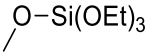	1	90 (65)
8	$(EtO)_3SiH$ (1.2)	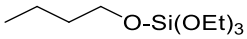	1.5	95 (81)
9	$(EtO)_3SiH$ (1.2)	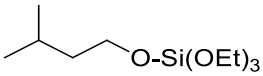	2	95 (71.2)
10	$(EtO)_3SiH$ (1.0)	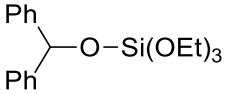	3	98 (64)
11	$(EtO)_3SiH$ (1.0)	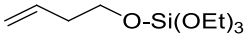	4	98 (71)
12	$(EtO)_3SiH$ (1.4)	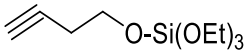	5	96 (65)
13	$(EtO)_3SiH$ (1.3)	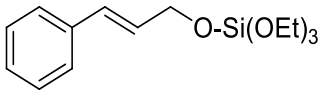	2.5	90 (64)
14	$(EtO)_3SiH$ (1.0)	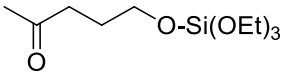	2.5	90 (73)

15[e]	$(EtO)_3SiH$ (1.0)	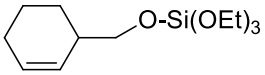	0.67	99
16	$(EtO)_3SiH$ (1.0)	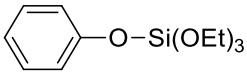	3	98 (81)
17	$(EtO)_3SiH$ (1.3)	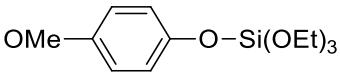	1	90 (78)
18	$(EtO)_3SiH$ (1.2)	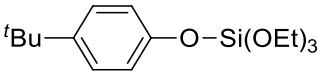	4	95 (57.1)
19	$(EtO)_3SiH$ (1.2)	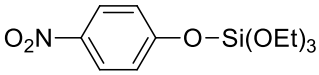	1.5	100 (73)
20	$(EtO)_3SiH$ (1.3)	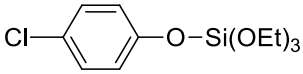	2	95 (57)

[a]Reaction conditions: Substrate (0.7-0.8 mmol), silane, and catalyst (0.5 mol%) at 80 °C. [b]the equivalent amounts of silanes used (vs alcohol). [c]Determined by ^1H NMR on the basis of consumption of alcohol and/or silane; isolated yields in parenthesis. [d]Reaction under N_2. [e]1 mol % catalyst used.

To examine the chemoselectivity of the dehydrogenative coupling process, we further worked with alcohol substrates having different functional groups such as C=C and C≡C multiple bonds (Entries 11-13, 15), since such groups may react with silanes under catalytic conditions. All these alcohols were converted to silylethers with excellent conversions and yields. As expected, there were no side products of hydrosilylation/hydrogenation of double and triple bonds with silanes. It is noted that saturated primary alcohols seem to be more reactive towards this dehydrogenative coupling with triethoxysilane than unsaturated ones, as it took less reaction time (Entry 8 *vs*. 11 & 12). The time profile of reactions under identical conditions with 1 equivalent of $(EtO)_3SiH$ confirms butan-1-ol is the fastest among them, though the difference is not large (Figure 14). Nevertheless, this suggests that even though the double and triple bonds are not reactive towards hydrosilanes under these conditions, they may still inhibit the coupling, presumably by

coordinating to the active metal sites. Since **Mn-1** known to catalyze the hydrosilylation of ketones, a multifunctional substrate, 5-hydroxy-2-pentanone was tested for the coupling reaction (Entry 14). Only the hydroxy group reacted with silane under these conditions, conditions, and the ketone moiety is preserved in the isolated product. The preference for hydroxy groups over carbonyls has been observed in other catalytic systems.

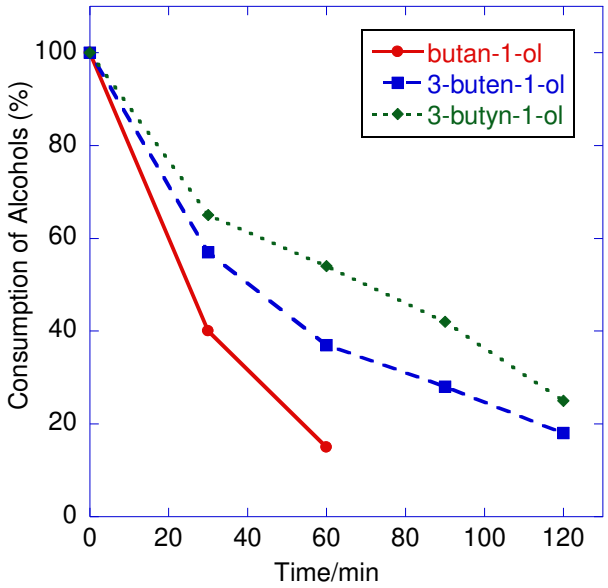

Figure 14. Comparison of reactions of three primary aliphatic alcohols with $(EtO)_3SiH$ (1:1).

To further probe the selectivity and electronic effect of different groups, we performed dehydrogenative coupling reactions of a series of *para*-substituted phenolic substrates and $(EtO)_3SiH$ (Table 2, entries 16-20). Halo, nitro, and methoxy groups were tolerated in the reaction and dehydrogenative coupling proceeded with high conversion and yields within a few hours. When the reactions of 1:1 $(EtO)_3SiH$:phenols under otherwise identical conditions were followed by ^1H NMR, the silane conversion profile indicated that both electron withdrawing and electron donating groups lead to faster reactions (Figure 15), with the exception of *p*-nitro-phenol, for which the reaction was considerably slower and featured an induction period. The peculiarity of

para-NO_2 substituted benzaldehyde and acetophenone has been noticed previously in hydrosilylation reactions,[81] though the reason behind is still unclear.

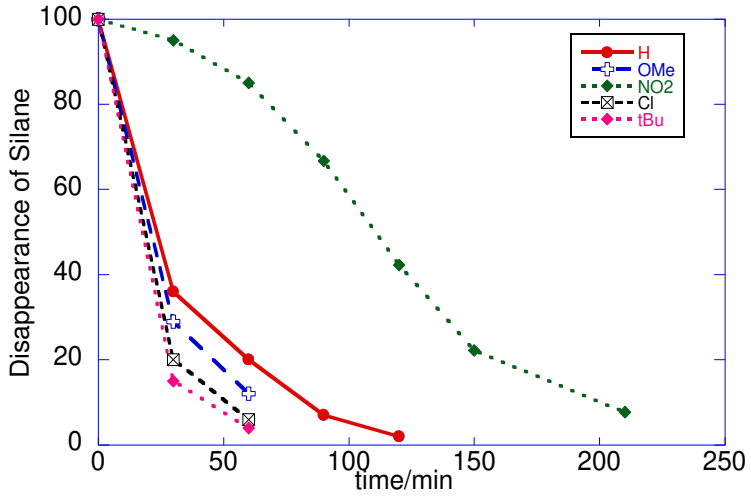

Figure 15. Reactions of substituted phenols *p*-X-C_6H_4OH (X = H, OMe, NO_2, Cl, ^{t}Bu) with $(EtO)_3SiH$ (1:1)

To extend the scope of dehydrogenative coupling reactions, several diols were also examined under the same conditions and results are summarized in Table 3. Diol substrates tend to be more demanding for the coupling because of the competing formation of cyclic and polymeric species. When 1,4-butanediol was allowed to react with two equivalents of $(EtO)_3SiH$, bissilylated $(EtO)_3SiO(CH_2)_4OSi(OEt)_3$ was the only product, as expected (Entry 1). When a slight excess of Ph_2SiH_2 was used, the seven-membered cyclic dioxasilacycle was obtained as the major product (Entry 2). Similarly, treatment of pinacol with one equivalent of Ph_2SiH_2 or $PhMeSiH_2$ afforded five-membered cyclic dioxasilacycles as the major products (Entries 3 & 4).[120]

Table 3. **Mn-1** catalyzed dehydrogenative coupling of diols with silanes[a]

Entry	Silane	diol:silane	Product (s)	t (h)	Conversion(%)[b]
1	$(EtO)_3SiH$	1:2	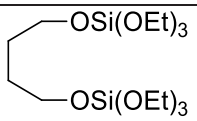	3	90 (56)
2	Ph_2SiH_2	1:1.2	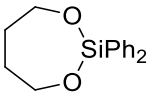	3.5	70 (65)
3	Ph_2SiH_2	1:1	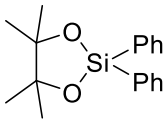	5.5	95
4	$PhMeSiH_2$	1:1	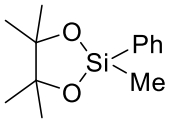	5	98

[a]Substrate (0.7-0.8 mmol), silane, and catalyst (0.5 mol%) at 80 °C. [b]Determined by ^1H NMR on the basis of consumption of diols and/or silane; isolated yields in parenthesis.

In another set of experiments, we repeated the reaction between benzyl alcohol and triethoxysilane to test the reusability of the catalyst. After the reaction was nearly complete (~60 min), second equivalent of alcohol and silane (1:1 molar ratio) was added to the reaction mixture and with a vigorous bubbling >90% of the substrates were consumed within 30 min. A third addition of 1:1 $PhCH_2OH$-$(EtO)_3SiH$ led to similar outcome (Figure 16). These results suggested that the catalyst can be effectively reused without much loss in reactivity.

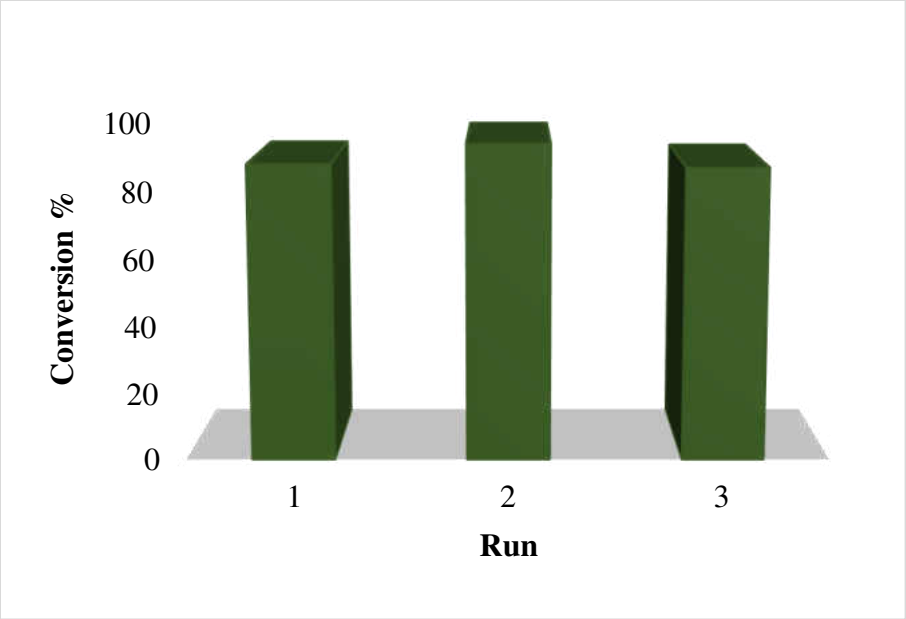

Figure 16. Reusability of the catalyst for dehydrogenative coupling

2.2.3. Dehydrogenative coupling of carboxylic acids and silanes

Based on the results of alcohols, we next extended this process for the dehydrogenative coupling of carboxylic acids and silanes to synthesize silylesters. Several reactions were performed in several solvents at different temperatures to optimize the reaction conditions and selected results are listed in Table 4. Among the solvents tested, $CDCl_3$ has generally given rise to better conversions (Complete solubility of carboxylic acids were observed in $CDCl_3$ and poor solubility was observed in other solvents). Compared with the dehydrogenative reactions of alcohols, carboxylic acids reactions are much slower, even with increased catalyst loading. Both aromatic (Entry 1) and aliphatic carboxylic acids (Entries 2 & 3) undergo dehydrogenative coupling reactions with $(EtO)_3SiH$ to yield corresponding silylesters.

Table 4. **Mn-1** catalyzed dehydrogenative coupling of carboxylic acids with $(EtO)_3SiH$[a]

Entry	Substrate	Acid:silane	Solvent	Products	t (h)	Conversion(%)[b]
1	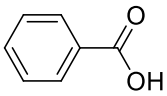	1:1	$CDCl_3$	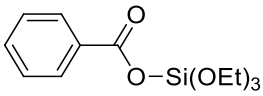	32	73
2	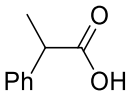	1:1.3	$CDCl_3$	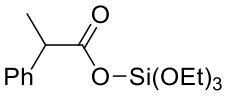	29	77
3	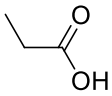	1:1	C_6D_6	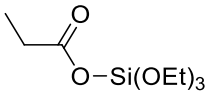	28	52

[a]SuReaction conditions: substrate (0.4–0.6 mmol), $(EtO)_3SiH$ and 1 (1 mol%); 80 °C. [b]Determined by ^1H NMR on the basis of consumption of acids and/or silane. Repeated attempts at isolation of silyl esters by column chromatography on silica led to decomposition, and isolated yields were not obtained.

2.3. Mechanistic consideration

During the reactions, one of the most notable features was the conspicuous change in color of the starting **Mn-1** complex from green to reddish brown, then to dark yellow, and finally to pale yellow, similar to the observations in hydrosilylation reactions.[15a] The color change can be attributed to the reduction of Mn(V) to lower oxidation states such as Mn(III) and Mn(II),[121,122]and appears to be correlated with the progress of the reaction. The observation that the reactions upon second and third additions of the reactants took place even faster, as discussed earlier (see Figure. 16), is in agreement with the hypothesis that Mn(V) is not the actual active species, and that it needs to be reduced first to act as the active catalyst. Conversely, when there was no reaction between the hydroxyl groups and tertiary hydrosilanes such as for $PhMe_2SiH$, Et_3SiH and $^tBuMe_2SiH$, the reaction mixture retained the same green color. In these cases, the less active tertiary hydrosilanes were not able to reduce manganese(V), and as a result, catalytic

dehydrogenative coupling did not occur. Hence, we believe that the activation of manganese by reduction is a crucial step for the reactivity.

2.4. Conclusions

In conclusion, we have reported a Mn-salen complex, **Mn-1**, for the effective synthesis of silyl ethers and silyl esters via dehydrogenative coupling of alcohols, phenols and carboxylic acids with hydrosilanes. The coupling reaction is compatible with a variety of functional groups, and seems to involve a reduced Mn active species. Our future studies will be focusing on the mechanistic understanding of the current dehydrogenative coupling reactions and further extension of the methodology to other applications.

2.5. Experimental section

General. Inert condition reactions were carried out under a dry nitrogen atmosphere, employing standard Schlenk line using J-Young NMR tube and dry box techniques and all the remaining reactions were carried out in air (at bench top). All the necessary solvents and liquid substrates were degassed and dried over molecular sieves prior to use. Deuterated solvents were purchased from Cambridge Isotope Laboratory. All ^{1}H NMR and all ^{13}C NMR spectra were recorded on a Bruker AVANCE-500 NMR spectrometer and referenced to $CDCl_3$ and CD_3CN. All the substrates were added inside the glovebox in an inert environment unless mentioned.

GC-MS instrumentation parameters. GC analyses were performed using a 5890 GC with 5972 MS equipped with an autosampler (6890 series, Agilent Technologies, Santa Clara, CA, USA). Injections were performed in the splitless mode for 0.50 min at 250 °C and the injection volume was 1 µL. The separation was performed using a 45-m long HP-5MS capillary column, with 0.25 mm internal diameter (I.D.) and 0.25 µL film thickness (J&W Scientific, Folsom, CA, USA). A constant carrier gas (helium) at a flow rate of 1.5 mL/min was maintained during the analysis. Two

temperature programs were used. The first started at 40°C held for 1 min, followed by a gradient of 35 °C/min to 80 °C, then a gradient of 20 °C/min to 300 °C and held for 10 min. The second program started at 50°C held for 1 min, followed by a gradient of 35 °C/min to 80 °C, then a gradient of 20 °C/min to 320 °C and held for 3 min. The MS data in total ion chromatograms (TIC) were acquired in the mass range of m/z of 50–700 at a scan rate 2.67 scan/s using the EI of 70 eV. The solvent delay was set to 3.8 minutes.

General procedure for the dehydrogenative coupling of alcohols and silanes. Following the optimized conditions, 0.5 mol% catalyst was loaded into J-Young NMR tube inside the glove box, stoichiometric equivalents of substrate and the reductant were added followed by the deuterated solvent (0.35 mL). The reaction mixture was heated to the 80 °C untill the conversion reached maximum. Reaction progress was confirmed by ^{1}H NMR.

General procedure for the dehydrogenative coupling of carboxylic acids and silanes. 0.5-1 mol% catalyst, stoichiometric equivalents of the substrate and reductant were loaded into a J-Young NMR followed by the addition of internal standard and deuterated solvent (CD_3CN, $CDCl_3$, toluene-*d*) as the solvent (0.35 mL). The reaction mixture was heated to the respective temparature (80 °C, 120 °C). Reaction progress was monitored by ^{1}H NMR and TLC. Procedure is same for the regular solvents (acetonitrile, toluene, DCM, $CHCl_3$) but the reactions were performed in a round bottom or Schleck flask.

Synthesis of catalyst. Following the work by Du Bois and coworkers,[123] we have synthesized **Mn-1**, tertiary butyl salen manganese(V) nitrido complex, using tertiary butyl H_2 salen as the ligand. Synthesis of salen manganese complex is a two-step process, first step is the synthesis of salen ligand from its precursors, salicylaldehyde and respective diamino alkanes followed by the synthesis of nitrido manganese(V) complex as a second step (Scheme 3). The synthesis involves

the addition of manganese acetate tetrahydrate to salen ligand solution followed by the subsequent addition of NH_4OH, NaOCl (bleach) using methanol and dichloromethane as the solvents. After workup with water, **Mn-1** was separated out as an emerald green powder (700 mg, 61%).

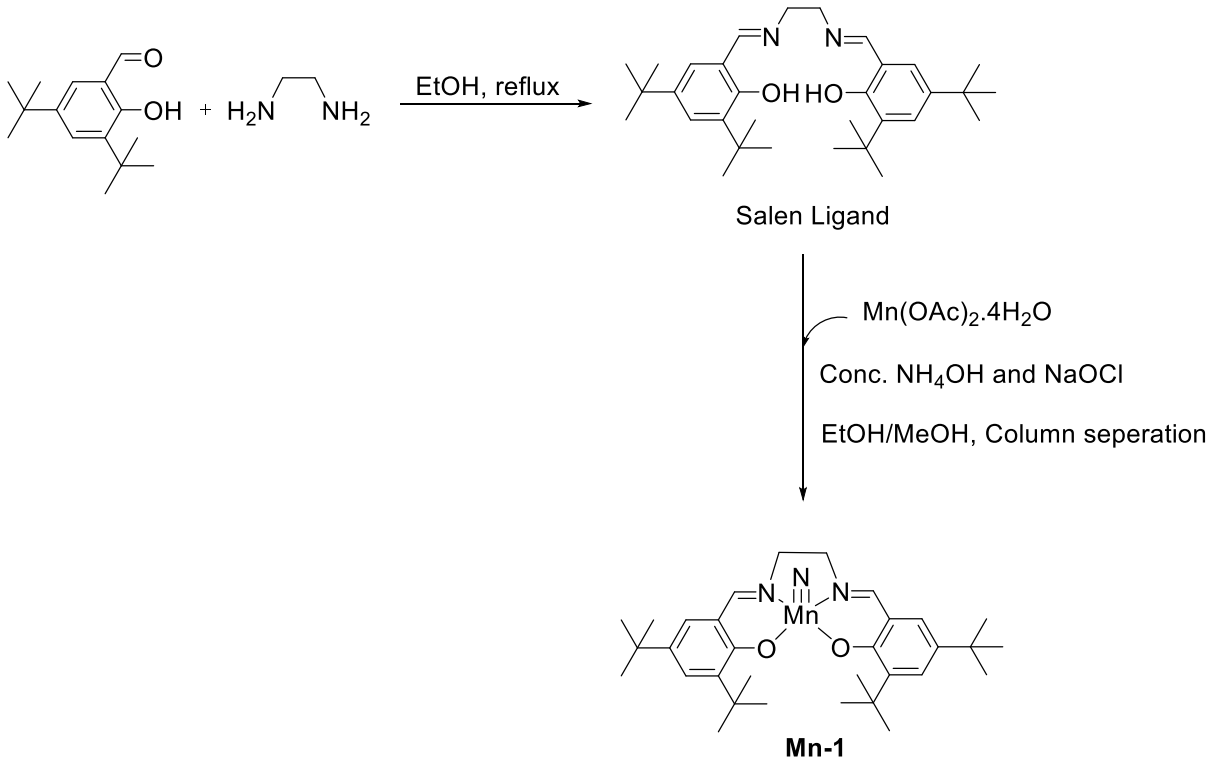

Scheme 3. Synthesis of salen-Mn(V) nitrido complex **Mn-1**

NMR and GCMS characterization data

Table 2, Entry 1: $(CH_3CH_2CH_2CH_2O)_2SiPh_2$: ^{1}H NMR (500 MHz, $CDCl_3$, 298K, δ): 7.7–7.66 (m, 4H, *Ph*), 7.45–7.35 (m, 6H, *Ph*), 3.81 (t, $J_{H\text{-}H}$ = 6.0, 2H, OCH_2CH_3), 1.61 (m, 2H, $OCH_2CH_2C_2H_5$), 1.24 (m, 2H, $OC_2H_4CH_2CH_3$), 0.92 (t, $J_{H\text{-}H}$ = 7.02, 3H, CH_3). ^{13}C {1H} NMR (500 MHz, $CDCl_3$, 298K, δ): 135.06, 134.79, 130.25, 127.93 (Ph), 63.03 (OCH_2), 34.75 ($OCH_2CH_2C_2H_5$), 19.12 (CH_2CH_3), 17.24 (CH_3).

Table 2, Entry 2: $(CH_3)_2CHOSiHPh_2$ [1]: ^{1}H NMR (500 MHz, $CDCl_3$, 298K, δ): 7.69 (dd, $J_{H\text{-}H}$ = 7.7, $J_{H\text{-}H}$ = 1.5, 4H, *o*-Ph), 7.6-7.35 (m, 6H, *m*/*p*-Ph), 4.85 (s, 1H, Si*H*), 4.22 (sept, $J_{H\text{-}H}$ = 6.2, 1H, C*H*), 1.27 (d, $J_{H\text{-}H}$ = 6.1, 6H, CH_3). ^{13}C {1H} NMR (500 MHz, $CDCl_3$, 298K, δ): 135.18 (*o*-

Ph), 134.84 (*i*-Ph), 130.42 (*p*-Ph), 128.16 (*m*-Ph), 67.56 (O*C*H(CH_3)$_2$), 25.49 (OCH(*C*H_3)$_2$). GC/MS: t_R = 10.06 min; m/z 241(M^+), 227, 211, 199, 183, 164 (100), 149, 136, 122, 105, 91.

Table 2, Entry 3: (CH_3)$_3$CSiHPh$_2$: ^{1}H NMR (500 MHz, $CDCl_3$, 298K, δ): 7.68–7.64 (m, 4H, *Ph*), 7.46−7.40 (m, 6H, *Ph*), 5.60 (s, 1H, Si*H*), 1.38 (s, 9H, C*H$_3$*). ^{13}C {1H} NMR (500 MHz, $CDCl_3$, 298K, δ): 135.24, 134.55, 130.62, 128.15 (Ph), 65.14 (O*C*H), 1.24 (*C*H_3). GC/MS: tR = 10.06 min; m/z 241(M+), 227, 211, 199, 183, 164 (100), 149, 122, 105, 91.

Table 2, Entry 4: (OCy)HSiPh$_2$: ^{1}H NMR (500 MHz, $CDCl_3$, 298K, δ): 7.61 (dd, J_{H-H} = 7.6, J_{H-H} = 1.6, 4H, *Ph*), 7.46–7.40 (m, 6H, *Ph*), 5.48 (s, 1H, Si*H*), 3.82 (m, 1H, C*H*), 1.87−1.22 (m, 10H, C*H$_2$*). ^{13}C {1H} NMR (500 MHz, $CDCl_3$, 298K, δ): 134.83, 134.58, 130.37, 128.08 (Ph), 73.27 (O*C*H), 35.53, 25.76, 24.31 (*C*H_2). GC/MS: t_R = 11.7 min; m/z 281(M^+), 267, 253, 239, 204 (100), 199, 183, 128, 105, 77. t_R = 14.3 min; m/z 380(M^+), 303, 281, 226 (100), 214, 205, 181, 152, 105, 77.

Table 2, Entry 5 and 6: (PhCH$_2$O)$_2$SiPh$_2$: ^{1}H NMR (500 MHz, $CDCl_3$, 298K, δ): 7.75 (dd, J_{H-H} = 7.8, 1.5, 4H, *o*-SiPh$_2$), 7.45–7.40 (m, 4H, *o*-CH$_2$Ph), 7.39–7.35 (m, 4H, *m*-CH$_2$Ph), 7.34–7.29(m, 6H, *m/p*-SiPh$_2$), 7.25–7.20 (m, 2H, *p*-CH$_2$Ph), 4.85 (s, 4H, PhC*H$_2$*). ^{13}C {1H} NMR (500 MHz, $CDCl_3$, 298K, δ): 140.72 (*i*-PhCH$_2$), 135.42 (*o*-PhSi), 132.29 (*i*-PhSi), 130.6 (*p*-PhSi), 128.4 (*m*-PhCH$_2$), 128.2 (*m*-PhSi), 127.5 (*p*-PhCH$_2$), 127.5 (*o*-PhCH$_2$), 65.05 (O*C*H$_2$Ph). GC/MS: t_R = 16.7 min; m/z 396(M^+), 376, 349, 335, 318, 305, 289, 275, 259, 240, 227, 212, 199, 183, 167, 151, 134, 121, 105, 91 (100).

Table 2, Entry 8: CH$_3$OSi(OEt)$_3$: ^{1}H NMR (500 MHz, $CDCl_3$, 298K, δ): 3.87 (q, J_{H-H} = 6.96, 6H, OC*H$_2$*CH$_3$), 3.60 (s, 3H, CH$_3$), 1.25 (t, J_{H-H} = 6.96, 9H, OCH$_2$C*H$_3$*). 0.93 (t, J_{H-H} = 6.97, 3H, CH$_3$). ^{13}C {1H} NMR (500 MHz, $CDCl_3$, 298K, δ): 59.38 (O*C*H$_2$CH$_3$), 51.30 (*C*H$_3$), 18.99

(OCH_2CH_3), 18.26 (CH_3). GC/MS: t_R = 4.41 min; m/z 194 (M^+), 179 (100), 165, 149, 135, 121, 105, 93, 77.

Table 2, Entry 9: $CH_3CH_2CH_2CH_2OSi(OEt)_3$: ^1H NMR (500 MHz, $CDCl_3$, 298K, δ): 3.86 (q, J_{H-H} = 6.96, 6H, OCH_2CH_3), 3.78 (t, J_{H-H} = 6.7, 2H, $OCH_2C_3H_7$), 1.57 (m, 2H, $OCH_2CH_2C_2H_5$), 1.38 (m, 2H, $OC_2H_4CH_2CH_3$), 1.24 (t, J_{H-H} = 6.96, 9H, OCH_2CH_3). 0.93 (t, J_{H-H} = 6.99, 3H, CH_3). ^{13}C {1H} NMR (500 MHz, $CDCl_3$, 298K, δ): 63.37 ($OCH_2C_3H_7$), 59.31 (OCH_2CH_3), 34.56 ($OCH_2CH_2C_2H_5$), 18.99 (OCH_2CH_3), 18.23 ($OC_2H_4CH_2CH_3$), 13.96 (CH_3). GC/MS: t_R = 6.62 min; m/z 235(M^+), 221, 207, 193, 179, 163, 149, 135, 119, 107, 91, 79 (100), 63, 45.

Table 2, Entry 10: $(CH_3)_2CHCH_2CH_2OSi(OEt)_3$: ^1H NMR (500 MHz, $CDCl_3$, 298K, δ): 3.87 (q, 6H, J_{H-H} = 6.96, OCH_2CH_3), 3.80 (t, 2H, J_{H-H} = 6.86, $OCH_2C_4H_9$), 1.73 (m, CH), 1.48 (m, 2H, $CH_2C_3H_7$), 1.24 (t, J_{H-H} = 6.96, 6H, OCH_2CH_3), 0.90 (t, J_{H-H} = 6.8, 3H, CH_3). ^{13}C {1H} NMR (500 MHz, $CDCl_3$, 298K, δ): 62.03 ($OCH_2C_4H_9$), 59.31 (OCH_2CH_3), 41.38 ($OCH_2CH_2C_3H_7$), 24.70 (CH), 22.76 $(CH_3)_2$, 18.29 (OCH_2CH_3). GC/MS: t_R = 7.8 min; m/z 249(M^+), 234, 219, 207, 191, 174, 163 (100), 149, 135, 119, 107, 91, 79, 63

Table 2, Entry 11: $(Ph)_2CHOSi(OEt)_3$: ^1H NMR (500 MHz, $CDCl_3$, 298K, δ): 7.43 (d, J_{H-H} = 7.8, 2H, *Ph*), 7.26-7.32 (m, 8H, *Ph*), 6.00 (s, 1H, OC*H*), 3.75 (q, J_{H-H} = 6.9, 6H, OCH_2CH_3), 1.19 (t, J_{H-H} = 6.9, 9H, OCH_2CH_3). ^{13}C {1H} NMR (500 MHz, $CDCl_3$, 298K, δ): 144.20, 128.34, 127.32, 126.66 (Ph), 66.3 (OCH), 59.38 (OCH_2CH_3), 18.18 (OCH_2CH_3). GC/MS: t_R = 11.57 min; m/z 346(M^+), 331, 317, 300, 289, 281, 269, 253, 239, 224, 211, 195, 181, 167 (100), 152, 135, 119, 107, 91, 79, 63.

Table 2, Entry 12: $CH_2CHCH_2CH_2OSi(OEt)_3$: ^1H NMR (500 MHz, $CDCl_3$, 298K, δ): 5.84 (m, 2H, CH_2CH), 5.09 (m, CH) 3.82-3.86 (m, 8H, $CH_2OSi(OCH_2CH_3)_3$, 2.35 (m, 2H, $C_2H_3CH_2)_3$ 1.24 (t, J_{H-H} = 6.9, 9H, OCH_2CH_3). ^{13}C {1H} NMR (500 MHz, $CDCl_3$, 298K, δ): 135.16 (CH_2CH),

116.88 (*C*H_2CH), 63.19 (C_3H_5*C*H_2O), 59.51 (O*C*H_2CH_3), 37.03 (C_2H_3*C*H_2), 18.32 (OCH_2*C*H_3). GC/MS: t_R = 5.93 min; m/z 234(M^+), 219, 204, 193 (100), 174, 163, 148, 135, 119, 105, 91.

Table 2, Entry 13: CHCCH_2CH_2OSi(OEt)$_3$: ^{1}H NMR (500 MHz, $CDCl_3$, 298K, δ): 3.82–3.88 (m, 8H, C*H*$_2$OSi(OC*H*$_2CH_3$), 2.49 (m, 2H, C_2HC*H*$_2$), 1.98 (m, C*H*), 1.24 (t, J_{H-H} = 6.9, 9H, OCH_2C*H*$_3$). ^{13}C {1H} NMR (500 MHz, $CDCl_3$, 298K, δ): 81.15 (CH_2*C*H), 69.66 (*C*H_2CH), 63.19 (C_3H_5*C*H_2O), 59.51 (O*C*H_2CH_3), 37.03 (C_2H_3*C*H_2), 18.32 (OCH_2*C*H_3). GC/MS: t_R = 6.13 min; m/z 231 (M^+), 217, 193 (100), 163, 149, 135, 119, 107, 91.

Table 2, Entry 14: PhCHCHCH_2OSi(OEt)$_3$: ^{1}H NMR (500 MHz, $CDCl_3$, 298K, δ): 7.3–7.4 (m, 5H, *Ph*), 6.66 (m, 1H, PhC*H)*, 6.37 (m, 1H, C*H*CH_2), 4.53 (m,2H, C*H*$_2$OSi(OEt), 3.93–3.91, (m, 6H, OC*H*$_2CH_3$), 1.29-1.27 (m, 6H, OCH_2C*H*$_3$). ^{13}C {1H} NMR (500 MHz, $CDCl_3$, 298K, δ): 81.15 (CH_2*C*H), 69.66 (*C*H_2CH), 63.19 (C_3H_5*C*H_2O), 59.51 (O*C*H_2CH_3), 37.03 (C_2H_3*C*H_2), 18.32 (OCH_2*C*H_3). GC/MS: t_R = 10.62 min; m/z 296(M^+), 281, 267, 252, 237, 223, 208, 193, 177, 163, 149, 135, 115 (100), 97, 79

Table 2, Entry 15: CH_3(CO)$CH_2CH_2CH_2$OSi(OEt)$_3$: ^{1}H NMR (500 MHz, $CDCl_3$, 298K, δ): 3.85 (q, J_{H-H} =6.99, 6H, OC*H*$_2CH_3$), 3.79 (t, J_{H-H} = 6.13, 2H, OC*H*$_2$), 2.56 (t, J_{H-H} = 7.3, 2H, OCH_2CH_2C*H*$_2$), 2.16 (s, 3H, C*H*$_3$), 1.85 (p, J_{H-H} = 6.72, 2H, OCH_2C*H*$_2$), 1.24 (m, 9H, OCH_2C*H*$_3$). ^{13}C {1H} NMR (500 MHz, $CDCl_3$, 298K, δ): 208.9 (*CO*), 62.57, (O*C*H_2), 59.31, (O*C*H_2CH_3), 39.98 (*C*H_3), 30.25 (OCH_2CH_2*C*H_2), 26.45 (OCH_2*C*H_2), 18.32 (OCH_2*C*H_3). GC/MS: t_R = 7.77 min; m/z 264 (M^+) is not observed, 249, 234, 219, 207, 191, 175, 163 (100), 149, 135, 119, 107, 91.

Table 2, Entry 16: (C_6H_9)CH_2OSi(OEt)$_3$: ^{1}H NMR (500 MHz, $CDCl_3$, 298K, δ): 5.72–5.77 (m, 1H, C*H*=CH), 5.59–5.64 (m, 1H, CH=C*H*), 3.85 (q, J_{H-H} = 6.8, 6H, OC*H*$_2CH_3$), 3.65 (b, 2H,

C*H*$_2$OH), 2.34–2.36 (m, 1H, C(3)*H*), 1.98–2.01 (m, 2H, C(4)*H*$_2$), 1.71–1.79 (m, 2H, C(5)*H*$_2$), 1.54 (b, 2H, C(6)*H*$_2$), 1.25 (t, J_{H-H} = 5.7, 9H, OCH$_2$C*H*$_3$).

Table 2, Entry 17: PhOSi(OEt)$_3$: ^{1}H NMR (500 MHz, CDCl$_3$, 298K, δ): 7.45 (m, 1H, *o*-Ph), 7.18–7.12 (m, 2H, *p*-Ph), 6.92 (m, 2H, *m*-Ph), 3.91 (q, J_{H-H} =6.96, 6H, OC*H*$_2$CH$_3$), 1.24 (t, J_{H-H} = 6.96, 9H, C*H*$_3$). ^{13}C {1H} NMR (500 MHz, CDCl$_3$, 298K, δ): 153.93 (*i*-Ph), 129.63, (*m*-Ph), 122.19, (*p*-Ph), 119.52 (*o*-Ph), 59.89 (O*C*H$_2$CH$_3$), 18.21 (OCH$_2$*C*H$_3$). GC/MS: t_R = 8.43 min; m/z 256(M$^+$) (100), 241, 228, 211, 197, 181, 167, 155, 137, 119, 107, 94, 79, 63, 45.

Table 2, Entry 18: *p*-MeOPhOSi(OEt)$_3$: ^{1}H NMR (500 MHz, CDCl$_3$, 298K, δ): 6.95–6.75 (m, 4H, Ph), 3.86 (m, 6H, O-C*H*$_2$), 3.77 (s, 3H, OC*H*$_3$), 1.24 (m, 9H, O-CH$_2$C*H*$_3$). ^{13}C {1H} NMR (500 MHz, CDCl$_3$, 298K, δ): 155-146 (2 Ar-C, *p*& *i*-Ph), 121.2–114.3 (2 Ar-C, *o* & *m*-Ph), 59.84 (O-*C*H$_2$CH$_3$), 55.85 (O*C*H$_3$), 18.24 (O-CH$_2$*C*H$_3$). GC/MS: t_R = 9.87 min; m/z 286(M$^+$), 271, 258, 242, 227, 215, 197, 185, 163 (100), 151, 135, 119, 108, 91, 79.

Table 2, Entry 19: *p*-^{t}BuPhOSi(OEt)$_3$: ^{1}H NMR (500 MHz, CDCl$_3$, 298K, δ): 7.25–6.58 (m, 4H, Ph), 3.96-3.92 (m, 6H, O-C*H*$_2$), 1.31 (s, 3H, ^{t}Bu), 1.23 (t, 9H, O-CH$_2$C*H*$_3$). ^{13}C {1H} NMR (500 MHz, CDCl$_3$, 298K, δ): 153.8 (*i*-Ph), 144.2 (*p*-Ph), 127.5–118.6 (2 Ar-C, *m*&*o*-Ph), 59.8 (O-*C*H$_2$CH$_3$), 34.27 (4° *C*), 31.68 (^{t}Bu), 18.2 (O-CH$_2$*C*H$_3$). GC/MS: t_R = 9.6 min; m/z 312 (M$^+$), 297(100), 281, 267, 253, 241, 223, 209, 194, 177, 155, 107, 91.

Table 2, Entry 20: *p*-NO$_2$PhOSi(OEt)$_3$: ^{1}H NMR (500 MHz, CDCl$_3$, 298K, δ): 8.18 (m, 2H, *m*-Ph), 6.94 (m, 2H, *o*-Ph), 3.89-3.87 (m,6H, O-C*H*$_2$), 1.25–1.22 (m, 9H, O-CH$_2$C*H*$_3$). ^{13}C {1H} NMR (500 MHz, CDCl$_3$, 298K, δ): 161.8 (*i*-Ph), 141.72 (*p*-Ph), 126.8 (*m*-Ph), 115.9 (*o*-Ph), 59.69 (O-*C*H$_2$CH$_3$), 18.02 (O-CH$_2$*C*H$_3$).

Table 2, Entry 21: *p*-ClPhOSi(OEt)$_3$: ^{1}H NMR (500 MHz, CDCl$_3$, 298K, δ): 7.21 (m, 2H, *m*-Ph), 6.96 (m, 2H, *o*-Ph), 3.94-3.91 (m, 6H, O-C*H*$_2$), 1.27–1.23 (t, 9H, O-CH$_2$C*H*$_3$). ^{13}C {1H} NMR

(500 MHz, $CDCl_3$, 298K, δ): 152.6 (*i*-Ph), 129.6 (*m*-Ph), 127.12 (*p*-Ph), 59.95 (O-*C*H_2CH_3), 18.24 (O-CH_2*C*H_3). GC/MS: t_R = 9.55 min; m/z 290 (M^+), 275, 262, 245, 230, 218, 202, 188, 174, 163, 147, 135, 119, 97, 79 (100).

Table 3, Entry 1: $(OEt)_3SiOCH_2CH_2CH_2CH_2OSi(OEt)_3$: ^{1}H NMR (500 MHz, $CDCl_3$, 298K, δ): 3.89–3.85 (m, 10H, $(CH_3CH_2O)_3SiOCH_2C_2H_4CH_2OSi(OCH_2CH_3)_3$, 1.64 (m, 4H, CH_2CH_2), 1.24 (m, 9H, OCH_2CH_3. ^{13}C {1H} NMR (500 MHz, $CDCl_3$, 298K, δ): 63.57 $(-C_3H_6CH_2OSi),)_3$, 59.70 (OCH_2CH_3), 28.9 $(CH_2CH)_3$, 18.51 (OCH_2CH_3).

Table 3, Entry 2: 1,3-Dioxa-2,2-diphenyl-2-silacycloheptane: ^{1}H NMR (500 MHz, $CDCl_3$, 298K, δ): 7.74 (m, 4H, *Ph*), 7.3–7.47 (m, 6H, *Ph*), 4.07 (m, 4H, CH_2CH_2OSi), 1.89 (d, 4H, CH_2OSi). ^{13}C {1H} NMR (500 MHz, $CDCl_3$, 298K, δ): 134.89, 133.41, 130.53, 128.12 (*Ph*). GC/MS: t_R = 11.4 min; m/z 270 (M^+), 192(100), 181, 114, 91, 77.

Table 3, Entry 3: 4,4,5,5-tetramethyl-2,2-diphenyl-1,3-dioxa-2-silacyclopentane: ^{1}H NMR (500 MHz, $CDCl_3$, 298K, δ): 7.67-7.64 (m, *m*, 4H, Ph), 7.44-7.38 (m, *p*, *o*, 6H, Ph), 1.33 (s, 12H, CH_3). ^{13}C {1H} NMR (500 MHz, $CDCl_3$, 298K, δ): 134.8 (*o*-Ph), 133.6 (*i*-Ph), 130.5 (*p*-Ph), 127.7 (*m*-Ph), 82.25 (*C*), 25.82 (CH_3). GC/MS: t_R = 11.07 min; m/z 298 (M^+), 283, 268, 253, 240, 225, 181(100), 123, 105, 77.

Table 3, Entry 4: 2,4,4,5,5-pentamethyl-2-phenyl-1,3-dioxa-2-silacyclopentane: ^{1}H NMR (500 MHz, $CDCl_3$, 298K, δ): 7.66 (m, *o*, 2H, *Ph*), 7.41-7.37 (m, *m*, *p*, 3H, *Ph*), 1.33 (s, 6H, CMe_2), 1.25 (s, 6H, CMe_2), 0.5 (s, $SiCH_3$). ^{13}C {1H} NMR (500 MHz, $CDCl_3$, 298K, δ): 135.66 (*i*-Ph), 133.7 (*o*-Ph), 130.42 (*m*-Ph), 128.08 (*p*-Ph), 82.01 (*C*), 25.96 (CH_3), 0.5 ($SiCH_3$).

Table 4, Entry 1: $PhCOOSi(OEt)_3$: ^{1}H NMR (500 MHz, $CDCl_3$, 298K, δ): 8.13–8.09 (m, 2H, *Ph*), 7.56-7.50 (m, 3H, *Ph*), 3.89-3.85 (m, 6H, O-CH_2), 1.29–1.25 (t, 9H, O-CH_2CH_3). ^{13}C {1H}

NMR (500 MHz, $CDCl_3$, 298K, δ): 165.5 (*C*O), 133.6, 130.9, 130. 5, 128.5 (*Ph*), 59.3 (O-*C*H_2CH_3), 18.16 (O-CH_2*C*H_3).

Table 4 Entry 2: C_2H_4(Ph)COOSi(OEt)$_3$: ^{1}H NMR (500 MHz, $CDCl_3$, 298K, δ): 7.35–7.3 (*m*, 2H, *Ph*), 7.26–7.22 (m, 3H, *Ph*), 3.85-3.82 (m, 6H, O-C*H*$_2$), 1.53-1.51 (m, 3H, C*H*$_3$), 1.25–1.22 (m, 9H, O-CH_2C*H*$_3$). ^{13}C {1H} NMR (500 MHz, $CDCl_3$, 298K, δ): 195 (*C*O), 135.5, 129.8, 129.2, 127.6 (*Ph*), 59.95 (O-*C*H_2CH_3), 43.5 (CH), 18.24 (O-CH_2*C*H_3), 18.1 (*C*H_3). GC/MS: t_R = 7.37 min; m/z 297 [M-CH_3]$^+$, 283, 269, 253, 225, 209, 150, 105 (100), 91, 77.

Table 4 Entry 3: C_2H_5COOSi(OEt)$_3$: ^{1}H NMR (500 MHz, $CDCl_3$, 298K, δ): ^{1}H NMR (500 MHz, $CDCl_3$, 298K, δ): 3.84–3.87 (m,6H, O-C*H*$_2$), 2.29 (q, 2H, C*H*$_2$), 1.21 (m, 9H, O-CH_2C*H*$_3$), 1.06 (t, 3H, C*H*$_3$). ^{13}C {1H} NMR (500 MHz, $CDCl_3$, 298K, δ): 173.5 (*C*O), 59.29 (O-*C*H_2CH_3), 28.91 (*C*H_2) 18.24 (O-CH_2*C*H_3), 9.3 (*C*H_3). GC/MS: t_R = 6.05 min; m/z 236 (M^+), 191, 163, 135, 119, 107, 91, 79 (100).

CHAPTER 3

VERSATILE MANGANESE CATALYSIS FOR THE SYNTHESIS OF POLYSILYLETHERS FROM DIOLS AND DICARBONYLS WITH HYDROSILANES

3.1. Introduction

Polymers with silicon in the main chain have received much attention in organic and material chemistry due to their various industrial and academic applications.[124,125,126,127] Polysilanes with Si-Si repeating units are promising in electronic devices because of their conductivity.[128] Poly(siloxane)s with Si-O-Si linkages and their copolymers are used extensively as elastomers, plastics and in other industrial applications because of their low temperature flexibility and high temperature stability.[129,130,131,132,133,134] Hydro-sensitive silicon polymers can be employed in medical applications such as controlled release of drugs.[135] Poly(siloxane)s are precursors for the synthesis of silicon oxy carbides (SiOC) via pyrolysis and direct photo-crosslinking methods.[136,137] The SiOC ceramic has been applied in coatings and as electrode materials in lithium batteries.[138,139,140,141,142,143] Recently there has been renewed interest in silicon-containing polymers, particularly poly(silylether)s with Si-O-C linkages, on account of their potential sustainability.[67,144] Silicon and oxygen are practically inexhaustible due to their abundance and carbon can be more readily sourced from biomass. The Si-O-C linkages are hydrolytically degradable, different from the typical biodegradable ester linkages that require enzymes for degradation. This makes the poly(silylether)-based materials particularly attractive in short-term and/or single use applications.[145] Importantly, the degradation behavior, along with the

thermomechanical properties, can be adjusted by changing substituent groups on silicon and/or carbon backbones of poly(silylether)s, and by copolymerization with other segments.[146]

Synthetically poly(silylether)s have been prepared by various methods depending on the nature of the actual linkages. Similar to the synthesis of silylethers, reaction of dichlorosilanes with diols through polycondensation leads to formation of poly(silylether)s.[147,148,149,150,151,152,153] Chlorosilanes can also react with bis(epoxide)s and bis(oxetane)s through additions catalyzed by quaternary onium salts to afford poly(silylether)s.[154,155,156,157] However, use of chlorosilanes has limitations.[158] Chlorosilanes are moisture sensitive and usually produce hydrogen chloride and other unwanted byproducts in polymerization reactions that require additional methods for separation. To overcome these problems, chlorosilanes have been replaced with diamino- and dialkoxysilanes as the coupling partners; in particular, diphenoxy- and dianilinosilanes have shown good activity towards the synthesis of high molecular weight polymers.[134,159] Still these methods may have limited substrate scope or require maintaining the high temperature conditions (200-300 °C) throughout the reaction.[134,160,161,162]

Alternatively, hydrosilanes have been deemed as optimal replacements for chlorosilanes because of their stability to air and ease of handling. Reactions with diols through dehydrogenative coupling [163] and with dicarbonyls through hydrosilylation polymerization[164,165,166] afford a variety of poly(silylether)s (Scheme 4). Notably, these methods are highly atom economical, producing H_2 as the sole byproduct or no byproduct. In general, these reactions are effected by catalysts derived from precious transition metals, usually ruthenium, palladium, and rhodium.[167,168,169] However, the high cost, low abundance of such metals and high catalyst loading (up to 10 mol %) are the main drawbacks of these methods. Other catalysts based on boranes[170] and alkali metals[171]

are also known. Recently the catalytic systems derived from inexpensive, earth abundant metals such as iron have been reported.[172]

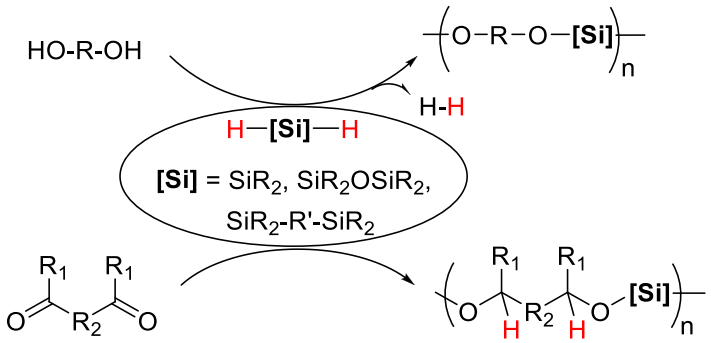

Scheme 4. Poly(silylether)s from hydrosilanes.

We have investigated the high-valent transition metal complexes for their roles in catalytic reductions and silane activation.[173,174] It is found that an air-stable and easily prepared salen-manganese complex [MnN(salen-3,5-^{t}Bu$_2$)] (**Mn-1**) is an effective catalyst for hydrosilylation of carbonyl compounds and dehydrogenative coupling of hydroxyl compounds with hydrosilanes.[81,175] Encouraged by these results and in connection with our interests in biodegradable materials,[176,177,178] we sought to synthesize poly(silylether)s from a variety of diols and dicarbonyls under manganese catalysis. Furthermore, taking advantage of the dual activity of **Mn-1**, we have employed substrates with mixed functional groups in the reaction with hydrosilanes to generate poly(silylether)s. As far as we are aware, no metal catalyst has been reported that could catalyze the synthesis of poly(silylether)s from three types of substrates (diols, dicarbonyls and hydroxyl carbonyl) with hydrosilanes.

3.2 Results and discussion

3.2.1. Optimization reactions

Our initial experiments started with optimizing suitable reaction conditions for the polycondensation of diols and hydrosilanes. 1,4-Benzenedimethanol and diphenylsilane were chosen as the representative coupling partarners in the presence of catalytic amount of manganese complex **1** (1 mol%), and selected results are presented in Table 5. According to the conditions in our previous work,[81] the reaction was performed using acetonitrile as the solvent at reflux temperature (entry 1). As expected, the initial green color of the reaction mixture arising from **Mn-1** turned brown and then yellow, indicating onset of the reaction. After 12 h, ^{1}H NMR spectroscopy showed greater than 95% conversion of diphenylsilane. Despite the high conversion, however, the number average molecular weight (M_n) of the polymer was determined by GPC as 4000 g/mol (M_w/M_n 1.28). In order to improve M_n, several solvents were next screened. When acetonitrile was replaced by tetrahydrofuran (THF) (entry 2), low M_n (1900 g/mol) polymers were obtained with only 50 % conversion of diphenylsilane in 12 h. Use of 1,4-dioxane as solvent resulted in 95 % conversion and higher molecular weight (M_n 7900 g/mol) (entry 3), suggesting that the coordination ability of cyclic ethers might not be the main culprit for the low conversion observed with THF. Reaction in refluxing toluene led to even higher M_n (9200 g/mol) within 12 h (entry 4). Given the above observations, it seemed that the reaction temperature played a key role in the polymerization reaction. In agreement with this, reaction performed at ambient temperature in toluene showed no reaction even after 48 h, and the green color remained the same during the period (entry 5). However, attempts at achieving high molecular weights by using high boiling aromatic solvents such as xylenes and mesitylene met with limited success (entries 6 & 7). Though the molecular weights obtained under refluxing condtions were decent, they were lower than that

in toluene. Finally, as air exclusion seemed to have little effect in our previous dehydrogenative coupling,[175] a reaction was performed under air in refluxing toluene for convenience (entry 8). However, conversion of monomers remained low (58%) even after extending the reaction time to 48 h, and M_n also dropped approximately by half (4500 g/mol). These results suggested the importance of inert conditions for the generation of high molecular weight polymers.

Table 5. Dehydrogenative coupling of 1,4-benzenedimethanol with diphenylsilane[a]

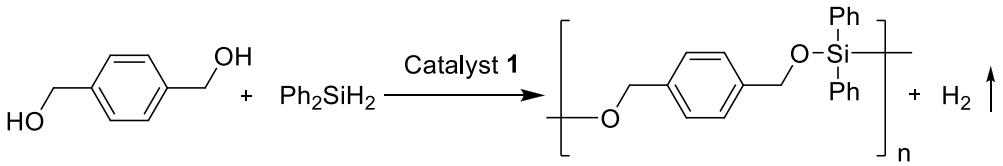

Entry	Solvent[b]	Temp	Condition	t (h)	Conv%	M_n (g/mol)[c]	M_w/M_n[c]
1	CD_3CN	reflux (81°C)	under N_2	12	> 95	4000	1.28
2	THF	reflux (66°C)	under N_2	12	50	1900	1.36
3[d]	1,4-Dioxane	reflux (101°C)	under N_2	20	> 95	7900	1.57
4[e]	Toluene	reflux (110°C)	under N_2	12	> 95	9200	1.66
5	Toluene	25°C	under N_2	48	0	-	-
6[f]	Xylenes	reflux (143°C)	under N_2	12	> 95	6000	1.14
7	Mesitylene	reflux (165°C)	under N_2	12	> 95	7200	1.23
8	Toluene	reflux (110°C)	under air	48	58	4500	1.15

[a]Reaction conditions: substrate (0.8–0.9 mmol), silane (1.0 equiv) and Mn catalyst **1** (1.0 mol%). [b]solvent used was 2.4-2.8 ml. [c]Determined by GPC calibrated with polystyrene standard. [d]Isolated yield 75.9 %. [e]Isolated yield 75.6 %. [f]Isolated yield 70 %.

The brown-colored reaction mixtures from entries 3 and 4 were purified by precipitation. The resulting whitish gray poly(silylether)s were obtained in 75.9 and 75.6 % yields, respectively.

In the ^{1}H NMR spectrum, the disappearances of hydroxyl groups at 2.0 ppm and silane hydrogens at 4.84 ppm, and the shift of benzylic protons from 4.65 to 4.81 ppm suggested the formation of poly(silylether) of 1,4-benzenedimethanol and diphenylsilane (Figure 17). ^{13}C NMR spectrum also supported the formation of poly(silylether), as only six peaks in aromatic region (129.71-139.47 ppm, four from silane and two from diol) and one peak at 64.98 ppm (benzylic carbon) were observed (Figure 18). In addition, the absence of both hydroxyl (3500 cm^{-1}) and SiH groups (2133 cm^{-1}) in the ATR FT-IR spectrum further supported the NMR assignments (Figure 19). The characteristic stretching frequencies at ~1040 cm^{-1} indicated the formation of Si-O-C connections.

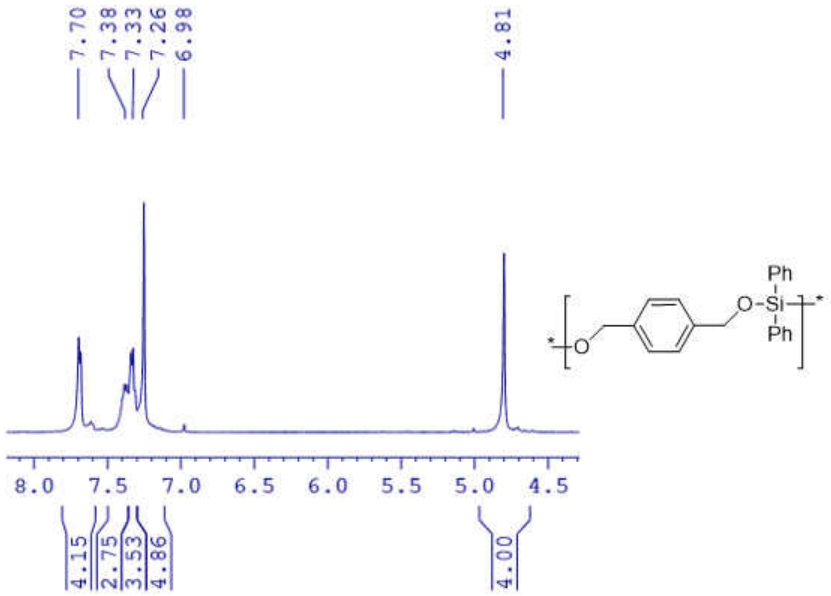

Figure 17. ^{1}H NMR of the poly(silylether) from 1,4-benzenedimethanol and diphenylsilane.

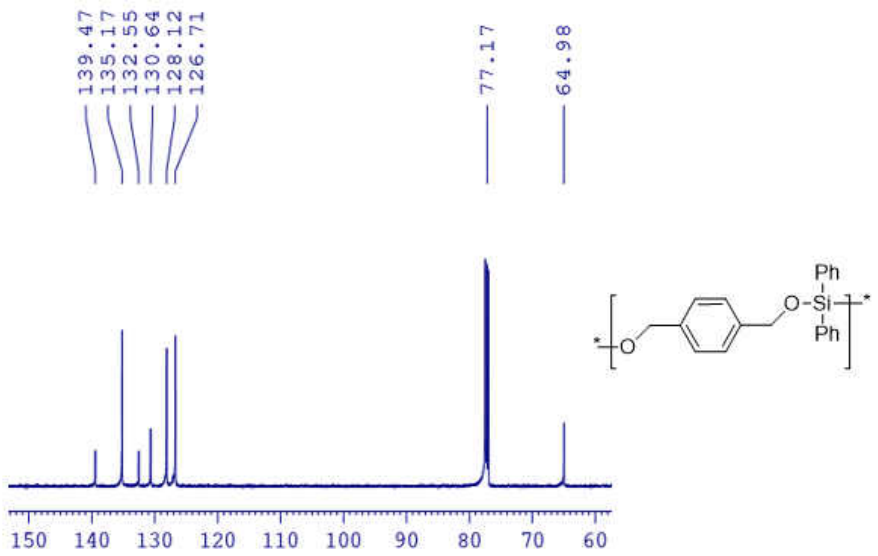

Figure 18. ^{13}C NMR of the poly(silylether) from 1,4-benzenedimethanol and diphenylsilane.

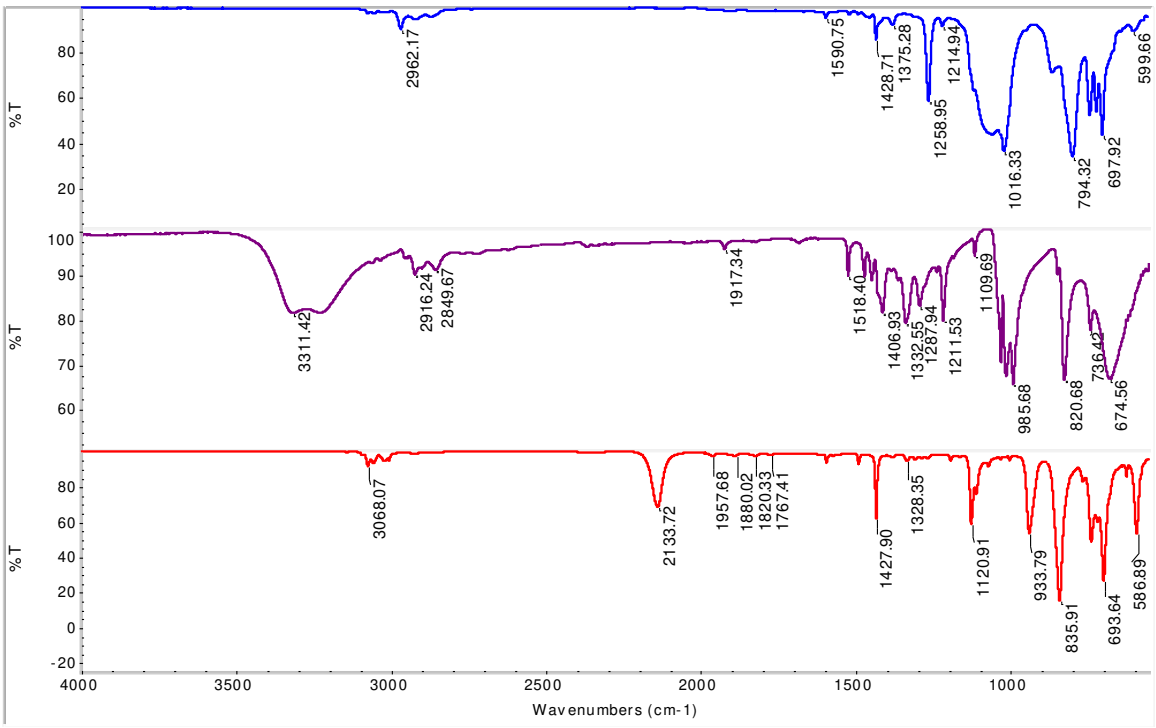

Figure 19. ATR FT-IR spectra of diphenylsilane (bottom), 1,4-benzenedimethanol (middle), and their poly(silylether) (top).

3.2.2. Step-growth polymerization

To learn more about the polymerization, we performed a set of reactions between 1,4-benzenedimethanol and diphenylsilane to explore the correlation between conversion, time and molecular weight of the polymer. During the reaction, samples were taken at each time interval and then were subjected to analysis by NMR and GPC. Conversion of diol was 19 % in 1 h and reached around 50 % in 4 h. However, at this point, the molecular weight of the polymer was only 1600 g/mol (M_w/M_n 1.33), indicating mostly oligomers were formed in the starting hours. At 8 h, the conversion increased to 91% with M_n 4600 g/mol, and at 22 h, the conversion was 96 % with 13000 g/mol. The sharp increase in the molecular weight in the later stage of the reaction suggested that the oligomers formed in the initial reaction time were still active and were later incorporated to form long chain polymers. The growth behavior in molecular weight (Figure 20) is typical of step-growth polymerization reactions.[179] The similar non-linear growth of the dispersities (M_w/M_n) also supported that these are step-growth type polymerization reactions.

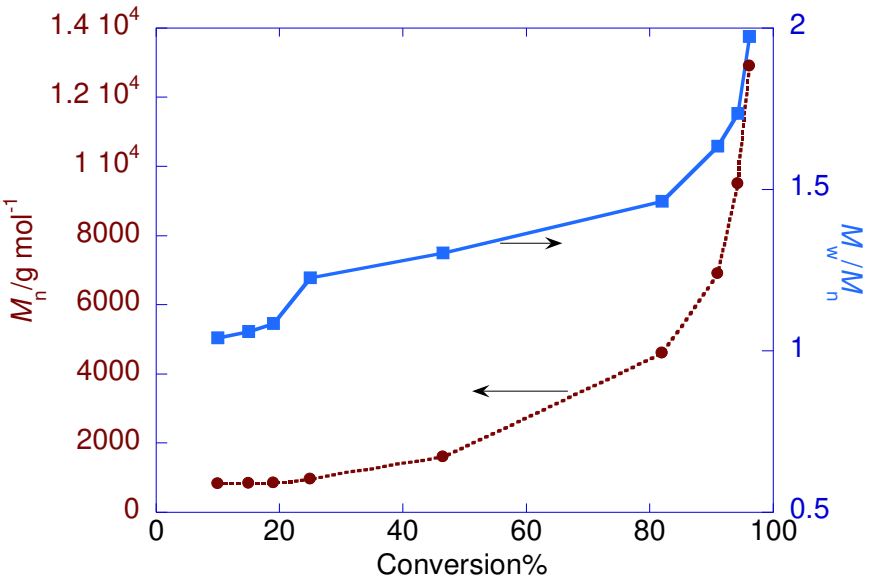

Figure 20. Plot of number average molecular weight (M_n, ●) and dispersity (M_w/M_n, ■) vs conversion

3.2.3. Substrate scope: Diols

To extend the substrate scope, we first chose a simple aryldiol 1,4-benzenediol (1,4-hydroquinone), because polymers with π-conjugated groups in the main or side chains are of interest for their prospective applications as electronic, photoic and ceramic materials (Table 6, entry 2).[180,181,182] Copolymerization reaction between 1,4-benzenediol and a disiloxane (1,3-bis(diethylamino)tetramethyldisiloxane) at melt conditions was reported in the literature, however the repoted molecular weight of the polymer was low (M_n 3600 g/mol).[148] In our current dehydrogenative coupling process between 1,4-benzenediol and diphenylsilane, >95% conversion of silane was observed in 12 h, and a white solid was obtained in 70% yield after purfication. The disappearence of hydroxyl and silicon hydrogen peaks in both ^{1}H NMR and FT-IR spectroscopies confimed the formation of the desired poly(silylether). In ^{29}Si NMR, a single peak at -37.42 ppm was observed. GPC analysis showed high molecular weight polymer with M_n 15000 g/mol (M_w/M_n 2.38). To expand on aryl diols, a dehydrogenative coupling reaction between a highly π-conjugated 4,4'-biphenol and diphenylsilane was performed (entry 3) under same conditions. The conversion reached 95% in 15 h and a whitish-gray polymer was obtained in 88.1 % yield after purification. However, the molecular weight obtained was somewhat lower, M_n = 7200 g/mol (M_w/M_n 1.87).

Table 6. Dehydrogenative coupling of symmetrical diols with hydrosilanes[a]

Entry	PSE	Diols	t (h)	M_n (g/mol)[b]	M_w/M_n[b]	Yield %[c]	T_g[d]
1	PSE 1	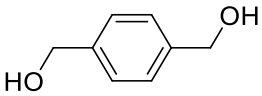	12	9200	1.66	76	22
2	PSE 2	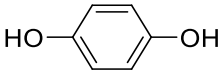	12	15000	2.38	70	-
3	PSE 3	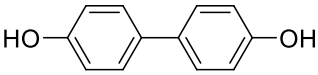	15	7200	1.87	88	101
4	PSE 4	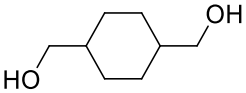	20	5100	1.41	62	38
5	PSE 5	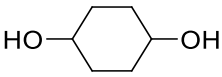	20	3100	1.73	70	60
6	PSE 6	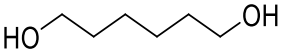	26	11400	2.00	84	-

[a]Reaction conditions: substrate (0.8–0.9 mmol), silane (1.0 equiv) and catalyst (1.0 mol%). The reactions were carried out in refluxing toluene under N_2 and the conversions of silane were greater than 95%. [b]Determined by GPC calibrated with polystyrene standard. [c]Isolated yield. [d]Determined by DSC in the second heating cycle.

Next, we carried out polycondensation reactions with aliphatic diols, namely 1,4-cyclohexanedimethanol and 1,4-cyclohexanediol (Table 6, entries 4 and 5). These two substrates can be viewed as the aliphatic analogs of 1,4-benzenedimethanol and 1,4-benzenediol respectively. Reaction between the primary diol 1,4-cyclohexanedimethanol and diphenylsilane was monitored up to 24 h, by which time silane conversion of 95 % was achieved. Purification afforded the corresponding poly(silylether) with 62 % isolated yield, and the observed M_n was 5100 g/mol (M_w/M_n 1.4). Reaction with a bulkier secondary diol 1,4-cyclohexanediol required longer reaction time, as only 80 % conversion was achieved after 20 h, although the isolated yield was good (70 %). Given the slow conversion, it was not surprising that the molecular weight of the resulting

polymer was rather low, M_n = 3100 g/mol ((M_w/M_n 1.73). In agreement with the low molecular weight, small peaks at around 5.3-5.4 ppm were observed in the ^{1}H NMR spectrum, which could be attributed to the tertiary Si-H end group in the polymer. Our previous results showed that diphenylsilane reacted with secondary alcohols in a two-step process but the second step was considerably slower than the first step.[81] Similarly here the steric hindrance plays a vital role in these two polycondensation reactions as reflected in the extended reaction times and low molecular weights of the polymers.

Conversely, when a sterically less hindered linear monomer 1,6-hexanediol was used as the substrate, a high molecular weight polymer, M_n = 11400 g/mol, was produced in high yields (84 %) (Table 6, entry 6). These results suggest that sterically less hindered monomers react readily to give the high molecular weight polymers. On the other hand, when another diol 1,4-butanediol was used, cyclic silylether was obtained as the main product instead of poly(silylether)s.[175,183] Obviously a rigid and/or long linker between the two hydroxyl groups of diols is desirable for the formation of poly(silylether)s.

3.2.4. Substrate scope: Dicarbonyls

Considering our previous results that the manganese complex **Mn-1** is also an efficient catalyst for the hydrosilylation of aldehydes and ketones,[81] we decided to apply the current system to dicarbonyl compounds for the synthesis of poly(silylether)s. In this study, benzene-1,4-dicarboxaldehyde (terephthalaldehyde) was chosen as the reaction partner with diphenylsilane, in part because the resulting polymer should be same as the polymer obtained from 1,4-benzenedimethanol (Table 6, entry 1 *vs* Table 7, entry 1). Under the optimized conditions, the consumption of terephthalaldehyde and the hydrosilylation of the carbonyl group were confirmed by the appearance of benzylic signals at 4.81 ppm in ^{1}H NMR and 65.0 ppm in ^{13}C NMR. The

conversion of terephthalaldehyde reached 90% in 24 h, and workup by precipitation gave 58% isolated yield of a polymer. The FT-IR spectrum of the polymer showed the disappearance of C=O stretching frequency at 1663 cm^{-1} and of silane hydrogens at 2134 cm^{-1} and a single peak at -30.3 was observed in ^{29}Si NMR. These spectroscopic data are essentially same as the data resulting from 1,4-benzenedimethanol. The main difference is that the molecular weight was low, $M_n = 2400$ g/mol (M_w/M_n 1.86). The low molecular weight is supposed to come from the less active nature of carbonyls in comparison with the hydroxyl groups in the reaction. The monitoring of the reaction profile of terephthalaldehyde and 1,4-benzenedimethanol under same conditions confirms the faster reaction of diol. This difference in reactivity with hydrosilanes has been observed in other systems and is attributed to the stronger nucleophilicity of hydroxyls over carbonyls (see below).[184] To further compare the activity of dicarbonyl monomers with diols, reactions were performed with 1,6-hexanedial[185] and 1,4-cyclohexanedione, the analogous structures of 1,6-hexanediol and 1,4-cyclohexane diol respectively (Table 7, entries 2 and 3). As expected, reaction with 1,6-hexanedial took 24 h to reach 90% conversion and the isolated yield was only 40%; it took even longer (48 h) for 1,4-cyclohexanedione to reach 90% conversion with a slightly higher isolated yield (49%). Both reactions resulted in low molecular weight polymers, M_n = 1800 and 2100 g/mol, respectively, consistent with the slow rate of reaction. The low yields in these reactions, despite of the >90% conversion, might be a result of the increased presence of short chain oligomers in these reactions that were lost during the precipitation process.

Table 7. Poly(silylethers) of dicarbonyls, hydroxy carbonyls and unsymmetrical diols.[a]

Entry	PSE	Substrate	t (h)	M_n (g/mol)[b]	M_w/M_n[b]	Yield %[c]	T_g[d]
1	PSE 7	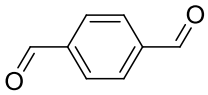	24	2400	1.88	58	20
2	PSE 8	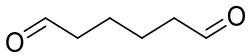	24	1800	1.59	40	-
3	PSE 9	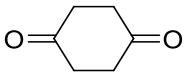	48	2100	1.73	49	51
4	PSE 10	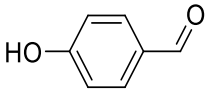	18	3800	1.77	69	18
5	PSE 11	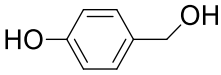	24	4500	1.93	73	25
6	PSE 12	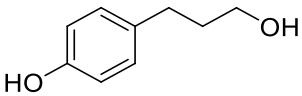	19	9000	1.59	80	21

[a]Reaction conditions: substrate (0.8–0.9 mmol), silane (1.0 equiv) and catalyst (1.0 mol%). [b]Determined by GPC calibrated with polystyrene standard. [c]Isolated yield. [d]Determined by DSC in the second heating cycle

3.2.5. Substrates with mixed functional groups

So far all of the substrates used are structurally symmetrical with two identical functional groups. Encouraged by the results that poly(silylether)s can be prepared from both diols and dicarbonyls using the same manganese catalyst, we sought to employ substrates with unsymmetrical, mixed functional groups to further extend the substrate scope. Thus, *p*-hydroxybenzaldehyde was selected as a monomer to react with diphenylsilane (Table 7, entry 4). Though the reaction time (18 h) required to reach 90% conversion of silane was less than the three reactions in entries 1-3, the isolated yield and the molecular weight (M_n = 3800 g/mol, M_w/M_n 1.73) were greater than those reactions. Relatively speaking, these values fall right in between those

obtained from 1,4-benzenediol and terephthalaldehyde in line with the difference in their respective reactivities toward polymerization reactions under manganese catalysis. As this substrate *p*-hydroxybenzaldehyde has two different termini, it can form polymers with different connectivities, which was supported by the presence of multiple peaks for the benzylic signals in both the ^{1}H and ^{13}C NMR spectra. These observations were consistent with the ^{29}Si NMR spectrum, in which three peaks at -37.1, -33.5, and -30.1 ppm were observed, as predicted from the three different silicon environments resulting from the head-to-head, head-to-tail, and tail-to-tail connections (Figure 21).

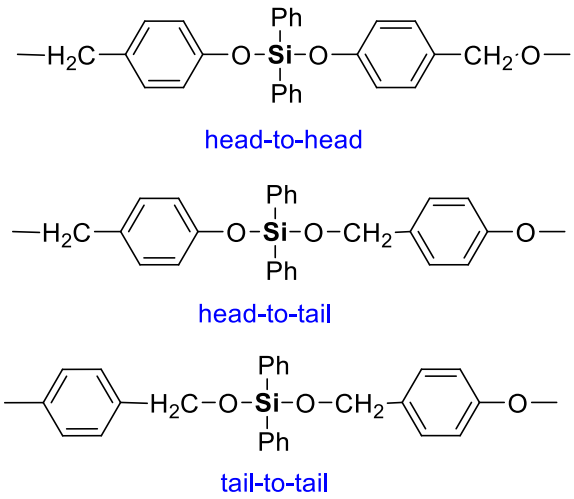

Figure 21. Three silicon centers in the poly(silylether) backbone

Similarly, reaction of *p*-hydroxybenzyl alcohol with diphenylsilane (Table 7, entry 5) yielded a polymer with slightly higher molecular weight (M_n = 4500 g/mol) that features three ^{29}Si NMR signals, as expected. It should be noted that the relative intensity of the three peaks are somewhat different from the result obtained with *p*-hydroxybenzaldehyde. Reaction with another unsymmetrical monomer 3-(4-hydroxyphenyl)-1-propanol gave comparable results (Table 7, entry 6): more than 95 % conversion and 80 % isolated yield were achieved in 19 h. The molecular weight (M_n = 9000 g/mol) was high when compared with polymers from dicarbonyls and hydroxyl

carbonyl. Again, three distinct peaks appeared in the ^{29}Si NMR, in agreement with the formation of three different types of connectivity. The high yield and M_n constitute additional evidence that hydroxyl compounds are faster than carbonyls in the polymerization reactions.

From these results and early studies, a plausible mechanism can be proposed for the manganese catalyzed polymerization of diols and dicarbonyls (Scheme 5). The high valent Mn(V) complex, **Mn-1**, is first reduced by diphenylsilane to a low valent Mn(II) or Mn(III) species, [186] which correlates with the color changes during the early stage of the reaction. The reduction of Mn(V) is not unexpected given the oxidizing power of high valent first-row transition metals. Hydrosilane is then activated by coordination with the metal center via either an η^1- or η^2-SiH adduct,[187] which may serve as a common intermediate for hydrosilylation and dehydrogenative cross coupling. Although not directly observed in the present system, such adducts with low valent manganese are well-documented in the literature.[188,189] Nucleophilic attack of hydroxyl or carbonyl groups on the silicon furnishes the Si-O bonds, accompanied by the hetereolytic cleavage of the Si-H bonds. The observation that diols are more active with hydrosilanes than dicarbonyls is in agreement with the stronger nucleophilicity of hydroxyls over carbonyls.[184] It should be mentioned that the oxidative addition of hydrosilane leading to a classical silyl hydride species cannot be ruled out at this stage;[190,191] however, our experimental observation that the present manganese catalyst is ineffective in catalyzing the hydrosilylation of allylic cyclohexane is more consistent with a Mn-SiH adduct intermediate.[184] The exact process following the nucleophilic attack may vary and a comprehensive investigation is needed to reveal these mechanistic details.

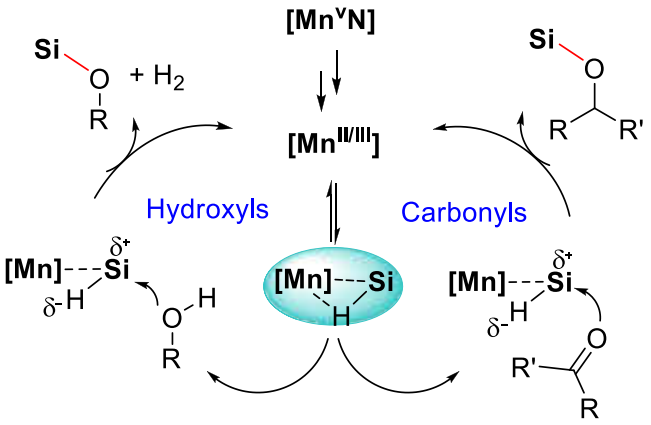

Scheme 5. A plausible mechanism for polymerization

3.3 Conclusions

In conclusion, we have demonstrated that a salen-manganese complex can effectively catalyze the synthesis of various poly(silylether)s from hydrosilanes and diols via dehydrogenative cross coupling and dialdehyde/diketone via hydrosilylation polymerization. Diol monomers show higher activity than dicarbonyls in these reactions, as reflected in the higher yields and molecular weights obtained under comparable conditions. Furthermore, due to the dual activity of the manganese catalyst, unsymmetrical monomers with mixed functional groups have been successfully incorporated into poly(silylether)s that contain different connectivity around the silicon center. The use of a catalyst derived from earth abundant, biocompatible metal via highly atom economical processes represents a sustainable strategy for the production of hydrolytically degradable materials. Further work improving the catalytic efficiency and integrating bio-based building blocks is underway in our laboratory.

3.4. Experimental section

Materials and instrument. All the solvents and liquid substrates were degassed and dried over activated molecular sieves 4Å prior to use. Deuterated solvents were purchased from Cambridge Isotope Laboratory. All ^{1}H and ^{13}C NMR spectra were recorded on a Bruker AVANCE-500 NMR spectrometer and referenced to the residue solvents in $CDCl_3$ or CD_3CN. Gel permeation

chromatography (GPC) analysis was performed on a Varian Prostar, using PLgel 5 µm Mixed-D column, a Prostar 355 RI detector, and THF as eluent at a flow rate of 1 mL/min (20 °C). Polystyrene standards were used for calibration. Infrared spectroscopy results were obtained on a Thermo Scientific Nicolet iS5 FT-IR instrument and analyzed with OMNIC 8.2 software. The samples for IR analysis were directly loaded using an iD5 ATR accessory as a thin film without any support. Differential scanning calorimetry (DSC) measurements were obtained on a Perkin Elmer Jade differential scanning calorimeter and the instrument was calibrated using zinc and indium standards. Glass transition temperatures (T_g) of polymer samples were determined from the second heating cycles with a heating/cooling rate of 20 °C/min under nitrogen atmosphere (20 mL/min). DSC data were analyzed using Pyris V9.0.2 software.

General procedure for the dehydrogenative coupling of alcohols and silanes. All the reactions were performed under inert conditions unless otherwise mentioned. A Schlenk flask (50-100 ml) was used as the reaction flask and oil baths equipped with digital thermometer and controller were used to set and read the temparature. The general procedure includes: loading the Schlenk flask with 1 mol % catalyst [MnN(salen-3,5-^{t}Bu$_2$)] (**Mn-1**), stoichiometric equivalents of substrate and diphenylsilane (1:1 molar ratio), followed by the addition of 2.5 to 3.0 mL of solvent in the glove box. The resulting reaction mixture was taken out of the glove box and connected to a Schlenk line under inert conditions. Then the reaction mixture was heated at reflux temperature for specific time (mentioned in the paper). The reaction was monitored by periodically taking out small amount of samples for NMR and GPC analysis.

Purification process. The polymers were purified via precipitation method. As all the polymers were soluble in dichloromethane (DCM) and insoluble in methanol (MeOH), these two solvents were used in the precipitation process. At the end of the reaction (>90% conversion), the brown

color viscous reaction mixture was first homogenized by addition of as low as possible amount of DCM (1-2 ml), then MeOH was added in portion wise (8-10 ml) until it turned to a biphasic mixture. The top layer, which has the unreacted materials, was taken out by pipette and the bottom viscous/solid layer was washed with MeOH for a few times (typically 2-3 times with 6-8 ml of MeOH each time) until it gave a white/light yellow color viscous/solid polymer. The resulting polymer was dried to a constant weight and characterized by ^{1}H NMR, ^{13}C NMR, FT-IR spectroscopies, gel permeation chromatography (GPC) and DSC.

NMR characterization data

Table 6, entry 1: Poly(silylether) of 1,4-benzenedimethanol: Scale: catalyst 5.0 mg, substrate 0.89 mmol. Polymer weight 214.0 mg, yield 76 %. ^{1}H NMR (500 MHz, $CDCl_3$, 298K, δ): 4.81 (s, 4H, OC*H*$_2$), 7.26 (m, 4H, *C*$_6$*H*$_4$), 7.33 (m, 4H, *m*-Ph), 7.38 (m, 2H, *p*-Ph), 7.70 (m, 4H, *o*-Ph). ^{13}C {^{1}H} NMR (125 MHz, $CDCl_3$, 298K, δ): 64.9 (O*C*H$_2$). 126.7 (*o*-C$_6$H$_4$), 128.1 (*m*-Ph), 130.6 (*p*-Ph), 132.5 (*i*-Ph), 135.1 (*o*-Ph), 139.4 (*i*- C$_6$H$_4$). ^{29}Si {^{1}H} NMR (99 MHz, $CDCl_3$, 298K, δ): -30.4. T_g: 22 °C.

Table 6, entry 2: Poly(silylether) of 1,4-benzenediol: Scale: catalyst 5.0 mg, substrate 0.89 mmol. Polymer weight 207.0 mg, yield 70 %. ^{1}H NMR (500 MHz, $CDCl_3$, 298K, δ): 6.64 (m, 4H, *C*$_6$*H*$_4$), 7.28 (m, 4H, *m-Ph*), 7.36 (m, 2H, *p-Ph*), 7.63 (m, 4H, *o-Ph*). ^{13}C {^{1}H} NMR (125 MHz, $CDCl_3$, 298K, δ): 120.5 (*C*$_6$*H*$_4$), 128.2 (*m-Ph*), 131.0 (*p-Ph*), 131.5 (*i-Ph*), 135.2 (*o-Ph*), 148.9 (*i-C*$_6$*H*$_4$). ^{29}Si {^{1}H} NMR (99 MHz, $CDCl_3$, 298K, δ): -35.2.

Table 6, entry 3: Poly(silylether) of 4,4'-biphenol: Scale: catalyst 5.0 mg, substrate 0.89 mmol. Polymer weight 299.0 mg, yield 88 %. ^{1}H NMR (500 MHz, $CDCl_3$, 298K, δ): 6.64 (m, 4H, *C*$_{12}$*H*$_8$), 7.26 (m, 4H, *C*$_{12}$*H*$_8$), 7.28 (m, 4H, *m-Ph*), 7.36 (m, 2H, *p-Ph*), 7.63 (m, 4H, *o-Ph*). ^{13}C {^{1}H} NMR (125 MHz, $CDCl_3$, 298K, δ): 120.2 (*C*$_{12}$*H*$_8$), 128.0 (*m-Ph*), 128.3 (*C*$_{12}$*H*$_8$), 131.1 (*p-Ph*), 131.4 (*i-*

Ph), 134.8 ($C_{12}H_8$), 135.3 (*o-Ph*), 153.4 (i-$C_{12}H_8$). ^{29}Si {^{1}H} NMR (99 MHz, $CDCl_3$, 298K, δ): -37.4. T_g: 101 °C.

Table 6, entry 4: Poly(silylether) of 1,4-cyclohexanedimethanol: Scale: catalyst 5.0 mg, substrate 0.89 mmol. Polymer weight 184.8 mg, yield 62 %. ^{1}H NMR (500 MHz, $CDCl_3$, 298K, δ): 0.98 (m, 4H, (CH_2) C_6H_{10}), 1.54 (m, 2H, (C*H*) C_6H_{10}), 1.86 (m, 4H, (CH_2) C_6H_{10}), 3.77 (m, 4H, OCH_2), 7.41 (m, 6H, *m & p-Ph*), 7.66 (m, 4H, *o-Ph*). ^{13}C {^{1}H} NMR (125 MHz, $CDCl_3$, 298K, δ): 29.2 ((*C*H$_2$) C_6H_{10}), 40.6 ((*C*H) C_6H_{10}), 68.7 ((*C*H$_2$) C_6H_{10}), 127.9, (*m-Ph*), 130.3 (*p-Ph*), 133.5 (*i-Ph*), 135.1 (*o-Ph*). ^{29}Si {^{1}H} NMR (99 MHz, $CDCl_3$, 298K, δ): -29.9. T_g: 38 °C.

Table 6, entry 5: Poly(silylether) of 1,4-cyclohexanediol: Scale: catalyst 5.0 mg, substrate 0.89 mmol. Polymer weight 222.5 mg, yield 70 %. ^{1}H NMR (500 MHz, $CDCl_3$, 298K, δ): 1.41 (m, 4H, (CH_2) C_6H_{10}), 1.84 (m, 4H, (CH_2) C_6H_{10}), 3.91 (m, 2H, (OC*H*) C_6H_{10}), 5.46 (m, 1H, Si*H*), 7.35 (m, 4H, *m-Ph*), 7.39 (m, 2H, *p-Ph*), 7.64 (m, 4H, *o-Ph*). ^{13}C {^{1}H} NMR (125 MHz, $CDCl_3$, 298K, δ): 30.7, 32.3 ((*C*H$_2$) C_6H_{10}), 68.9, 70.1 ((O*C*H) C_6H_{10}), 127.7, 128.1 (*m-Ph*), 130.1, 131.3 (*p-Ph*), 134.3, 134.7 (*i-Ph*), 135.1, 135.1 (*o-Ph*). ^{29}Si {^{1}H} NMR (99 MHz, $CDCl_3$, 298K, δ): -35.4, -35.6. T_g: 60 °C.

Table 6, entry 6: Poly(silylether) of 1,6-hexanediol: Scale: catalyst 5.0 mg, substrate 0.89 mmol. Polymer weight 222.5 mg, yield 84 %. ^{1}H NMR (500 MHz, $CDCl_3$, 298K, δ): 1.32 (m, 4H, OCH$_2$CH$_2$CH_2), 1.56 (m, 4H, OCH$_2$CH_2CH$_2$), 3.74 (m, 4H, OCH_2CH$_2$CH$_2$), 7.33 (m, 4H, *m-Ph*), 7.38 (m, 2H, *p-Ph*), 7.63 (m, 4H, *o-Ph*). ^{13}C {^{1}H} NMR (125 MHz, $CDCl_3$, 298K, δ): 25.7 (OCH$_2$CH$_2$*C*H$_2$), 32.6 (OCH$_2$*C*H$_2$CH$_2$), 63.3 (O*C*H$_2$CH$_2$CH$_2$), 127.9 (*m-Ph*), 130.3 (*p-Ph*), 133.4 (*i-Ph*), 135.1 (*o-Ph*). ^{29}Si {^{1}H} NMR (99 MHz, $CDCl_3$, 298K, δ): -32.6.

Table 7, entry 1: Poly(silylether) of terephthalaldehyde: Scale: catalyst 5.0 mg, substrate 0.89 mmol. Polymer weight 178.0 mg, yield 58 %. ^{1}H NMR (500 MHz, $CDCl_3$, 298K, δ): 4.81 (m, 4H,

OC*H*$_2$), 7.26 (m, 4H, *C*$_6$*H*$_4$), 7.37 (m, 4H, *m-Ph*), 7.71 (m, 6H, *p & o-Ph*). ^{13}C {^{1}H} NMR (125 MHz, $CDCl_3$, 298K, δ): 65.0 (O*C*H$_2$). 126.7 (*p & o-C*$_6$*H*$_4$), 128.1 (*m-Ph*), 130.6 (*p-Ph*), 132.5 (*i-Ph*), 135.1 (*o-Ph*), 139.4 (*i- C*$_6$*H*$_4$). ^{29}Si {^{1}H} NMR (99 MHz, $CDCl_3$, 298K, δ): -30.3. T_g: 20 °C.

Table 7, entry 2: Poly(silylether) of 1,6-hexanedial: Scale: catalyst 5.0 mg, substrate 0.89 mmol. Polymer weight 105.6 mg. yield 40 %. ^{1}H NMR (500 MHz, $CDCl_3$, 298K, δ): 1.26-1.62 (m, 8H, OCH$_2$C*H*$_2$C*H*$_2$), 3.82 (m, 4H, OC*H*$_2$CH$_2$CH$_2$), 7.30-7.40 (m, 10H, *Ph*). ^{13}C {^{1}H} NMR (125 MHz, $CDCl_3$, 298K, δ): 26.82 (OCH$_2$CH$_2$*C*H$_2$), 33.21 (OCH$_2$*C*H$_2$CH$_2$), 64.15 (O*C*H$_2$CH$_2$CH$_2$), 127.8 (*m-Ph*), 131.1(*p-Ph*), 133.8 (*i-Ph*), 135.2 (*o-Ph*).

Table 7, entry 3: Poly(silylether) of 1,4-cyclohexanedione: Scale catalyst 5.0 mg, substrate 0.89 mmol. Polymer weight 130.1 mg, yield 49 %. ^{1}H NMR (500 MHz, $CDCl_3$, 298K, δ): 1.38 (m, 4H, (C*H*$_2$) *C*$_6$*H*$_{10}$) 1.81 (m, 4H, (C*H*$_2$) *C*$_6$*H*$_{10}$), 3.87 (m, 2H, (OC*H*) *C*$_6$*H*$_{10}$), 7.27 (m, 6H, *m & p-Ph*), 7.58 (m, 4H, *o-Ph*). ^{13}C {^{1}H} NMR (125 MHz, $CDCl_3$, 298K, δ): 30.9, 32.0 ((*C*H$_2$) *C*$_6$*H*$_{10}$), 68.8, 70.0 ((O*C*H) *C*$_6$*H*$_{10}$), 127.7 (*m-Ph*), 130.1 (*p-Ph*), 134.1 (*i-Ph*), 135.0 (*o-Ph*). ^{29}Si {^{1}H} NMR (99 MHz, $CDCl_3$, 298K, δ): -35.6, -35.7. T_g: 51 °C.

Table 7, entry 4: Poly(silylether) of *p*-hydroxy benzaldehyde: Scale: catalyst 5.0 mg, substrate 0.89 mmol. Polymer weight 188.0 mg, yield 69 %. ^{1}H NMR (500 MHz, $CDCl_3$, 298K, δ): 4.66-481 (m, 2H, OC*H*$_2$), 6.88 (m, 2H, *m-C*$_6$*H*$_4$), 7.08 (m, 2H, *o-C*$_6$*H*$_4$), 7.32 (m, 6H, *m & p-Ph*), 7.68 (m, 4H, *o-Ph*). ^{13}C{^{1}H} NMR (125 MHz, $CDCl_3$, 298K, δ): 64.7, 65.1 (O*C*H$_2$), 119.6, 119.7 (*Ph*), 128.2, 130.5, 130.7, 131.0, 132.0, 133.7, 134.5, 135.1 (*m, p, i & o-Ph*), 153.5 (*i-C*$_6$*H*$_4$). ^{29}Si {^{1}H} NMR (99 MHz, $CDCl_3$, 298K, δ): -30.1, -33.5, -37.1. T_g: 18 °C.

Table 7, entry 5: Poly(silylether) of *p*-hydroxy benzylalcohol: Scale: catalyst 5.0 mg, substrate 0.89 mmol. Polymer weight 198.5 mg, yield 73 %. ^{1}H NMR (500 MHz, $CDCl_3$, 298K, δ): 4.83-4.60 (m, 2H, OC*H*$_2$), 6.97 (m, 2H, *C*$_6$*H*$_4$), 7.45-7.35 (m, 2H, *C*$_6$*H*$_4$ and m, 6H, *m & p-Ph*), 7.72 (m,

4H, *o-Ph*). $^{13}C\{^1H\}$ NMR (125 MHz, $CDCl_3$, 298K, δ): 64.7, 65.2 (O*C*H_2), 119.6, 119.9 (*C_6H_4*), 128.2, 128.40, 130.6, 130.8, 133.3, 134.6, 134.9, 135.3 (*m, p, i & o-Ph*), 153.5, 154.2 (*i-C_6H_4*). $^{29}Si\ \{^1H\}$ NMR (99 MHz, $CDCl_3$, 298K, δ): -30.5, -33.5, -37.7. T_g: 25 °C.

Table 7, entry 6: Poly(silylether) of 3-(4-hydroxyphenyl)-1- propanol: Scale: catalyst 5.0 mg, substrate 0.89 mmol. Polymer weight 238.0 mg, yield 80 %. ^1H NMR (500 MHz, $CDCl_3$, 298K, δ): 1.73 (m, 2H, $OCH_2CH_2CH_2C_6H_4$), 2.51 (m, 2H, $OCH_2CH_2CH2C_6H_4$), 3.75 (m, 2H, $OCH_2CH_2CH_2C_6H_4$), 6.79 (m, 4H, *C_6H_4*), 7.30 (m, 6H, *m & p-Ph*), 7.65 (m, 2H, *o-Ph*). $^{13}C\{^1H\}$ NMR (125 MHz, $CDCl_3$, 298K, δ): 31.3, 31.3 ($OCH_2CH_2CH_2C_6H_4$), 34.1, 34.2 ($OCH_2CH_2CH_2C_6H_4$), 62.5, 63.0 ($OCH_2CH_2CH_2C_6H_4$), 119.5, 119.6 (*C_6H_4*), 128.0, 128.1, 129.5, 130.4, 130.7, 131.7, 132.5, 133.2, 135.1 (*m, p, i & o-Ph*), 152.2, 152.6 (*i-C_6H_4*). $^{29}Si\{^1H\}$ NMR (99 MHz, $CDCl_3$, 298K, δ): -31.9, -34.5, -37.8. T_g: 21 °C.

CHAPTER 4

POLYMERS FROM BIO-DERIVED RESOURCES: SYNTHESIS OF POLY(SILYLETHER)S FROM FURAN DERIVATIVES CATALYZED BY A SALEN–MN(V) COMPLEX

4.1 Introduction

Synthetic materials play a vital role in every aspect of modern life. There is a need for advanced technologies for accessing elastomers, plastics, textiles, packaging, and sophisticated materials applied in electronics and medicine. The vast majority of these materials are synthesized from non-renewable fossil fuel resources.[192,193] However, increasing consumption of fossil fuels will lead to their eventual depletion and continuous release of greenhouse gases. In addition, the majority of these polymers are non-degradable thus their accumulation in the environment has been a threat to the ecosystem.[194] At present, there is no primary remedy for these problems; one possibility is to synthesize polymers from sustainable starting materials. In recent years, growing effort has been dedicated to providing access to key chemical building blocks derived from biomass.[195,196,197] These biomaterials, including starch, cellulose, lignin and side products of bio-derived oils, are environmentally benign, and highly abundant as a renewable source of carbon.[198,199] Among a large number of building blocks, furan based monomers such as furfural, 5-hydroxymethylfurfural (HMF) and their derivatives are a promising platform to synthesize bio resins, biofuels, biopolymers, and various value-added chemicals.[200,201,202,203,204,205,206]

Although several furan based monomers have been used in polymer synthesis,[207] to our knowledge, poly(silyl ether)s (PSEs) from furan derivatives have not been reported. PSEs are an important class of polymers with unique and significant properties and applications.[56,58] The

presence of a labile Si-O-C linkage in the backbone allows them to degrade easily as it is susceptible to acid or base catalyzed hydrolysis.[56,67,208] The rate of hydrolysis depends on the nature of substituents on silicon and carbon atoms, and the bond distance of Si–O and Si–C in the Si–O–C chain.[209] The hydrolytic lability of Si–O–C linkage attenuates their long-term environmental impact and makes them highly attractive in applications where their degradation is desirable such as in drug delivery processes.[210] In comparison, the corresponding siloxanes (Si–O–Si) and ethers (C–O–C) are resistant to hydrolysis and thus degradation.[211,212]

PSEs have been synthesized by various methods from several available sources. The most commonly employed method is condensation polymerization of diols with either dihalosilanes, dialkoxysilanes, or diaminosilanes. Quaternary ammonium salt catalyzed reaction of dichlorosilanes with bis(oxetane)s and bis(epoxide)s also provide PSEs.[68,69,71] However, chlorosilanes are air/moisture sensitive and generate undesired side products, such as HCl.[213] Hydrosilanes can be advantageous as they are air-stable, inexpensive and produce H_2 as the only by-product. Reactions between hydrosilanes and bifunctional hydroxyl or carbonyl monomers, catalyzed by transition metal complexes such as palladium, rhodium, and ruthenium, are widely used to synthesize PSEs.[214] However, the high cost and toxicity of precious metals are the main limitations. With these considerations, we have been interested in manganese-catalyzed reactions because it is an inexpensive, earth abundant, biocompatible, and has great potential as a sustainable alternative to precious metal catalysts.[215] An air stable, easily prepared high valent Mn salen nitrido complex [MnN(salen-3,5-^{t}Bu$_2$)] (**Mn-1**, see Scheme 6) has been shown to be an effective catalyst for dehydrogentaive coupling of alcohols with hydrosilanes and hydrosilylation of carbonyls.[81,175] Because of its versatility, **Mn-1** has been employed to synthesize a wide range of PSEs from diols, dicarbonyls, and hydrosilanes.[216] Presumably, the reduced manganese center activates

hydrosilanes by formation of an η^2- or η^1-SiH adduct, which undergoes nucleophilic attack by the hydroxyl or carbonyl groups in the substrate, generating the silylether linkages. Combining our interests in high-valent transition metal complexes in catalysis[173,174] and in utilizing renewable feedstock for degradable polymers,[217] herein we report the synthesis of a variety of PSEs from bio-derived furanic monomers and hydrosilanes catalyzed by **Mn-1**.

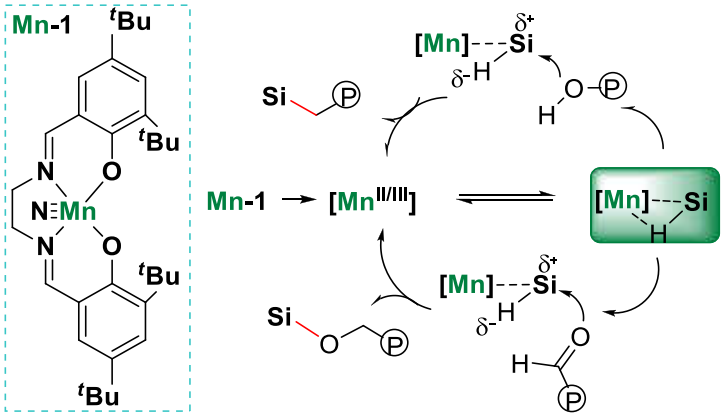

Scheme 6. Structure of the **Mn-1** catalyst and a possible polymerization mechanism

4.2 Results and discussion

The four furan monomers examined in this study, 5-(hydroxymethyl)furfural (HMF),[218] 2,5-bishydroxymethylfuran (BHMF),[219,220] 2,5-diformylfuran (DFF),[221,222,223,224] and 5,5'-oxymethylenebisformylfuran (OBMF),[225,226] are all known compounds and can be derived from cellulosic biomass. HMF is now commercially available from nonedible sources.

4.2.1 Reactions between BHMF with hydrosilanes

The diol, 2,5-bis(hydroxymethyl)furan (BHMF), is a reduced product of HMF and was chosen as the standard monomer. The two hydroxyl groups in BHMF makes it a versatile building block for various polymers such as polyesters via condensation with carboxylic acids; some of the cross-linked polymers are known for their self-healing ability.[227] Our initial efforts were geared towards establishing suitable conditions for the polymerization reactions between BHMF and various

hydrosilanes in the presence of **Mn-1** (1 mol%). A reaction between BHMF and Ph_2SiH_2 in toluene at reflux temperature under inert conditions was monitored at regular time intervals by NMR spectroscopy. Also, change in the reaction mixture's color from green to brown indicated the reaction progress. The monomer conversion reached >95 % in 12 h; however, the reaction was allowed to continue for 24 h in order to obtain high molecular weight PSEs since the reaction proceeds by a step-growth polymerization reaction. The resultant polymer product PSE (13) was purified by the precipitation method and characterized by spectrometric techniques (Table 8, entry 1). According to the ^{1}H NMR analysis, the disappearance of silane hydrogens (Si*H*) at 4.92 ppm and hydroxyl groups of BHMF peaks at 1.87 ppm confirmed the consumption of starting materials. Simultaneously, shifting of the two methylene groups (CH_2) of monomer in ^{1}H NMR from 4.62 to 4.66 ppm (Figure 22) and in ^{13}C NMR (CH$_2$) from 56.5 to 58.0 ppm suggested the formation of PSE (12) (Figure 23).

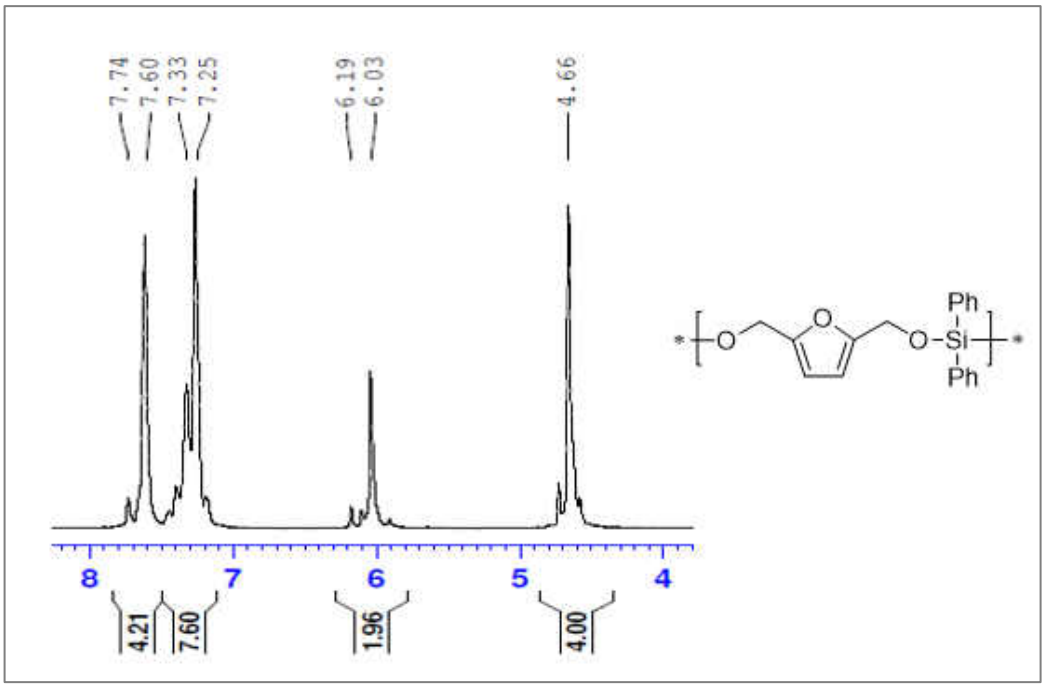

Figure 22. ^{1}H NMR spectra of the PSE prepared from of BHMF and Ph_2SiH_2

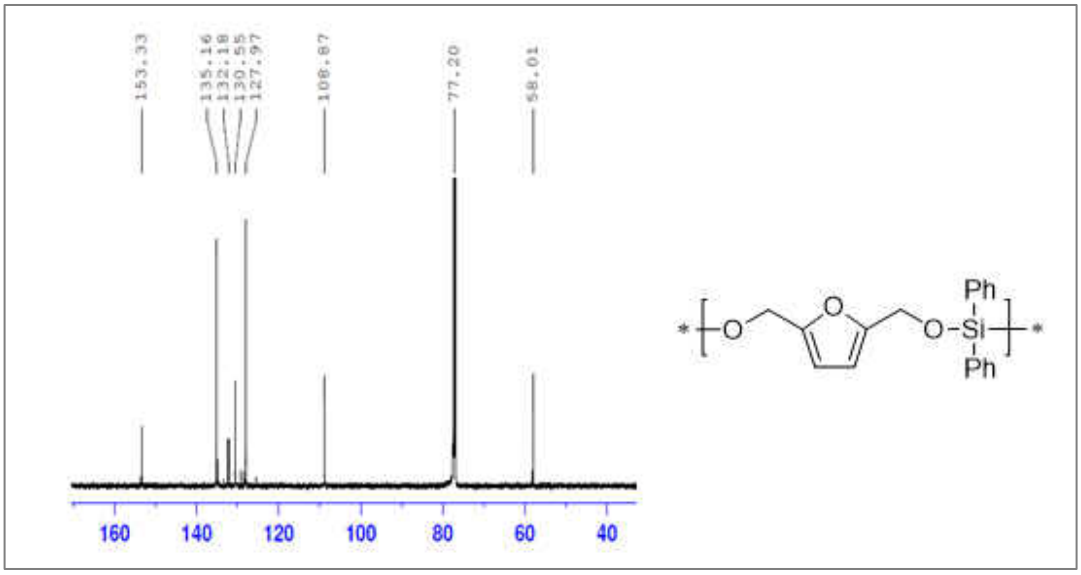

Figure 23. ^{13}C NMR spectra of the PSE prepared from of BHMF and Ph_2SiH_2

In the ^{29}Si NMR spectrum, a single peak was observed at −39.61ppm, which was consistent with the single silicon center of a repeating unit. In addition to the NMR studies, the disappearance of hydroxyl (OH) groups at 3200 cm^{-1} and Si-H groups at 2130 cm^{-1}, and the appearance of Si-O-C linkage around 1200 cm^{-1} in FT-IR supports the formation of PSE (13). GPC studies reveal that the resultant PSE (12) has M_n of 4300 g/mol (Table 2, entry 1). It should be mentioned that the synthesized PSE has a light brownish color after repeated purifications by precipitation. No further darkening was observed after two months of ambient storage and GPC analysis showed no significant change in molecular weights.

To explore the effect of hydrosilanes in the polycondensation, we sought to vary one of the phenyl groups of Ph_2SiH_2 with substituents possessing different electronic and steric features. First, a less hindered alkyl group i.e. methyl was chosen to replace one phenyl group. However, the reaction between the corresponding methylphenylsilane, $PhMeSiH_2$ and BHMF for 24 h

produced low molecular weight PSE (14) (M_n 3200 g/mol, Table 8, entry 2). The results are consistent with prior observation that alkylsilanes showed lower activity than arylsilanes in **Mn-1** catalyzed dehydrogenative coupling reactions. When a more hindered 1-naphthylphenylsilane, $NpPhSiH_2$, was used in the reaction under the same conditions, an even lower molecular weight polymer PSE (15) with M_n 2100 g/mol was obtained, presumably due to the high steric hindrance of naphthyl group (Table 8, entry 3). Furthermore, a bis(hydrosilane), 1,4-bis(dimethylsilyl)benzene (BDMSB) was tested because of its known high reactivity in the preparation of PSEs. However, the reaction mixture retained its initial green color, which indicated that the reaction was not proceeding (Table 4, entry 4). NMR studies of the reaction confirmed that BDMSB was not active in **Mn-1** catalyzed reactions. The lack of reactivity of BDMSB could be attributed to the fact that it is a tertiary silane having two alkyl (methyl) groups. In these cases, it was also noted that the activity of hydrosilanes correlated well with the isolated yields.

In our previous study, it was shown that the reaction temperature plays a role in producing high M_n PSEs,[216] thus a variety of high boiling solvents including xylenes (140 °C), bromobenzene (156 °C), and mesitylene (165 °C) were examined in the polymerization. A set of reactions between BHMF and Ph_2SiH_2 were performed in these solvents at reflux temperatures. However, very low M_n PSEs were produced due to the poor solubility of BHMF. Furthermore, in all these reactions, considerable amount of a dark brown insoluble solid was formed at elevated temperatures. Efforts to characterize these insoluble materials were not successful because of their poor solubility in common organic solvents. Thus, toluene was chosen as the standard solvent in further polymerization runs.

Table 8. Polymerization of HMF with different hydrosilanes[a]

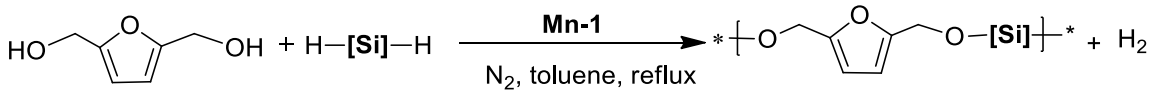

Entry	PSE	[Si]	M_n (g/mol)[b]	Đ[b]	Yield %
1	PSE 13	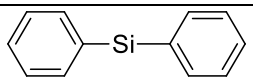	4300	1.33	88
2	PSE 14	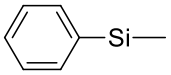	3200	2.22	63
3	PSE 15	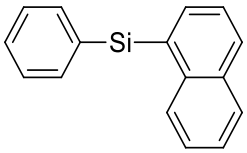	2100	1.24	40
4	-	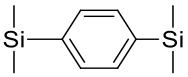	N.R.	-	-

[a]Reaction conditions: substrate HMF, 0.89 mmol; silane, 1.0 equiv; and catalyst **Mn-1**, 1.0 mol %; reaction time, 24 h. [b]Determined by GPC calibrated with polystyrene standards. Đ = polydispersity index.

4.2.2 Substrate scope

Given the versatility of the current catalyst, we are interested in extending the substrate scope to include other furan derivatives with different functional groups. First, we decided to lengthen the reaction time in order to produce high-M_n PSEs. Thus, a 40 h reaction between BHMF and Ph_2SiH_2 was performed under the optimized condition (Table 9, entry 1). As expected, the isolated product PSE (16) has a high molecular weight (M_n 11000 g/mol), more than double that of the 24 h reaction. This agrees with the step-growth nature of condensation polymerization reactions.

In the biomass conversion process, furan derivatives with different functional groups have been routinely produced. We targeted HMF, as an interesting bio-derived building block bearing both hydroxyl and formyl functionalities. The reaction between HMF and Ph_2SiH_2 under optimized conditions was carried out for 40 h, and the resulting PSE (17) has M_n of 8000 g/mol with Đ of 2.26 (Table 9, entry 2). The comparatively lower molecular weight of PSE (17) can be

explained by the general observation that hydroxyl groups are more nucleophilic and thereby more active than carbonyl groups in **Mn-1** catalyzed reaction with Ph_2SiH_2. Though HMF has two different functional groups, the resulting structure of PSE with Ph_2SiH_2 would be same as the PSE of BHMF i.e. PSE (16) because the –C*H*O functional group will be reduced to –CH_2O– during the reaction.

In the ^{1}H NMR spectrum, the disappearance of aldehyde peak at 9.63 ppm and appearance of two new hydrogens at 4.66 ppm (i.e. conversion of -C*H*O to -CH_2O-) and shifting of the two hydrogens of the furan ring from 6.55 and 7.34 ppm to 6.07 ppm confirm the formation of PSE (17). In addition, the disappearance of the C=O stretching frequency at 1660-1670 cm^{-1} in FT-IR spectrum also supports the consumption of monomers and formation of PSE (17). Interestingly, small but consistent peaks at 9.63 ppm in ^{1}H NMR spectrum and at 1672 cm^{-1} in FT-IR spectrum indicate the presence of formyl-capped end groups of the polymer chain.

Encouraged by these results, another furan derivative, 2,5-diformylfuran (DFF) was examined as monomer under the optimized condition (Table 9, entry 3). The M_n of the resultant PSE (18) was 5500 g/mol with Đ of 1.74. Comparatively, the M_n of PSE (18) was lower than the analogous PSE (16) and (17) (Table 9, entries 1-2). These values again are in line with the fact that the hydrosilylation of carbonyls catalyzed by **Mn-1** is slower than the dehydrogenative coupling of alcohols. Notably, PSE (18) has the same backbone as PSE (16) and (17), which was verified by NMR spectroscopy. The disappearance of –C*H*O peak at 9.65 ppm and the simultaneous appearance of two –CH_2 protons (4 H) at 4.65 ppm in ^{1}H NMR and appearance of a new peak at 65.0 ppm in ^{13}C NMR confirms the formation of PSE (18). Together, these reactions represent a rather unique example in which polymers with the same backbone structure can be synthesized from monomers having different functional groups using the same catalyst.

Table 9. Polymerization reactions of various furan monomers[a]

Entry	PSE	Substrate	M_n (g/mol)[b]	Đ [b]	Yield %
1	PSE 16	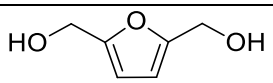	11000	1.98	81
2	PSE 17	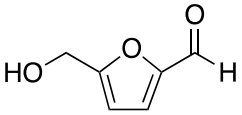	8000	2.26	74
3	PSE 18	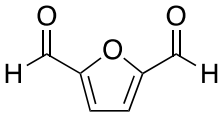	5500	1.74	76
4	PSE 19	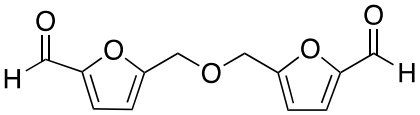	6400	1.69	78

[a]Reaction conditions: substrate, 0.89 mmol; silane Ph_2SiH_2, 1.0 equiv; and catalyst **Mn-1**, 1.0 mol %; reaction time: 40 h. [b]Determined by GPC calibrated with polystyrene standards.

We next chose cirsiumaldehyde (5,5'-[oxybis(methylene)]di(2-furaldehyde) (OBMF), as the monomer. OBMF features two characteristic ether linked C*H*$_2$ groups (-C*H*$_2$-O-C*H*$_2$-) at 4.45 ppm and two -C*H*O groups at 9.90 ppm. The reaction between OBMF and Ph_2SiH_2 for 40 h under optimized conditions resulted in PSE (19), which has a M_n of 6400 g/mol (Table 2, entry 4). Similar to the NMR spectra of PSEs (17) & (18), a new characteristic peak appeared at 4.66 ppm, corresponding to the newly formed –C*H*$_2$ protons from the reduction of C*H*O groups. Also like in PSE (17) and (18), the presence of small peaks at 9.57 ppm in ^{1}H NMR and 178.1 ppm in ^{13}C NMR indicates the formyl group as an end group of the polymer.

4.2.3 Thermal properties of PSEs

Differential scanning calorimetry. The thermal properties of the synthesized PSEs were investigated under nitrogen atmosphere using differential scanning calorimetry (DSC) and

thermogravimetric analysis (TGA) techniques, and the characteristic results were summarized in Table 10.

Table 10. DSC and TGA data of PSEs

Polymer #	T_g/°C	$T_{-50\%}$/°C	**Final residue %**
PSE (12)	9.8	445	21.2
PSE (13)	3.5	427	22.6
PSE (14)	27.8	473	22.4
PSE (16)	15.6	445	21.2
PSE (17)	9.0	453	25.4
PSE (18)	3.3	427	22.6
PSE (19)	2.5	422	29.0

The long Si–O and Si–C bond lengths in Si–O–C linkages of PSEs can raise the flexibility of the polymer backbone, which leads to low glass-transition temperatures (T_g). PSEs bearing aromatic backbones or secondary α-carbons typically exhibit higher T_g, whereas those bearing aliphatic backbones or primary α-carbons typically have lower T_g. According to the DSC analysis, T_g of the PSEs (1-3) are in the range of 3.5–27.8 °C (Figure 24). Here PSEs with sterically more hindered groups such as naphthylphenylsilane ($NpPhSiH_2$) exhibits higher T_g values PSE (15), T_g = 27.8 °C), while PSEs with sterically less hindered groups exhibits lower T_g values (PSE (13 & 14), T_g = 9.8 & 3.5 °C respectively). These results clearly demonstrate that steric hindrance around the silicon atom plays a significant role in determining the T_g. In addition to the steric hindrance, molecular weights may also play a role in determining the T_g of PSEs. In this context, it is informative to compare PSE (16-18), a series of polymers with same backbone linkages but different molecular weights. PSE (16), with a M_n of 11000 g/mol exhibits a T_g of 15.6 °C, whereas PSE (17) with a M_n of 8000 g/mol exhibits a T_g of 9.0 °C, and PSE (18) with a M_n 5500 g/mol shows a low T_g of 3.3 °C. PSE (19) has the lowest T_g of 2.5 °C among all the listed PSEs in this

work. This may be attributed to the additional flexible ether linkages between two furan rings. These specific trends demonstrate the importance of steric hindrance of substituent groups and the molecular weights in determining the thermal properties of PSEs.

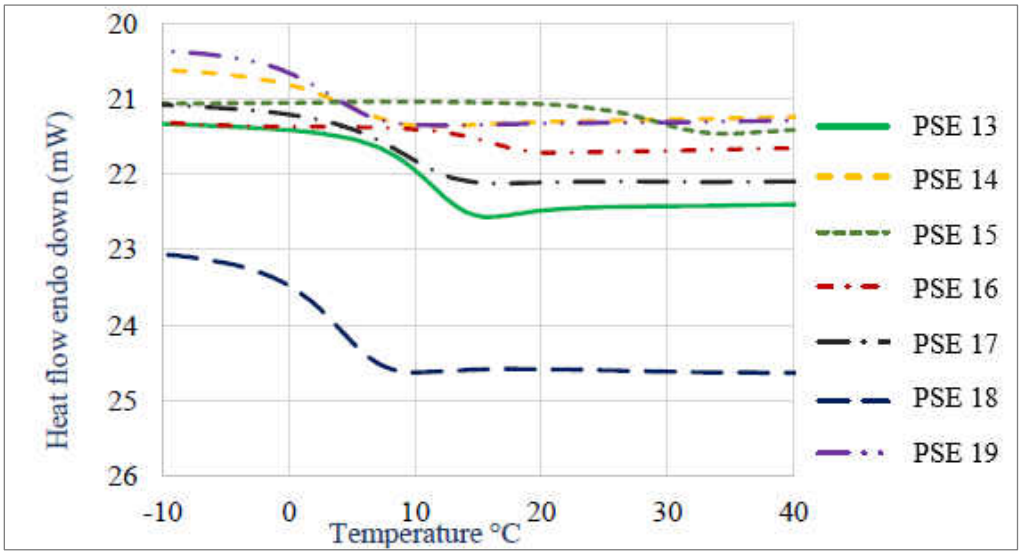

Figure 24. DSC Thermograms of PSEs

Thermogravimetric analysis. TGA of PSEs was carried out from 20 to 800 °C. According to the TGA analysis (Figure 25), the onset of decomposition occurs at about 187–250 °C. The temperatures for 50% gravimetric loss ($T_{-50\%}$), a vital criterion for assessment of thermal stability, are in the range of 422-473 °C. The final residue weights of all the PSEs are between 21.2 to 29.0 %. Similar to DSC studies, steric hindrance and molecular weights of PSEs are important factors influencing the thermal stability of PSEs. PSE (15) produced from $NpPhSiH_2$ showed highest thermal stability, with $T_{-50\%}$ at 473 °C, even though its molecular weight is not high. This can be attributed to the protection provided by the sterically more hindered Np group. Along the same line, PSE (13) and PSE (14) derived from less hindered Ph_2SiH_2 and $MePhSiH_2$ show progressively lower resistance to heat. On the other hand, a smaller variation in $T_{-50\%}$ values were observed for PSEs (16, 17, and 18) with the same repeating units; which may be a result of the

difference in the respective molecular weights. The additional ether linkage again leads to the low $T_{-50\%}$ of PSE (19).

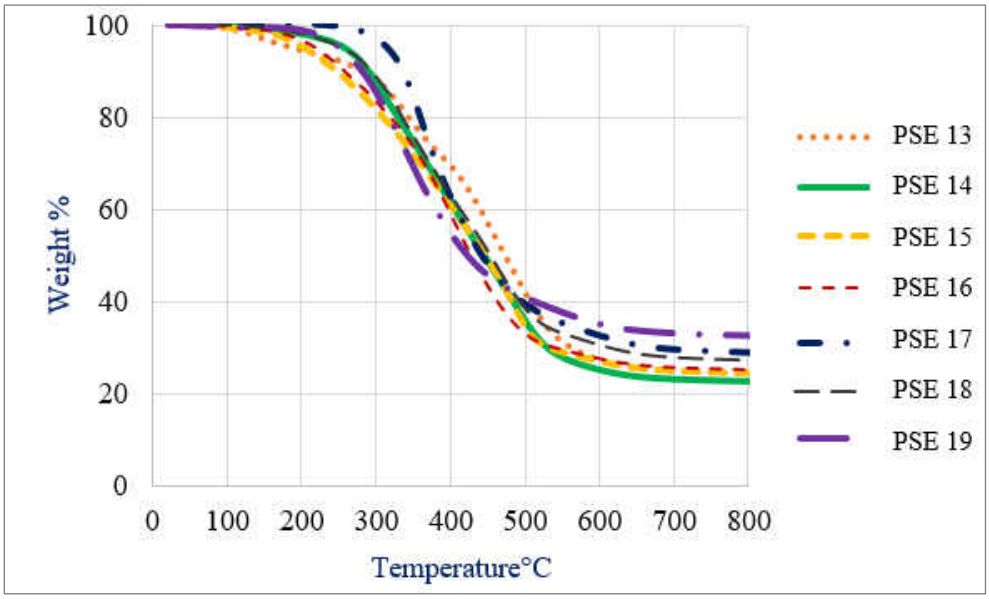

Figure 25. TGA Thermograms of PSEs

4.2.4 Degradation studies

To test the hydrolytic stability of the PSE polymers, we have performed degradation studies under hydrolytic conditions. For this study, a high molecular weight PSE (20) (M_n of 25,000 g/mol) was synthesized from BHMF and Ph_2SiH_2 under optimized conditions by extending the reaction time from 40 h to 96 h. This polymer exhibited a T_g of 17.9 °C, higher than the corresponding PSE obtained at 40 h. A homogeneous solution was first prepared by dissolving this PSE in THF (~10 mg/mL), and aliquots of HCl/H_2O (pH=2.0) at 2 vol% were added at room temperature to induce polymer degradation. Changes in the molecular weight of PSE over time were monitored by GPC (Figure 26). As expected, a rapid drop in the molecular weight was observed initially (M_n nearly halved in 3 hours), followed by a slow degradation resulting in M_n of 8500 g/mol at 48 h. In

comparison, increasing the amount of HCl/H_2O (pH=2.0) from 2 vol% to 17 vol% led to complete degradation within the first few hours, while no significant degradation was observed when 2 vol% neutral H_2O was added instead of HCl/H_2O. These observations demonstrated that the cleavage of the Si–O–C linkage in our PSE correlated with the amounts of active acidic hydrogens in the mixture, comparable to the literature report on the degradation of PSEs.

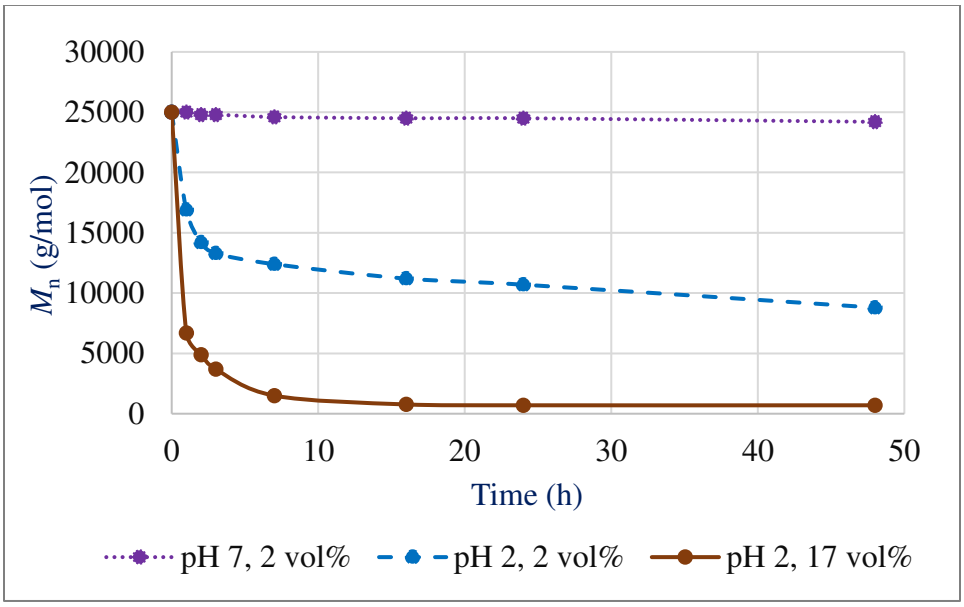

Figure 26. Degradation plots of PSE 20 (M_n vs time)

4.3. Conclusions

In summary, a variety of degradable poly(silylether)s (PSEs) based on renewable furan derivatives were successfully synthesized by using an efficient Mn salen catalyst. Monomers with hydroxyl functional groups reacted via dehydrogenative cross coupling with hydrosilanes, whereas carbonyl functional groups reacted via hydrosilylation. Under similar conditions using Mn catalyst, hydroxyl functionalized monomers display higher activity than carbonyl monomers, leading to high molecular weight PSEs. It is notable that the PSEs with same polymer backbone can be obtained from different monomers with different functional groups. The thermal stability

of PSEs, as indicated by the T_g and $T_{-50\%}$, can be correlated with, and thus modified by the steric features of the substituent groups on silicon. Interestingly, the polymers can be completely degraded under acidic conditions. Further studies on synthesizing other PSEs from different renewable feedstock and their degradation are underway in our laboratory.

4.4. Experimental Section

Materials and instrumentation. 5-Hydroxymethyl furfural and its derivatives were supplied by Prof. Sibi's group at NDSU. Deuterated solvent, $CDCl_3$ was purchased from Cambridge Isotope Laboratory. Hydrosilanes were purchased from Sigma-Aldrich. All the solvents were degassed and dried over molecular sieves (4 Å) prior to use. All ^1H, ^{13}C NMR, and ^{29}Si NMR spectra were recorded on a Bruker AVANCE-500 NMR spectrometer and referenced to the residual $CHCl_3$ in $CDCl_3$. ^{29}Si NMR spectra were referenced to internal TMS. Infrared spectroscopy (IR) results were obtained on a Thermo Scientific Nicolet iS5 FT-IR instrument and analyzed with OMNIC 8.2 software. The samples for IR analysis were directly loaded as a thin film without support using an iD5 ATR accessory. Molecular weights were determined via gel permeation chromatography (GPC). A Varian Prostar system, using the PLgel 5 μm Mixed-D column, a Prostar 355 refractive index detector was used. Elution rate was maintained at 1 mL/ min (20 °C) and THF was used as the eluent. Polystyrene standards were used for calibration. DSC thermograms were collected using a Perkin Elmer Jade differential scanning calorimeter, and the instrument was calibrated using zinc and indium standards. Samples were analyzed in hermetically sealed pans under a nitrogen atmosphere. T_gs of PSEs were determined from the second heating cycles with a heating/cooling rate of 20 °C/min under the nitrogen atmosphere (20 mL/min). DSC data were analyzed using Pyris V9.0.2 software. TGA of PSEs was performed on SDT Q 600 instrument at a flow rate of 100 mL/min of nitrogen (furnace purge gas). The temperature was increased at 5

°C/min rate from 23 to 800 °C. Alumina (Al_2O_3) sample cups were used to weigh the polymer samples and to run the TGA. Advantage™ software was used to analyze the TGA data.

General procedure for the synthesis and purification of PSEs. All reactions were performed under inert atmosphere of dry nitrogen unless otherwise mentioned. Oil baths equipped with digital thermometers and controllers were used to set and read the temperature. For a typical synthesis, to a 50-100 mL Schlenk flask equipped with a magnetic stir bar, 1 mol% catalyst [MnN(salen-3,5-^{t}Bu$_2$)] (**Mn-1**), stoichiometric equivalents of monomer and diphenylsilane (0.89 mmol of each, 1:1 ratio) were added, followed by the addition of 2.5 to 2.8 mL of solvent in a glove box. Later the reaction flask was taken out and connected to Schlenk line under an inert atmosphere. Then, the reaction mixture was heated at reflux temperature for a specific time. The reaction progress was monitored until >90% conversion was achieved by periodically taking out a small amount of samples for NMR and GPC analyses.

PSEs were purified by precipitation method from dichloromethane (DCM) and methanol (MeOH) solvents. The brown colored crude reaction mixture was homogenized by adding small amount of DCM (1-2 mL), then MeOH was added portion wise (10−12 mL) as the solution turned into a biphasic mixture. The top layer of any soluble, unreacted materials was separated using a pipette, and the bottom solid/viscous layer was further washed with MeOH a couple of times which resulted in a solid/viscous light yellow colored polymer. Finally, the polymer was dried under vacuum to a constant weight and characterized by ^{1}H NMR, ^{13}C NMR, and FT-IR and GPC, DSC and TGA.

General procedure for PSEs degradation. PSE (10 mg) and 1 mL of THF were added to a 10 mL sample vial equipped with a magnetic stirrer. After getting a homogenous solution, calculated volumes of HCl/H_2O solution (pH=2) or distilled water were added to the reaction mixture at

ambient temperature. Samples were taken at specific times using pipets and diluted for molecular weight determination.

NMR characterization data of PSEs

Table 8. Entry 1, PSE (12): Scale: catalyst 5.0 mg, substrate 0.89 mmol. Yield 88%. ^{1}H NMR (500 MHz, $CDCl_3$, 298 K, δ): 4.66 (m, 4H, OC*H₂*), 6.03 (m, 2H, C*H*-C*H*), 7.33 (m, 6H, *m* & *p-Ph*), 7.60 (m, 4H, *o-Ph*). ^{13}C {1H} NMR (125 MHz, $CDCl_3$, 298 K, δ): 58.0 (O*C*H$_2$), 108.9 (*C*H-*C*H), 128.0 (*m-Ph*), 130.5 (*p-Ph*), 132.2 (*i-Ph*), 135.2 (*o-Ph*), 153.3 (=*C*). ^{29}Si {1H} NMR (99 MHz, $CDCl_3$, 298 K, δ): −39.81.

Table 8. Entry 2, PSE (13): Scale: catalyst 5.0 mg, substrate 0.89 mmol. Yield 63%. ^{1}H NMR (500 MHz, $CDCl_3$, 298 K, δ): 0.37 (m, C*H₃*), 4.5-4.65 (m, 4H, OC*H₂*), 6.16 (m, 2H, C*H*-C*H*), 7.36 (m, 3H, *m* & *p-Ph*), 7.60 (m, 2H, *o-Ph*). ^{13}C {1H} NMR (125 MHz, $CDCl_3$, 298 K, δ): -3.8 (*C*H$_3$), 57.7 (O*C*H$_2$), 108.6 (*C*H-*C*H), 128.0 (*m-Ph*), 130.3 (*p-Ph*), 133.2 (*i-Ph*), 134.2 (*o-Ph*), 153.4 (=*C*). ^{29}Si {1H} NMR (99 MHz, $CDCl_3$, 298 K, δ): −36.36.

Table 8. Entry 2, PSE (14): Scale: catalyst 5.0 mg, substrate 0.89 mmol. Yield 40%. ^{1}H NMR (500 MHz, $CDCl_3$, 298 K, δ): 4.63 (m, 4H, OC*H₂*), 5.96 (m, 2H, C*H*-C*H*), 7.31-8.21 (m, 10H, *Ph* & *Naph*). ^{13}C {^{1}H} NMR (125 MHz, $CDCl_3$, 298 K, δ): 58.0 (O*C*H$_2$), 109.0 (*C*H-*C*H), 125.2–137.1 (14 C, *Ph* & *Naph*). 153.3 (=*C*). ^{29}Si {1H} NMR (99 MHz, $CDCl_3$, 298 K, δ): −40.10.

Table 8. Entry 1, PSE (16): Scale: catalyst 5.0 mg, substrate 0.89 mmol. Yield 81%. ^{1}H NMR (500 MHz, $CDCl_3$, 298 K, δ): 4.63 (m, 4H, OC*H₂*), 6.16 (m, 2H, C*H*-C*H*), 7.36 (m, 3H, *m* & *p-Ph*), 7.60 (m, 2H, *o-Ph*). ^{13}C {^{1}H} NMR (125 MHz, $CDCl_3$, 298 K, δ): -3.8 (*C*H$_3$), 57.7 (O*C*H$_2$), 108.6 (*C*H-*C*H), 128.0 (*m-Ph*), 130.3 (*p-Ph*), 133.2 (*i-Ph*), 134.2 (*o-Ph*), 153.4 (=*C*). ^{29}Si {1H} NMR (99 MHz, $CDCl_3$, 298 K, δ): −39.61

Table 9. Entry 2, PSE (17): Scale: catalyst 5.0 mg, substrate 0.89 mmol. Yield 74%. ^{1}H NMR (500 MHz, $CDCl_3$, 298 K, δ): 4.65 (m, 4H, OC*H*$_2$), 6.07 (m, 2H, C*H*-C*H*), 7.33 (m, 6H, *m* & *p-Ph*), 7.62 (m, 4H, *o-Ph*). ^{13}C {1H} NMR (125 MHz, $CDCl_3$, 298 K, δ): 58.0 (O*C*H$_2$), 108.9 (*C*H-*C*H), 128.0 (*m-Ph*), 130.6 (*p-Ph*), 134.6 (*i-Ph*), 135.2 (*o-Ph*), 153.5 (=*C*). ^{29}Si {1H} NMR (99 MHz, $CDCl_3$, 298 K, δ): −40.22

Table 9. Entry 3, PSE (18): Scale: catalyst 5.0 mg, substrate 0.89 mmol. Yield 76%. ^{1}H NMR (500 MHz, $CDCl_3$, 298 K, δ): 4.65 (m, 4H, OC*H*$_2$), 6.07 (m, 2H, C*H*-C*H*), 7.33 (m, 6H, *m* & *p-Ph*), 7.62 (m, 4H, *o-Ph*). ^{13}C {1H} NMR (125 MHz, $CDCl_3$, 298 K, δ): 58.0 (O*C*H$_2$), 108.9 (*C*H-*C*H), 128.0 (*m-Ph*), 130.5 (*p-Ph*), 134.5 (*i-Ph*), 135.2 (*o-Ph*), 153.3 (=*C*). ^{29}Si {1H} NMR (99 MHz, $CDCl_3$, 298 K, δ): −41.03

Table 9. Entry 4, PSE (19): Scale: catalyst 5.0 mg, substrate 0.89 mmol. Yield 78%. ^{1}H NMR (500 MHz, $CDCl_3$, 298 K, δ): 4.38 (m, 4H, C*H*$_2$OC*H*$_2$), 4.73 (m, 4H, OC*H*$_2$), 6.15 (m, 2H, C*H*-C*H*), 7.32 (m, 6H, *m* & *p-Ph*), 7.64 (m, 4H, *o-Ph*), 9.57. ^{13}C {1H} NMR (125 MHz, $CDCl_3$, 298 K, δ): 58.8 (O*C*H$_2$), 63.1 (*C*H$_2$O*C*H$_2$), 108.9 (*C*H=CCH$_2$OSi), 110.6 (*C*H=CCH$_2$OCH$_2$), 128.0 (*m-Ph*), 130.6 (*p-Ph*), 134.9 (*i-Ph*), 135.2 (*o-Ph*), 151.4 (=*C*CH$_2$OSi), 154.0 (=*C*CH$_2$OCH$_2$). ^{29}Si {1H} NMR (99 MHz, $_{CDCl3}$, 298 K, δ): −40.42.

CHAPTER 5

RENEWABLE ISOHEXIDES-BASED, HYDROLYTICALLY DEGRADABLE POLY(SILYLETHER)S WITH HIGH THERMAL STABILITY

5.1 Introduction

Petrochemical-based synthetic polymers have played a significant role in the chemical industry due to their attractive properties like durability, elasticity, and other valuable features.[2,3] However, depletion of fossil fuel feedstock and environmental persistence of most petrochemical polymers limit their sustainability perspective.[228,229,230] To overcome these challenges, naturally originated and eco-friendly polymers have emerged as a major sustainable alternative.[231,232,233] In this regard, a variety of biobased renewable monomers and their derivatives have been extensively reported in the polymer synthesis.[234,235,236] Yet, the low thermal stability of most of the bio-based polymers, particularly low glass transition temperature (T_g) and low thermal decomposition (T_d) are a major limitation for high temperature industrial processes and applications.[237] On the other hand, design and development of various degradable polymers, hydrolytically or enzymatically, have been growing due to their wide diversity of applications in biomedical fields; representative examples include orthopedic implants, tissue engineering, drug delivery systems, and imaging agents.[238,239,240,241]

Driven by these considerations, isohexides (1,4:3,6-dianhydrohexitols) namely isosorbide (IS; 1,4:3,6-dianhydro-D-mannitol), isomannide (IM; 1,4:3,6-dianhydro-D-glucitol), and isoidide (II; 1,4:3,6-d-dianhydro-L-iditol) have received significant attention in polymer chemistry (Figure 27).[16,36] Isohexides are commonly prepared from carbohydrate sources via multistep reactions

including hydrogenation and dehydration.[242,243]Among the three isomers, IS, a C2 *exo,* C5 *endo* diol and IM, a C2/C5 *endo endo* diol are readily available due to their high yield production from D-sorbitol and D-mannitol, respectively, whereas the C2/C5 *exo exo* isomer, II is rare due to the negligible existence of its precursor, L-idose in plants.[43,244] These bifunctional isohexides are chiral and non-toxic;[245] the unique aliphatic bicyclic structure with two fused tetrahydrofuran rings provides high strength and rigidity to the molecule.[246] Consequently, the incorporation of isohexides into the polymer backbone can dramatically enhance the thermal and mechanical properties of polymers, which makes them attractive for high thermal applications such as flame-retardants.[247]

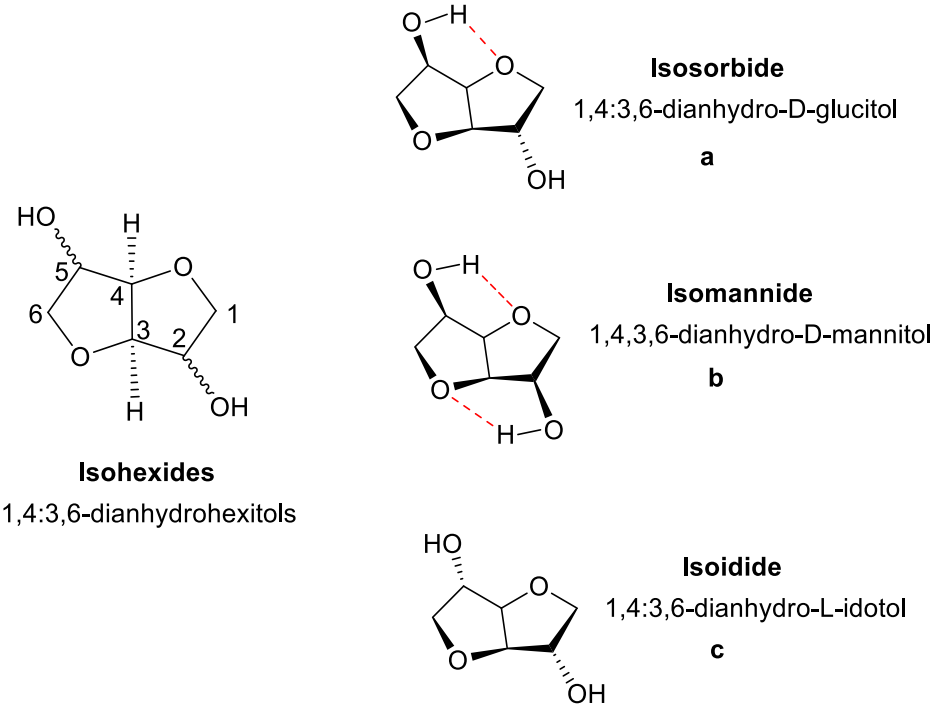

Figure 27**.** Chemical structure of isohexide (left). (a) isosorbide (b) isomannide, (c) isoidide. Dotted lines in (a) and (b) represent intramolecular hydrogen bonds

Interestingly, a variety of reactive functionalities such as amine, azide, isocyanate, carboxylic acid, and ester groups can be installed to replace or extend the original hydroxyl groups

for new starting materials, which further broadens the scope of accessible polymers.[248,249] Hence, a wide range of thermally stable polyesters,[250] polyamides,[251,252,253] poly(ester amide)s,[254] poly(ether imide)s,[255] polymethacrylates,[256] polyurethanes,[257] polycarbonates,[258] and poly(isosorbide fatty alkylates)[259] have been synthesized through either chain or step growth polymerization. Notably, poly(ester amide)s derived from isohexides have been shown to be degradable in bioanalogous studies and can be successfully used in biological applications.[260,261] To our knowledge, isohexide-based poly(silyl ether)s (PSEs) have not been reported to date, although there is significant industrial and academic interest in them. PSEs are potentially susceptible to hydrolytic degradation due to the presence of a labile silyl ether (Si–O–C) linkage.[262] A variety of synthetic methods have been reported to produce silylethers from various available resources.[263,264,265] One of the most commonly used methods is transition metal catalyzed condensation polymerization of alcohols with silanes.[59,60,68] Recently, we have reported the synthesis of degradable PSEs from biobased furan derivatives and silanes catalyzed by an air-stable manganese nitrido salen complex [$Mn^{V}N$(salen-3,5-$^{t}Bu_2$)] (**Mn-1**).[216,262] Mn has great potential as a sustainable alternative to precious metals such as platinum, rhodium, and ruthenium, because it is inexpensive, earth abundant, nontoxic and biocompatible. Use of readily available hydrosilanes as co-monomer over moisture sensitive chlorosilanes is also advantageous as nontoxic H_2 is the only by-product in this dehydrogenative coupling reactions. Motivated by these results, herein we present the synthesis and characterization of IS and IM based PSEs via polycondensation method catalyzed by **Mn-1**. Remarkably, PSEs derived from isohexides exhibit high glass transition and thermal stabilities, yet are hydrolytically degradable.

5.2 Results and discussion

The PSEs were synthesized by polycondensation reactions of IS and IM with secondary hydrosilanes (Scheme 7). The polymerization reactions were performed according to our recent work, and toluene was again chosen as the solvent in this study because of the formation of low molecular weight polymers in other solvents such as benzene, mesitylene, xylene, and dioxane (Table 11).

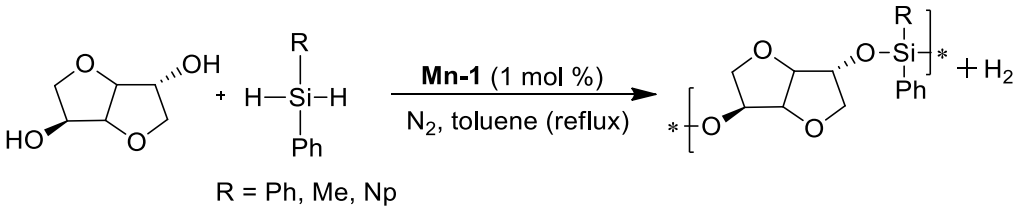

Scheme 7. Polymerization of IS with different silanes

The reactions were monitored at regular time intervals by NMR spectroscopy. The resulting PSEs were purified through the precipitation method, and the details are described in the experimental section. The reaction between Ph_2SiH_2 and IS went smoothly and the conversion reached >95% in less than 10 h, nevertheless, the reaction time was prolonged to 24 h (Table 12, entry 1). The disappearance of IS's hydroxyl peak at 2.96 ppm and silane hydrogens (Si*H*) at 4.92 ppm in ^{1}H NMR confirmed the consumption of starting materials. Appearance of six characteristic peaks at 71.3, 73.9, 76.0, 78.0, 82.0, and 88.3 ppm in ^{13}C NMR spectrum (Figure 28b) indicates that the resulting PSE (21) still possesses the C2 *exo* and C5 *endo* configurations. Besides, attribution of four peaks in ^{13}C NMR between 128.0 and 140.0 ppm and a single peak in ^{29}Si NMR at -31.48 ppm confirms the presence of diphenylsilyl moiety in the resultant polymer. The GPC analysis showed the M_n as 3300 g/mol with poly dispersity index (Đ) of 1.31.

Table 11. Polycondensation reaction of IS and Ph_2SiH_2 in different solvents[a]

Entry	PSE	Solvent	Time (h)	M_n g/mol [b]	Đ [b]
1	PSE 21	Dioxane	24	2500	1.25
2	PSE 22	Benzene	24	2400	1.42
3	PSE 23	Xylenes	24	2300	1.31
4	PSE 24	Mesitylene	24	2400	1.29

[a]Substrate, 0.87−0.90 mmol; silane, 1.0 equiv; and Mn catalyst **1**, 1.0 mol %. 1 mL of solvent under reflux. [b] Determined by gel permeation chromatography (GPC) calibrated with polystyrene standards

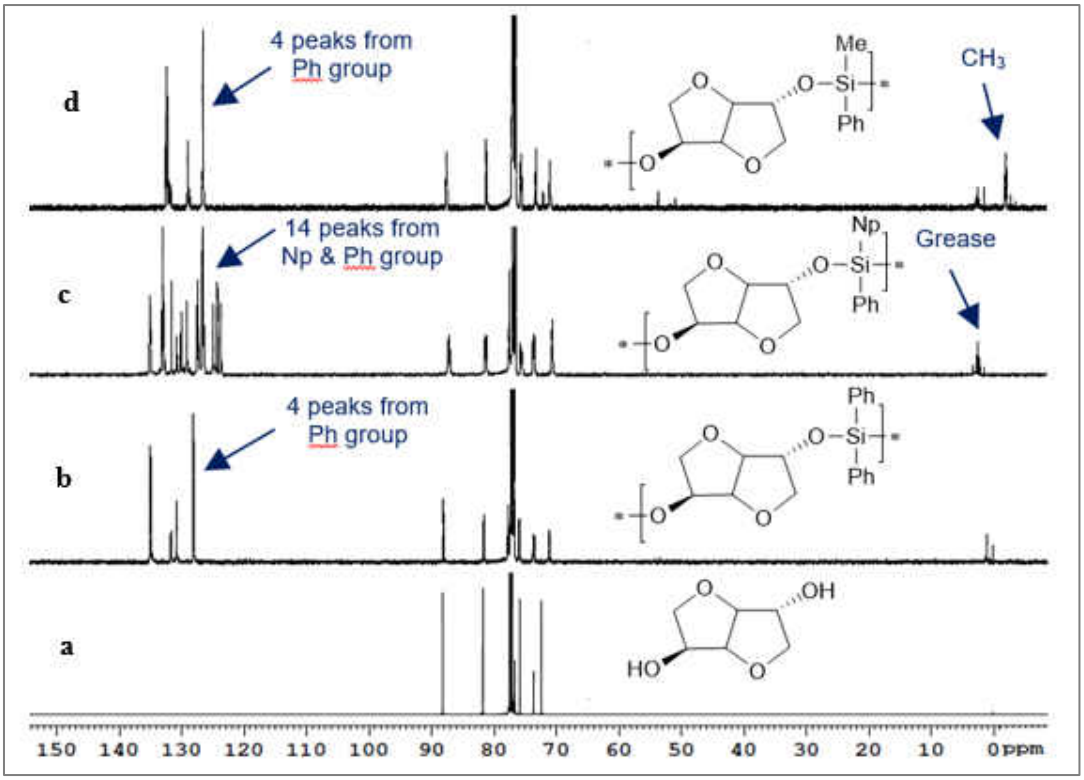

Figure 28. Comparison of ^{13}C NMR spectra for IS and IS-derived PSEs. (a) IS monomer, (b) PSE (25), (c) PSE (27), (d) PSE (28)

In another reaction between the same monomers over 40 h, the M_n of the resulting PSE (26) was increased to 5700 g/mol (Table 12, entry 2). Compared with PSEs derived from 2,5-

bis(hydroxymethyl) furan under identical conditions,[262] IS has produced lower molecular weight PSEs. Although direct comparison of GPC-based molecular weights of different polymers should be taken with caution, we attribute it to the secondary hydroxyl groups of isohexides being relatively less reactive than primary hydroxyl groups, as observed in similar reactions.[175,216] Additionally, the intramolecular hydrogen bonding between the proton of endo hydroxyl group and an endocyclic oxygen may also decrease the reactivity of the *endo* hydroxyl group (see Figure 27).[266]

Table 12. Polymerization of IS with different hydrosilanes

Entry	PSE	Structure (time h)	M_n (g/mol)[b]	Đ[b]	Yield %
1	PSE 25	$ISPh_2$-(24)	3300	1.31	78
2	PSE 26	$ISPh_2$-(40)	5700	1.66	86
3	PSE 27	ISPhNp-(40)	4000	1.44	70
4	PSE 28	ISPhMe-(40)	3500	1.57	72

[a] Reaction conditions: substrate, 0.87−0.90 mmol; silane, 1.0 equiv; and Mn catalyst **1**, 1.0 mol %. Conversion is >95% as judged by the consumption of hydrosilanes by NMR. [b] Determined by gel permeation chromatography (GPC) calibrated with polystyrene standards

To explore the reactivity of hydrosilanes in manganese catalyzed polycondensation reactions, sterically hindered 1-naphthylphenylsilane ($PhNpSiH_2$) was next employed in the reaction. A low molecular weight PSE (27), M_n = 4000 g/mol was produced at 40 h (Table 12, entry 3). The appearance of fourteen peaks between 125.0 and 145.0 ppm in ^{13}C NMR confirms the incorporation of naphthylphenyl moiety into the polymer structure (Figure 28c). If a less hindered silane, methylphenylsilane ($PhMeSiH_2$) was used, PSE (28) with even lower molecular weight was obtained (Table 12, entry 4), presumably due to the lower reactivity of $PhMeSiH_2$ than

Ph_2SiH_2 in the reaction. The appearance of silylmethyl peak at -3.50 ppm in ^{13}C NMR confirms the formation of PSE (28) (Figure 28d).

The formation of low molecular weight polymers with hindered and alkyl hydrosilanes in **Mn-1** catalyzed reactions are consistent with our previous observations. These polymers were further characterized by FT-IR. As shown in Figure 29, the disappearance of hydroxyl (OH) and Si–H stretching frequencies around ν = 3300 cm^{-1} and 2100 cm^{-1} respectively in FT-IR also supports the formation of PSEs between isohexide and hydrosilanes. The entire series of PSEs exhibit similar FT-IR absorption patterns.

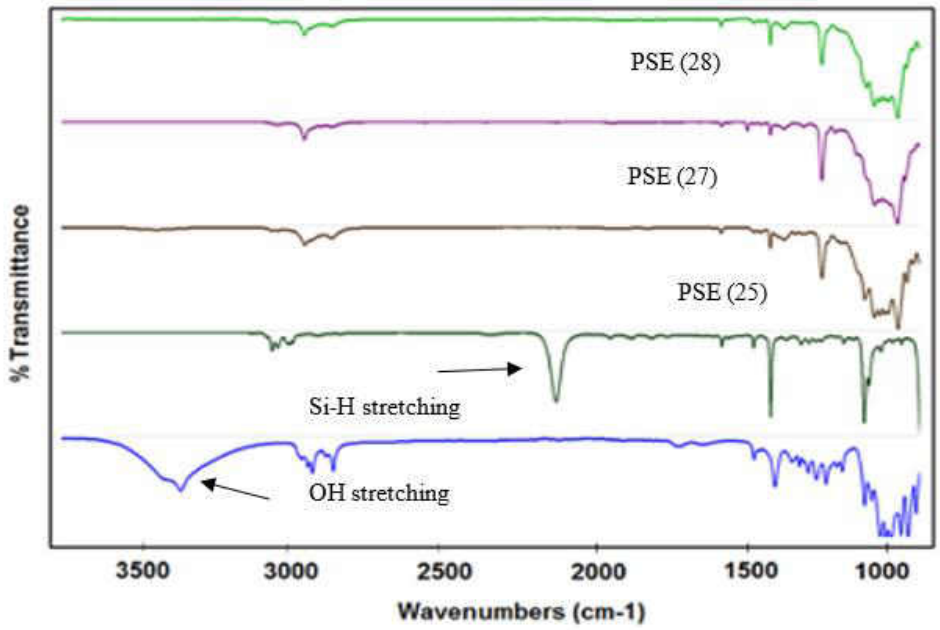

Figure 29**.** Attenuated total reflectance FT-IR spectra of isosorbide (bottom), hydrosilane, PSE (25), PSE (27), and PSE (28)

5.2.1 Synthesis of PSEs from isosorbide and isomannide at extended reaction times

In consideration of the low reactivity of isohexides and the step-growth polymerization pathway of current polycondensation reactions, we further increased the reaction time to synthesize polymers with high molecular weight. Thus, a new reaction between IS and Ph_2SiH_2

was performed under optimized conditions for 80 h. GPC analysis displayed that high molecular weight polymer PSE (29) was indeed achieved, and M_n was observed to be 17000 g/mol with Đ of 2.08 (Table 13, entry 1). Therefore, the reaction time was kept as 80 h in further reactions. Similarly, the longer reaction time boosted the molecular weight of the PSE (30) from IS and sterically hindered $PhNpSiH_2$ up to 14000 g/mol with the Đ of 2.00 (Table 13, entry 2). In another reaction between a less active silane, $PhMeSiH_2$ and IS, the molecular weight of the resulting PSE (31) was observed as 13300 g/mol with the Đ of 1.92 (Table 13, entry 3).

Table 13. Polymerization of IS and IM with hydrosilanes

Entry	**PSE**	**Structure (time h)**	**M_n (g/mol)[b]**	**Đ[b]**	**Yield %**
1	PSE 29	$ISPh_2$-(80)	17000	2.08	90
2	PSE 30	ISPhNp-(80)	14000	2.00	82
3	PSE 31	ISPhMe-(80)	13300	1.92	73
4	PSE 32	$IMPh_2$-(80)	13000	2.25	71
5	PSE 33	IMPhNp-(80)	9500	1.56	72
6	PSE 34	IMPhMe-(80)	6100	2.05	70

[a]Reaction conditions: substrate, 1.78 mmol; silane, 1.0 equiv; and catalyst **Mn-1** 1.0 mol %. Conversion is >95% as judged by the consumption of hydrosilanes by NMR. [b]Determined by GPC calibrated with polystyrene standards.

Encouraged by these results, IM, a symmetric isohexide was examined as monomer and polymerization reactions were performed with the three hydrosilanes mentioned above. Reaction with Ph_2SiH_2 under the typical polymerization conditions resulted in PSE (32), exhibiting M_n of 13000 g/mol with Đ of 2.25 (Table 13, entry 4). In contrast to IS-derived PSE (29), IM-derived PSE (32) have displayed significantly different NMR spectra. Appearance of only three peaks at

3.70, 4.20, and 4.40 ppm in ^{1}H NMR for the eight alicyclic protons and three peaks at 72.0, 75.3, and 82.0 ppm in ^{13}C NMR demonstrates the structural difference of IS and IM, which is in agreement with the symmetric nature of IM. We next performed two polymerization reactions under standard conditions with $PhNpSiH_2$ and $PhMeSiH_2$, as depicted in Table 13 (Entries 5 and 6), M_n values of the resulting PSEs (33) and (34) were 9500 g/mol and 6100 g/mol, respectively. Comparatively, IM-derived PSEs (32-34) showed lower molecular weights than the corresponding IS-derived PSEs (29-31). These results suggest that orientation of hydroxyl groups of isohexides has a significant influence on their reactivity: the two *endo* hydroxyl groups of IM could both participate in intramolecular hydrogen bonding with adjacent oxygen atom, whereas only one endo hydroxyl group for intramolecular hydrogen bonding in IS (Figure 27). For a direct comparison of IS and IM, reactions with Ph_2SiH_2 were performed under identical conditions, which demonstrated that IS reacted faster than IM in the reaction, though the difference was small. Nevertheless, all these polymerization reactions gave reasonable isolated yields of 70-90% (Table 13).

Thermo gravimetric analysis: The thermal stabilities of the PSEs were evaluated by TGA from 30 to 800 °C under inert (nitrogen) atmosphere, and results are illustrated in Figure 30. All the synthesized PSEs have displayed a single-stage decomposition profile. Irrespective of the molecular weights and polymer backbone structure, majority of PSEs have shown a remarkable thermal stability as indicated by $T_{-5\%}$ around 347-446 ºC and $T_{-50\%}$ between 470-509 ºC, which is at the high end of the PSEs reported to date.[70,168] PSEs derived from $PhNpSiH_2$, namely PSE (27), (30), and (33) have exhibited the highest $T_{-50\%}$, while PhMeSiH2- derived PSEs such as PSE (28), (31), and (34) showed the lowest $T_{-50\%}$. The $T_{-50\%}$. values (480-490 °C) of Ph_2SiH_2-derived PSEs (25, 26, 29, and 32) were in between the values of $PhNpSiH_2$ and $PhMeSiH_2$ derived PSEs. This observed trend illustrates that steric bulk around the silicon has played an important role in

enhancing the thermal stability of the PSEs. In this context, it is worth noting that these PSEs exhibit high thermal stabilities (as judged by $T_{-5\%}$, $T_{-50\%}$, or T_{max} /°C) when compared to other isohexide-based polymers such as polyesters, polyamides, and poly(ether amides).[252,267]

Furthermore, molecular weights of polymers also can impact the thermal stability of PSEs, which is evident when comparing the M_n and $T_{-50\%}$ of PSEs (25), (26), and (29). The PSE (25) with low M_n of 3300 g/mol has displayed $T_{-50\%}$ of 487 °C, whereas PSE (29) with high M_n of 17000 g/mol has displayed $T_{-50\%}$ of 492 °C.

5.2.2 Thermal analysis

The thermal properties of these PSEs have been comparatively examined by techniques including differential scanning calorimetry (DSC) and TGA, and the results are summarized in Table 14.

Table 14. DSC and TGA data of PSEs

Entry	PSE	Structure (time)	T_g/°C[b]	$T_{-5\%}$/°C[c]	$T_{-50\%}$/°C[c]	T_{max} /°C[c]	Final residue % (800 °C) [c]
1	PSE 25	ISPh2-(24)	75	382	487	479	32
2	PSE 26	ISPh2-(40)	78	408	488	481	18
3	PSE 27	ISPhNp-(40)	115	419	495	482	25
4	PSE 28	ISPhMe-(40)	38	347	482	470	26
5	PSE 29	ISPh2-(80)	85	410	498	484	30
6	PSE 30	ISPhNp-(80)	120	446	509	489	27
7	PSE 31	ISPhMe-(80)	43	397	486	476	27
8	PSE 32	IMPh2-(80)	76	384	494	484	27

9	PSE 33	IMPhNp-(80)	116	432	505	480	30
10	PSE 34	IMPhMe-(80)	42	367	484	476	27

[a]Reaction conditions: substrate, 1.78 mmol; silane, 1.0 equiv; and catalyst Mn-1, 1.0 mol %. [b]Determined by DSC. [c]Determined from TGA. $T_{-5\%}$ and $T_{-50\%}$ refer to the temperatures at which 5% and 50% weight losses were observed, respectively, whereas T_{max} refers to the temperatures at which maximum rate of weight loss occurs

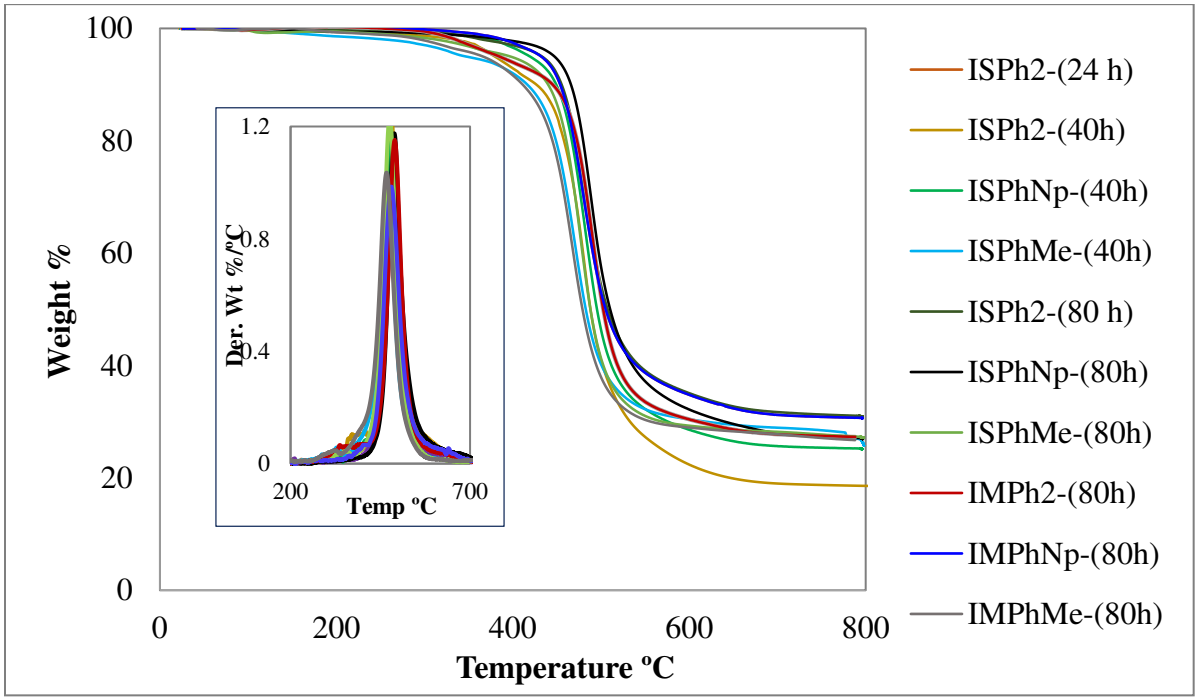

Figure 30. TGA thermograms of isohexide-derived PSEs, recorded from 30 to 800 °C at a heating rate of 20 °C/min under a N_2 atmosphere. Inset is the DTG curve of the same data set.

Differential scanning calorimetry: Glass transition data acquired from DSC analysis are listed in Table 14, and thermograms from the second heating cycles are displayed in Figures 31-33. It can be seen that the T_g values of these PSEs were in the range of 38-120 °C, and only T_g was observed without any melting or crystallization transitions, which suggests they are amorphous in

nature. As noted above, these PSEs generally feature higher T_g's than other isohexide-based polymers including polyesters, polyurethanes, and poly(ester urethanes),[232,245,268] though a few polyesters, poly(ether imides), and IS incorporated poly(butylene terephthalate)s have greater T_g's.[255] In this study, the $PhNpSiH_2$-derived PSEs (27), (30), and (33) have displayed the highest T_g's at 115, 120 and 116 ºC, respectively, which could be attributed to the presence of a highly hindered naphthyl group in the polymer backbone. Notably, polyesters based on isohexides with rigid aromatic diacids can reach comparable T_g's (up to 105 ºC).[267] Similar to the trend in thermal degradation temperatures observed above, the $PhMeSiH_2$-derived PSEs (28), (31) and (34) with a less hindered methyl group have exhibited comparatively lowest T_g's (38-43 ºC), while the Ph_2SiH_2-derived PSEs (25), (26), (29) and (32) have shown modest T_g's in between (75–85 °C). In addition, high molecular weight PSEs have shown higher T_g's over low molecular weight PSEs (25, 26, 29). All these observations are in accord with the literature report that the T_g values of polymers can be enhanced by high molecular weight and sterically hindered groups.[269]

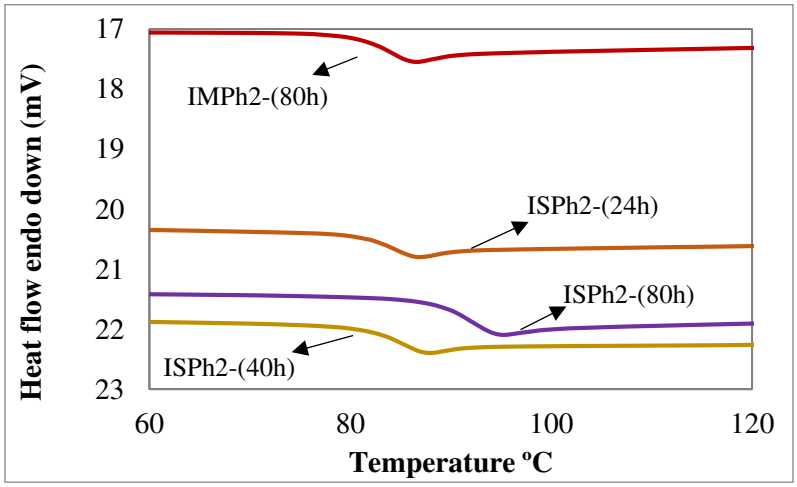

Figure 31. DSC thermograms from the second heating cycles of the PSEs of IS and IM with Ph_2SiH_2.

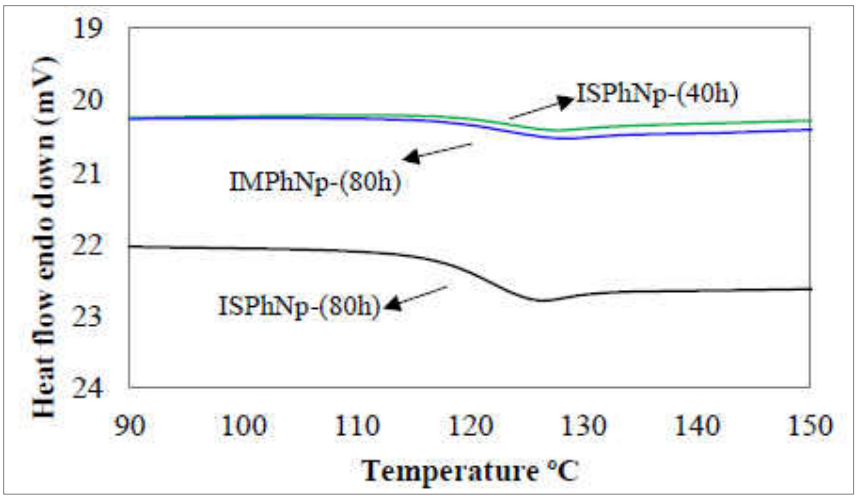

Figure 32. DSC thermograms from the second heating cycles of the PSEs of IS and IM with $PhNpSiH_2$.

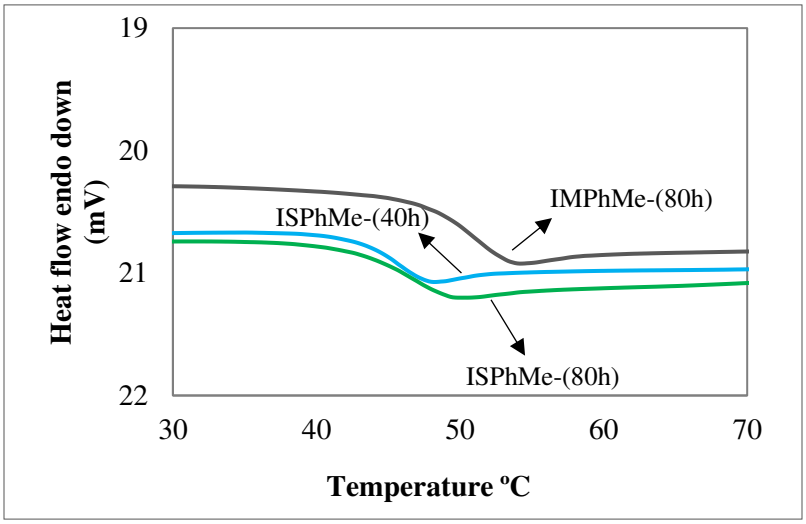

Figure 33. DSC thermograms from the second heating cycles of the PSEs of IS and IM with $PhMeSiH_2$

To better understand the role of the rigidity of isohexides in affecting the thermal properties of PSEs, we have compared the glass transition temperatures of IS-derived PSEs with that of 2,5-bis(hydroxymethyl)furan (BHMF) derived PSEs (Figure 34). It is clear that IS-derived PSEs have higher T_g's than the corresponding BHMF-derived PSEs, and in both series, the T_g's increase with the steric bulk at the silicon, i.e. in the order of SiPhMe < $SiPh_2$ < SiPhNp, in line with the literature

observations.[270] Furthermore, the difference in T_g's between the two series are observed to be 75, 92, and 35 ºC respectively, for Ph_2SiH_2, $PhNpSiH_2$, and $PhMeSiH_2$ derived PSEs. In other words, the same bulky SiPhNp group would impart a larger influence when combined with a rigid, secondary diol than with a primary diol. This suggests a synergy between the steric bulk and rigidity of two co-monomers in affecting the thermal properties of the polymers.

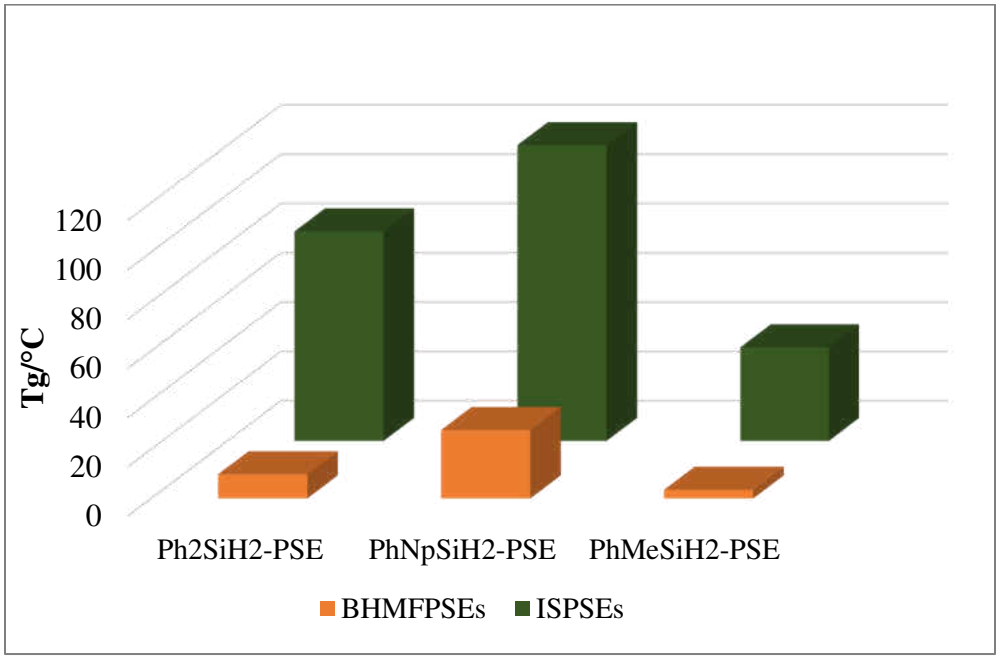

Figure 34. Comparison of *Tg*'s of IS-PSEs with BHMF-PSEs

5.2.3. Hydrolytic degradation

Environmental degradability is one of the key considerations in the sustainable development and applications.[271] Hydrolytically sensitive polymers are of special interest owing to their potential applications in biomedical fields such as in the delivery of protein based vaccines and nucleic acids, and treatment of inflammatory related diseases.[272,273,274] We have investigated the degradation behavior of PSEs under various conditions by monitoring the molecular weight

change over time (Figure 35). A high molecular weight PSE (29) was chosen as a representative. As anticipated, no or little degradation occurred at neutral conditions, but a considerable decrease in the molecular weight was observed in the first few hours when 2 vol % HCl/H_2O (pH 2) in THF was used as the medium at room temperature (RT). However, the degradation slowed down and resulted in partial degradation with Mn of 6900 g/mol in 24 h. This may suggest that the extent of degradation depends on the amount of acidic hydrogens available.[262] In accord with this, when the amount of HCl/H_2O (pH 2) was increased to 10 vol %, a rapid decrease in the molecular weight was observed and the total degradation was completed in less than 10 h. Raising the temperature greatly accelerated the degradation process, as a complete degradation occurred in less than an hour when the temperature was raised to 50 °C from RT. In addition, PSE (29) also underwent hydrolysis in basic medium, as partial degradation was observed when 2 vol % KOH/H_2O (pH 11) in THF was used as the medium at RT. The extent of degradation apparently correlated with the amount of available hydroxide ions, as the resultant polymer had a higher molecular weight (~8200 g/mol) compared to that of 2 vol % HCl/H_2O (pH 2) condition.

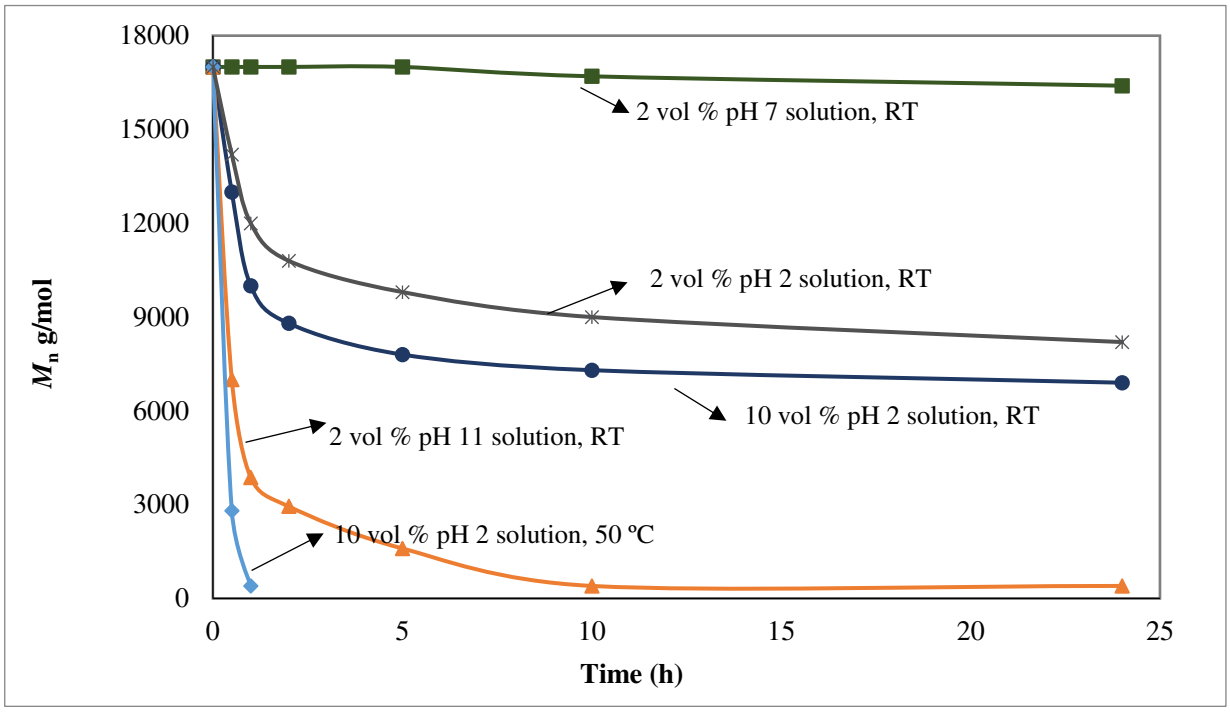

Figure 35**.** Degradation plots of PSE (29) (M_n vs time) under neutral, acidic, and basic conditions. Conditions employed are 0.02 mL of HCl/H2O (pH 2) in 0.98 mL of THF (2 vol % pH 2) and 0.10 mL of HCl/H2O (pH 2) in 0.90 mL of THF (10 vol % pH 2) at RT or 50 ºC and 0.02 mL of KOH/H_2O (pH 11) in 0.98 mL of THF (2 vol % pH 11. ■ 2 vol % pH 7 solution, RT. ∗ 2 vol % pH 2 solution, RT. ● 10 vol % pH 2 solution, RT. ► 10 vol % pH 2 solution, 50 ºC. ♦ 2 vol % pH 11 solution, RT.

To explore the effect of steric hindrance in degradation, IS-derived PSEs with Ph_2SiH_2 (29), $PhNpSiH_2$ (30), and $PhMeSiH_2$ (31) were compared in the degradation processes. As expected, all three PSEs exhibited a rapid initial degradation under the similar conditions using 2 vol. % HCl/H_2O (pH 2) acidic medium (Figure 36). Apparently, PSE (30) with highly hindered naphthyl group has shown some hydrolytic stability over the other two PSEs. It should be noted that complete degradation was not observed even after six days. Similar dependence on the availability of acidic hydrogens has been mentioned in the degradation of PSEs.[146]

Additionally, gas chromatography-mass spectrometry (GC/MS) analysis on the fully degraded samples of PSE (29) clearly showed the presence of the starting monomer IS (m/z 146.1 g/mol) and silanol derivatives, such as diphenylsilanediol (m/z 216 g/mol), hexaphenylcyclotrisiloxane (m/z 594 g/mol), and octaphenylcyclotetrasiloxane (m/z 792.3 g/mol).

Also, another compound having two IS and one Ph_2SiH_2 units (m/z of 472.1 g/mol) was observed. Quantification by NMR with an internal standard ($PhMe_3Si$) indicated nearly quantitative regeneration of the diol monomer IS. Since no IS degradation products were detected, we assume the mechanism of hydrolytic degradation relied on the labile Si-O-C linkage. It is worth mentioning that the degradation products of PSEs, mainly alcohols and silanol derivatives, are nontoxic and neutral, which would lead to no extreme pH changes in the surrounding environment upon degradation.[275]

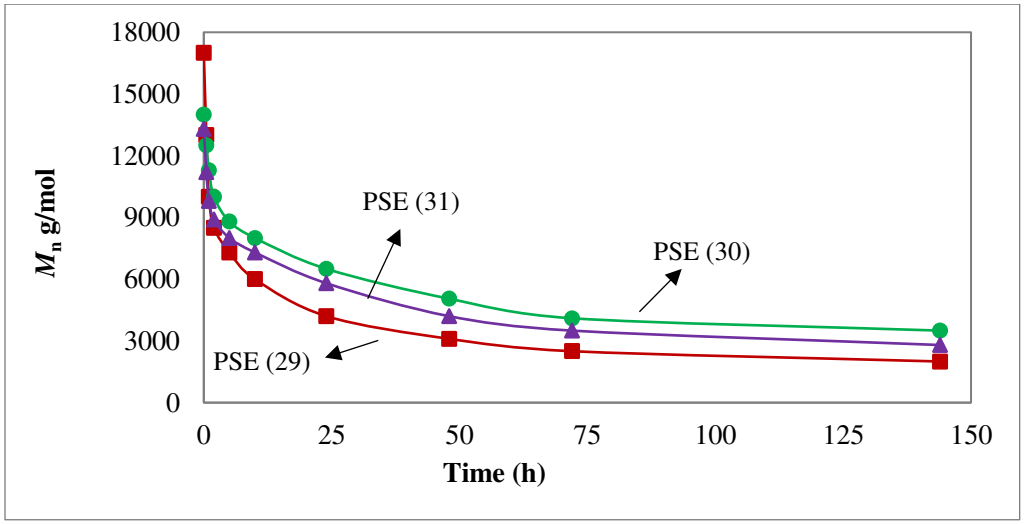

Figure 36. Degradation plots of PSE (29, 30, and 31) (M_n vs time) under acidic conditions. Conditions employed are 0.02 mL of HCl/H_2O (pH 2) in 0.98 mL of THF (2 vol % pH 2) at RT. ■ PSE (29). ● PSE (30). ▲ PSE (31).

5.3. Conclusions

Degradable and partially biobased poly(silylether)s (PSEs) have been synthesized by manganese catalyzed dehydrogenative cross coupling between isohexides and a series of hydrosilanes. The PSEs have shown excellent thermal stabilities ($T_{-5\%}$ up to 446 °C and $T_{-50\%}$ up to 509 °C) and high glass transition temperatures (T_g up to 120 °C). This is attributed to the presence of built-in rigidity from isohexide bicyclic rings, as well as the bulky substituent groups like naphthyl on silicon. The two factors may interact synergistically in enhancing the thermal

stability of PSEs. At the same time, these PSEs are readily degradable via hydrolysis under acidic and basic conditions, which can be modulated by the available active ions (H^+ and OH^-) and temperature. This combination of high thermal resistance and easy hydrolytic degradability may lead to novel applications, particularly in consideration of their low toxicity and partially biobased origin. Further studies on improving the properties of PSEs and their potential applications are underway in our lab.

5.4. Experimental section

Materials, methods, and instrumentation. Isosorbide, isomannide and hydrosilanes were purchased from Sigma Aldrich. Deuterated solvents were purchased from the Cambridge Isotope Laboratories. Solvents were degassed and dried over molecular sieves (4 Å) overnight prior to use. Glassware was dried overnight prior to use. ^{1}H, ^{13}C, and ^{29}Si NMR spectra were recorded on a Bruker AVANCE 500 NMR spectrometer in deuterated chloroform ($CDCl_3$) with tetramethylsilane (TMS) as the internal reference. FT-IR was performed on a Thermo Scientific Nicolet iS5 FT-IR instrument, and analyzed with OMNIC 8.2 software. The samples for analysis were directly loaded as a thin film using an iD5 ATR accessory. GPC analysis was performed on a Varian Prostar system equipped with a PLgel 5 μm Mixed-D column and a Prostar 355 refractive index (RI) detector. THF was used as the eluent and elution rate was maintained at 1 mL/min (20 °C). Polystyrene standards were used for the instrument calibration. TGA were performed on a SDT Q 600 instrument with Advantage software. The samples in Al_2O_3 cups were heated in the 30 to 800 °C range with a ramp rate of 20 °C/min and a flow rate of 100 mL/min of nitrogen (furnace purge gas). DSC thermograms were collected on a PerkinElmer Jade differential scanning calorimeter calibrated with indium and zinc standards. Samples were analyzed in hermetically sealed pans under an inert (N_2) atmosphere (20 mL/min). Glass transition temperatures (T_g's) of

PSEs were determined from the second heating cycles from −30 to 350 °C with a heating/cooling rate of 20 °C/min. Obtained data were analyzed using the Pyris V9.0.2 software. GC-MS analyses were performed with a 5890 GC with 5972 MS equipped with an autosampler (6890 series, Agilent Technologies, Santa Clara, CA, USA). Injections were performed in the split mode with 10:1 ratio and the injection volume was 1 μL. The temperature program started at 70°C for 1 min, followed by a gradient of 40 °C/min to 140 °C, then a gradient of 10 °C/min to 350 °C and held for 10 min. The separation was performed using a 39.7 m long Agilent HP-5MS column. A constant carrier gas (helium) at a flow rate of 1.5 mL/min (total flow is 19.5 mL/min) was maintained during the analysis. The MS data in total ion chromatograms (TIC) were acquired in the mass range of m/z of 35–1000 at a scan rate of 1.56 scan/s.

General procedure for the synthesis and purification of PSEs. The polymerization reactions were performed under an inert atmosphere of dry nitrogen (N_2). Oil baths equipped with digital thermometers and controllers were used to set and read the temperature during the reaction. For a typical synthesis, to a Schlenk flask (50−100 mL) fitted with a magnetic stirrer, a condenser, and nitrogen inlet and outlet, catalyst [$Mn^{V}N$(salen-3,5-$^{t}Bu_2$)] (**Mn-1**) (10 mg, 0.018 mmol, 1 mol %) and stoichiometric equivalents of isohexide or isomannide and hydrosilane (1.78 mmol of each, 1:1 ratio) were added, followed by the addition of 2.0-2.5 mL of solvent inside the glovebox. The reaction flask was then taken out, connected to a Schlenk line under nitrogen flow, and heated to reflux for specified time. The reaction progress was monitored periodically taking out a small amount of samples for NMR analyses. After the reaction, a small amount of DCM (1−2 mL) was first added to the brown colored crude reaction mixture, and MeOH was then added portion-wise (10−12 mL) which resulted in a biphasic mixture. The top layer containing the unreacted material was removed, and the bottom pale/off-white colored solid/viscous part was washed with MeOH

for a couple of times. Finally, the resulting polymers were dried under vacuum to a constant weight for characterization.

Degradation procedure of PSEs. To a sample vial PSEs (15-16 mg), calculated amount of THF, deionized water, and calculated amount of HCl/H_2O or KOH/H_2O were added. The amounts for the neutral condition were 0.98 mL of THF and 0.02 mL of deionized water; for acidic conditions 0.98 mL of THF and 0.02 mL HCl/H_2O (pH 2), and 0.90 mL of THF and 0.10 mL of HCl/H_2O (pH 2), for basic conditions 0.98 mL of THF and 0.02 mL KOH/H_2O (pH 11). A magnetic stir bar was added and the homogenized mixture was stirred on a magnetic stirrer at RT or 50 ºC. Samples were taken at specified time intervals and analyzed by GPC.

NMR characterization data

Table 12. Entry 1, IS+Ph2SiH2 (24h), PSE (25): Scale: catalyst 10 mg, substrate 1.78 mmol. Yield 78%. ^{1}H NMR (500 MHz, $CDCl_3$, 298 K, δ): 3.47 (m, 1H, -C*H*$_2$), 3.63 (m, 1H, -C*H*$_2$), 3.89-3.98 (m, 2H, -C*H*$_2$), 4.35-4.58 (m, 4H, -OC*H* & -C*H* bridged), 7.37 (m, 6H, *m* & *p-Ph*), 7.63 (m, 4H, *o-Ph*). ^{13}C {1H} NMR (125 MHz, $CDCl_3$, 298 K, δ): 71.30, 73.86, 76.09, 77.19, 77.89, 81.82, 88.83 (6 C from IS unit), 128.30 (*m-Ph*), 131.04 (*p-Ph*), 131.81 (*i-Ph*), 135.14 (*o-Ph*). ^{29}Si {1H} NMR (99 MHz, $CDCl_3$, 298 K, δ): -31.48.

Table 12. Entry 2, IS+Ph2SiH2 (40h), PSE (26): Scale: catalyst 10 mg, substrate 1.78 mmol. Yield 86%. ^{1}H NMR (500 MHz, $CDCl_3$, 298 K, δ): Same as PSE (25)

Table 12. Entry 3, IS+PhNpSiH2 (40h), PSE (27): Scale: catalyst 10 mg, substrate 1.78 mmol. Yield 70%. ^{1}H NMR (500 MHz, $CDCl_3$, 298 K, δ): 3.34 (m, 2H, -C*H*$_2$), 3.37-3.96 (m, 2H, -C*H*$_2$), 4.42-4.54 (m, 4H, -OC*H* & -C*H* bridged), 7.37-7.56 (m, 6H, *m* & *p-Ph*), 7.69 (m, 1H, *Ph*), 7.79 (m, 1H, *o-Ph*), 7.93 (m, 1H, *o-Ph*), 8.03 (m, 1H, *o-Ph*). ^{13}C {1H} NMR (125 MHz, $CDCl_3$, 298 K, δ): -3.35 (-Ph*Me*), 71.01, 73.93, 76.12, 78.01, 81.84, 87.94 (6 C peaks from -IS unit), 128.36,

125.9, 126.6, 128.31, 129.0, 129.26, 130.96, 131.88, 132.58, 133.38, 133.92, 134.77, 134.91, 136.92 (14 C peaks from -*PhNp* unit). ^{29}Si {1H} NMR (99 MHz, $CDCl_3$, 298 K, δ): -30.31.

Table 12. Entry 4, IS+PhMeSiH2 (40h), PSE (28): Scale: catalyst 10 mg, substrate 1.78 mmol. Yield 72%. ^{1}H NMR (500 MHz, $CDCl_3$, 298 K, δ): 0.43 (m, 3H, Ph*Me*) 3.52 (m, 2H, -CH_2), 3.66 (m, 2H, -CH_2), 4.37-4.48 (m, 4H, -OC*H* & -C*H* bridged), 7.37 (m, 3H, *m* & *p-Ph*), 7.61 (m, 2H, *o-Ph*). ^{13}C {1H} NMR (125 MHz, $CDCl_3$, 298 K, δ): -3.35 (-Ph*Me*), 71.35, 72.52, 73.61, 76.03, 77.60, 81.76 (6 C from IS unit), 128.23 (*m-Ph*), 130.71 (*p-Ph*), 133.60 (*i-Ph*), 134.12 (*o-Ph*). ^{29}Si {1H} NMR (99 MHz, $CDCl_3$, 298 K, δ): -16.47.

Table 13. Entry 1, IS+Ph2SiH2 (80h), PSE (29): Scale: catalyst 10 mg, substrate 1.78 mmol. Yield 90%. ^{1}H NMR (500 MHz, $CDCl_3$, 298 K, δ): Same as PSE (25)

Table 13. Entry 2, IS+PhNpSiH2 (80h), PSE (30): Scale: catalyst 10 mg, substrate 1.78 mmol. Yield 82%. ^{1}H NMR (500 MHz, $CDCl_3$, 298 K, δ): Same as PSE (27)

Table 13. Entry 3, IS+PhMeSiH2 (80h), PSE (31): Scale: catalyst 10 mg, substrate 1.78 mmol. Yield 73%. ^{1}H NMR (500 MHz, $CDCl_3$, 298 K, δ): Same as PSE (28)

Table 13. Entry 2, IM+Ph2SiH2 (80h), PSE (32): Scale: catalyst 10 mg, substrate 1.78 mmol. Yield 71%. ^{1}H NMR (500 MHz, $CDCl_3$, 298 K, δ): 3.89 (m, 2H, -CH_2), 4.10 (m, 2H, -CH_2), 4.50 (m, 2H, -OC*H*), 4.79 (m, 2H, -C*H* bridged), 7.37-7.41 (m, 6H, *m* & *p-Ph*), 7.71-7.72 (m, 4H, *o-Ph*). ^{13}C {1H} NMR (125 MHz, $CDCl_3$, 298 K, δ): 74.04, 77.95, 82.96 (3 C from IM unit), 127.88 (*m-Ph*), 131.15 (*p-Ph*), 134.55 (*i-Ph*), 135.78 (*o-Ph*). ^{29}Si {1H} NMR (99 MHz, $CDCl_3$, 298 K, δ): -29.95.

Table 13. Entry 2, IM+PhNpSiH2 (80h), PSE (33): Scale: catalyst 10 mg, substrate 1.78 mmol. Yield 72%. ^{1}H NMR (500 MHz, $CDCl_3$, 298 K, δ): 3.67 (m, H, -CH_2), 4.19 (m, 2H, -OC*H*), 4.79 (m, 2H, -C*H* bridged), 7.31-7.46 (m, 6H, *m* & *p-Ph*), 7.69-7.89 (m, 2H, *Ph*), 8.10-8.17 (m, 2H,

Ph). ^{13}C {1H} NMR (125 MHz, $CDCl_3$, 298 K, δ): 72.53, 73.81.46 (3 C from IM unit), 125.35, 125.87, 126.44, 127.92, 128.24, 128.48, 128.97, 129.36, 130.85, 131.72, 132.71, 133.39, 135.02, 137.06 (14 C peaks from -*PhNp* unit). ^{29}Si {1H} NMR (99 MHz, $CDCl_3$, 298 K, δ): -29.69

Table 13. Entry 2, IM+PhMeSiH2 (80h), PSE (34): Scale: catalyst 10 mg, substrate 1.78 mmol. Yield 70%. ^{1}H NMR (500 MHz, $CDCl_3$, 298 K, δ): 0.49 (m, 3H, -Ph*Me*), 3.84 (m, 1H, -CH_2), 4.02 (m, 2H, -CH_2), 4.27 (m, 1H, -CH_2), 4.35 (m, 1H, -OC*H*), 4.42 (m, 1H, -OC*H*), 4.75 (m, 2H, -C*H* bridged), 7.37 (m, 3H, *m* & *p-Ph*), 7.71 (m, 4H, *o-Ph*). ^{13}C {1H} NMR (125 MHz, $CDCl_3$, 298 K, δ): 0.29 (-Ph*Me*) 73.46, 78.16, 82.59 (3 C from IM unit), 127.70 (*m-Ph*), 129.74 (*p-Ph*), 133.34 (*i-Ph*), 137.53 (*o-Ph*). ^{29}Si {1H} NMR (99 MHz, $CDCl_3$, 298 K, δ): -16.25.

CHAPTER 6

HYDROBORATION OF CARBONYLS BY A MANGANESE CATALYST

6.1. Introduction

The chemical transformations of unsaturated organic compounds plays a significant role in fine chemical production and synthesis of complex organic molecules.[276,277,278,279] Among the several unsaturated compounds such as C=C, C=N, C=O, and C≡C, reduction of carbonyl functional groups to alcohols is a key transformation since the resultant products, boronate esters, are a wide variety of valuable intermediates.[280] Hydroboration has been found to be one of the significant fundamental and powerful tools to perform these transformations.[281,282,283] The most common methods of hydroboration is addition of a stoichiometric amount of borane to a carbonyl compound followed by the hydrolysis of boronate esters. Typically, metal hydrides are widely employed for these transformations;[284] however, poor functional group tolerance, modest reaction rates, and vigorous reaction conditions increased the interest in the development of efficient and selective reduction methods.[285] Notably, transition metals (Mo,[286] Ru,[287] Rh,[288] Co, Ni,[289] Cu,[290] and Zn[291]) main group elements (Li,[292] Mg,[293,294] Ca,[295] Al,[296,297] Ga,[298] Ge,[299] Sn[300], and P[301]), alkali metals, and rare earth metals,[302,303,304] as catalysts have been reported extensively for the catalytic hydroboration of aldehydes and ketones, because of their excellent chemo- and regioselectivity and high atom economy. However, due to the low abundance and high economic cost of precious metal catalysts, there is always a surge of interest in the development of inexpensive and earth abundant metal catalysts.[305,306,307] In this context, a great effort has been implemented to develop a variety of first row transition metal based catalysts (Ti,[308,309] Fe, [310,311]

and Cu[312,313]) since they are widely available. In contrast, manganese catalysts have been widespread in hydrogenation,[314,315,316] hydrosilylation,[81] nitrogen transfer reactions,[317,318] and oxidation processes,[319,320] but they have remained largely unexplored in hydroboration of carbonyl compounds. However, the excellent efficiency of manganese in this field has only just been established in greater contributions by Zhang,[312] Trovitch,[47] Gade,[321] and others.[322] Taking this into consideration along with recent concerns about sustainability, manganese is of particular interest, since it is one of the most abundant transition metals in the earth's crust and biocompatible.[323,324,325]

We have investigated the catalytic activity of several high-valent transition metal complexes in reduction processes and silane activation.[81,116,117] Interestingly, an air stable and easily prepared salen-manganese complex, [MnN(salen-3,5-^{t}Bu$_2$)] (**Mn-1**) has found to be an efficient catalyst in carbonyls hydrosilylation and dehydrogenative coupling reactions.[81,175,216,262,326] Encouraged by these results, herein we are reporting the catalytic hydroboration of carbonyl compounds by employing **Mn-1** as the catalyst and pincolborane (HBpin) as an efficient reductant. Significantly, **Mn-1** has shown excellent activity and chemo selectivity towards aldehydes over ketones under mild conditions.

6.2. Results and discussion

We began our catalytic studies by examining the hydroboration of acetophenone as the test substrate and HBpin, and the results were presented in Table 15. Reactions were performed by adding equimolar amount of acetophenone (**30**) and HBpin to a catalyst solution in CD_3CN in a J-Young NMR tube, and the reaction progress was conveniently monitored by ^{1}H and ^{11}B NMR spectroscopy. The control experiment between acetophenone and HBpin in the absence of **Mn-1** at room temperature (rt) showed no reaction (Table 15, entry 1). With 1 mol % of **Mn-1,**

quantitative formation of acetophenone reduction product, boronate ester, **31** was detected in less than 5 minutes at rt (Table 15, entry 2). Appearance of a single quartet peak in ^{1}H NMR at δ 5.66 ppm and a single peak in ^{11}B NMR at δ 25.42 ppm, which is in the spectral region of boronate esters (24 to 26 ppm), confirms the formation of 3.[327] The rapid conversion in the catalytic reaction at rt led us to further assess the catalytic activity of **Mn-1** by gradually lowering its loadings. It was found that >95 % conversion could be obtained in less than 5 min at 0.2 mol % **Mn-1** loading, corresponding to a TOF of 5700 h^{-1}, which is comparable to some of the most active hydroboration catalysts in the literature (Table 15, entry 3).[287,290,293,296,311] A nearly complete reaction in 30 minutes (TOF of 1960 h^{-1}) and 90 % conversion in 4 h (TOF of 1125 h^{-1}) were achieved with loadings of 0.1 and 0.02 mol %, respectively (Table 15, entries 4 and 5). However, further decreasing the catalyst loading to 0.002 mol % resulted in only 2 % conversion in 24 h (Table 15, entry 6) and increasing the reaction temperature to 50 ºC under these conditions did not improve the conversion much (15 % in 24 h) (Table 15, entry 7). On the other hand, the reaction with catecholborane (HBcat) instead of HBpin was comparatively slow and only 75 % conversion was achieved in 24 h (Table 15, entry 8).

To evaluate the general applicability and substrate scope of this catalytic system, a wide range of carbonyl substrates were subjected to the standard conditions. In all the cases, hydroboration of carbonyl substrates followed by silica prompted hydrolysis of the alkoxyboronate pinacol esters afforded the corresponding 1º and 2º alcohols in excellent yields.

Table 15. Screening of reaction conditions for hydroboration of carbonyls

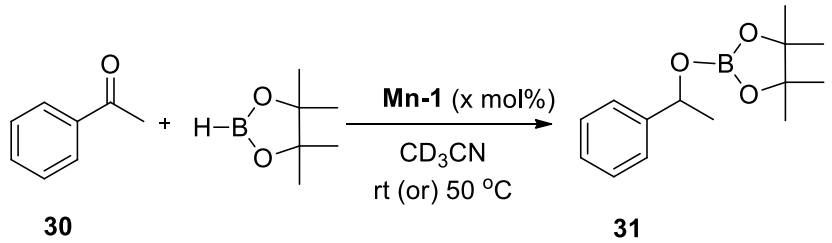

#	Catalyst mol%	Temperature	Time	Conv. %[b]	TON	TOF [h^{-1}]
1	-	rt	24 h	0	0	0
2	1	rt	< 5 min	100	100	1200
3	0.2	rt	< 5 min	95	475	5700
4	0.1	rt	30 min	98	980	1960
5	0.02	rt	4 h	90	4500	1125
6	0.002	rt	24 h	2	1000	42
7	0.002	50 ºC	24 h	15	7500	312
8[c]	0.2	rt	24 h	75	375	17

[a] Reaction conditions: Catalyst (Mn-1) 0.002 to 1 mol%, Acetophenone 1 eqv. HBpin 1.1 eqv. [b] Confirmed by using NMR spectroscopy. [a] HBcat was used instead of HBpin.

6.2.1. Hydroboration of ketones

Under the optimized conditions (0.2 mol % catalyst at rt) we examined the substrate scope of ketones and a representative set of substrates with yields were summarized in Table 16. Hydroboration reactions of acetophenones bearing both electron withdrawing and donating groups at *para* position afforded the corresponding boronate esters in quantitative yields (Table 16, entries 1-6). In the process, synthetically significant halide functional groups, such as Cl (**32a**) and Br (**32b**), were tolerated and no hydrodehalogenated products were observed. Similarly, substrates bearing challenging functional groups such as 4-trifluoromethyl (**32c**) and 4-nitro (**32d**) were also

successfully converted to corresponding boronate esters without losing catalyst efficiency. In addition, excellent yields were observed in less than 5 minutes for substrates with electron donating groups such as methyl (**32e**) and methoxy (**32f**), whereas previously reported catalysts afforded moderate yields even at extended reaction times.[297,312] Cyclopropyl phenyl ketone (**32g**) was completely converted to the desired product without the observation of any ring-opening product, demonstrating that a radical intermediate was not likely involved (Table 16, entry 7).[328] Moreover, increasing the steric demands also has no effect on the yields of boronate esters as seen in the case of hydroboration of benzophenone (**32h**), which resulted in 99 % of corresponding boronate ester in less than 10 minutes (Table 16, entry 8). A complete conversion of simple saturated aliphatic, 2-pentanone (**32i**), and cyclohexanone (**32j**) to corresponding boronate esters were also achieved under the standard conditions in less than 10 minutes (Table 16, entries 9-10). Interestingly, α-β unsaturated ketones such as 2-cyclohexenone (**32k**), benzylideneacetophenone (**32l**), and 4-phenyl-3-butyne-2-one (**32m**), containing both C=O, C=C, and C≡C bonds were also selectively hydroboronated on the C=O bond to generate corresponding boronate esters though slightly extended reaction times (1-4 h) were required (Table 16, entries 11-13).[284] This wide functional group tolerance with high selectivity and efficiency is rare for carbonyl hydroboration.

Table 16. **Mn-1** catalyzed hydroboration of various ketone substrates

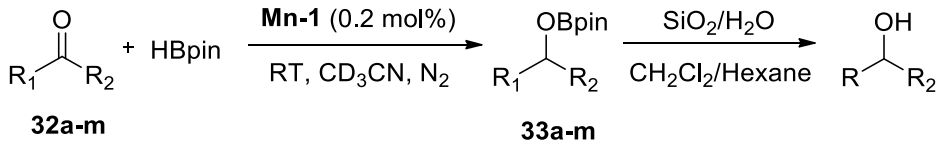

Entry	Ketone	Time	Boronate ester yield %[b]
1	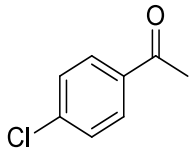	5 min	100
2	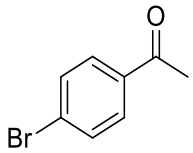	5 min	100
3	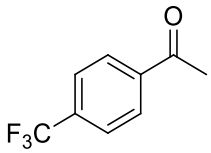	5 min	100
4	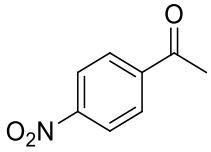	5 min	100
5	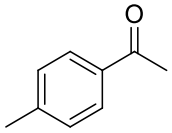	5 min	100
6	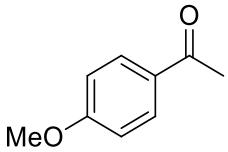	5 min	100
7	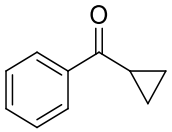	5 min	90

8	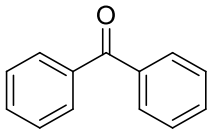	10 min	100
9	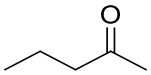	10 min	100
10	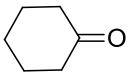	10 min	100
11	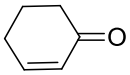	1 h	100
12	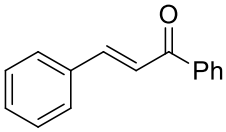	2 h	60
13	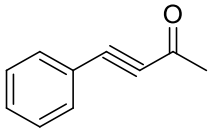	4 h	70

[a] Reaction conditions: Catalyst (Mn-1) 0.2 mol%, ketone 1 eqv. HBpin 1.1 eqv. [b] Confirmed by using NMR spectroscopy. [c] Confirmed by using NMR spectroscopy.

6.2.2. Hydroboration of aldehydes

The capability of **Mn-1** in hydroboration of ketones under mild conditions encouraged us to explore the hydroboration of aldehydes, and the results were summarized in Table 17. Surprisingly, a simple benzaldehyde (**34**) hydroboration reaction under the optimized conditions required 1 h to afford 100 % conversion (Table 17, entry 1). In addition, introducing an electron-donating group, methoxy (**34b**) at *para* position to benzaldehyde increased the reaction time to 24 h to afford the corresponding boronate ester (Table 17, entry 2). Because, it is known that aldehydes are prone to autoxidation to carboxylic acids, we purified the substrates for further examination. Expectedly, hydroboration reactions with purified substrates resulted in corresponding boronate esters in quantitate yields in less than 5 minutes (Table 17, entries 3-4).

Addition of a 1 mol % of benzoic acid to a reaction mixture of purified benzaldehyde and HBpin resulted in formation of 80% boronate ester after 3 h. These findings suggested the inhibiting nature of carboxylic acids in the current hydroboration reactions. With these findings in hand, scope of the aldehyde substrates was examined at standard conditions. Electron withdrawing (**34c-34f**) groups including Cl, Br, CN, and NO_2 at *para* position were well tolerated and the corresponding boronate esters were obtained in less than 5 min (Table 17, entries 5-8). Increasing the steric hindrance by employing Br, an electron withdrawing and bulky group, at the *ortho* position of benzaldehyde (**34g**) also has no effect on catalytic efficiency (Table 17, entry 9). Significantly, both conjugated (**34h**) and non-conjugated (**34i**) aldehydes were successfully hydroboronated on C=O part without compromising in yields though non-conjugated substrates required longer reaction times (Table 17, entries 10-11). These findings again demonstrate there is no competing side reactions such as C=C bond hydroboration. Further, we tested the catalytic activity of **Mn-1** by choosing an aliphatic aldehyde, 1-decanal (**34j**), as a substrate. The reaction successfully afforded the corresponding boronate ester in quantitative yields in less than 30 minutes (Table 17, entry 12). The feasibility of this method was next demonstrated with heterocyclic aromatic aldehydes, 2-pyridinecarboxaldehyde (**34k**), 2-furancarboxaldehyde (**34l**), and 2-thiophenecarboxaldehyde (**34m**). The desired boronate esters were exclusively obtained without dearomatization of the heterocyclic ring, which underscores the catalyst selectivity for C=O functionality (Table 17, entries 13-15).

Table 17. **Mn-1** catalyzed hydroboration of aldehyde substrates

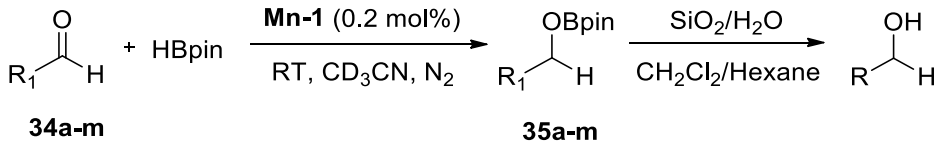

Entry	Aldehyde	Time	Boronate ester yield %[b]
1	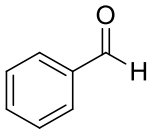	1 h	100
2	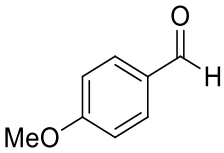	24 h	80
3*	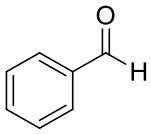	5 min	100
4*	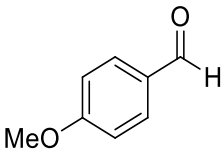	5 min	96
5	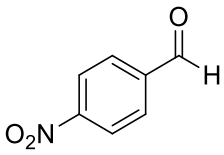	5 min	100
6	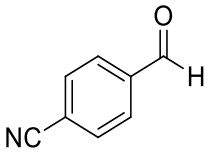	5 min	100
7	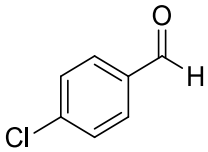	5 min	100

8	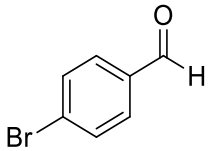	5 min	100
9	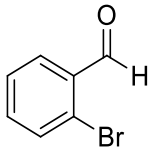	5 min	100
10	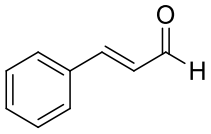	24 h	96
11	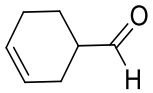	10 min	99
12	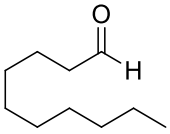	30 min	95
13	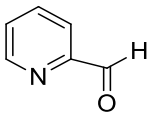	10 min	100
14	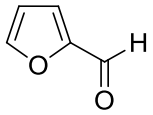	10 min	95
15	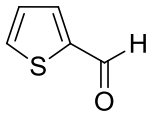	20 min	98

[a] Reaction conditions: Catalyst (Mn-1) 0.2 mol%, ketone 1 eqv. HBpin 1.1 eqv. [b] Confirmed by using NMR spectroscopy. [c] Confirmed by using NMR spectroscopy. [*]substrate was purified and used for hydroboration.

6.2.3. Chemoselective reactions

Importantly, it was found that **Mn-1** can catalyze both inter- and intramolecular chemoselective hydroboration of aldehydes over ketones. The intermolecular competition reaction

between equimolar amounts of benzaldehyde (30a) and acetophenone (26a) with HBpin resulted in an exclusive conversion of benzaldehyde to benzyl boronate ester, with the ketone intact (Scheme 8.A). ^{1}H NMR analysis showed the complete disappearance of –CHO peak at 10.08 ppm and appearance of -CH_2 peak of benzyl boronate ester at 4.95 ppm and the presence of unreacted acetophenone in reaction mixture. These results are similar to the observations in previous reports.[284,303,329] Likewise, a high degree of chemoselectivity and an exclusive conversion of aldehydes over ketones was achieved with *p*-substituted substrates with electron-donating (*p*-methoxy) and electron-withdrawing (*p*-nitro) groups. (Scheme 8.B & C). The intra-molecular competitive hydroboration reaction was carried out with 4-acetylbenzaldehyde (**36**) with HBpin, and exclusive chemoselective hydroboration of aldehyde group (**37**) (98%) over ketone group was observed. (Scheme 9). Adding another equivalent of HBpin to the reaction resulted in complete conversion of the acetyl group (**38**).

A.

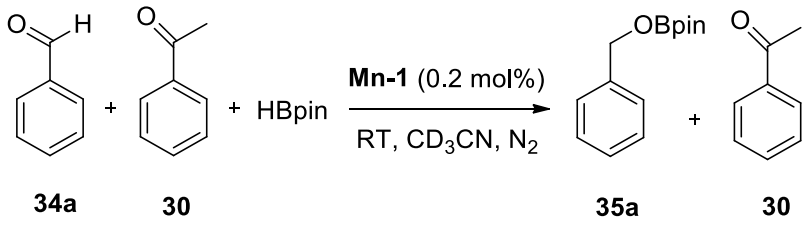

B.

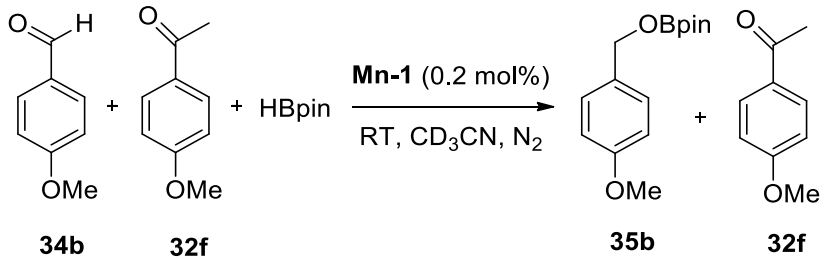

C.

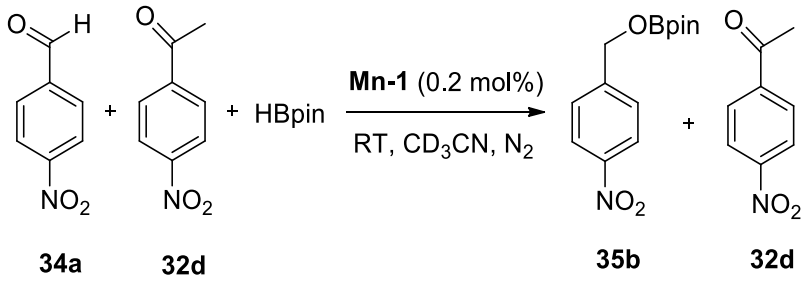

Scheme 8. Intermolecular chemoselective reactions catalyzed by **Mn-1**

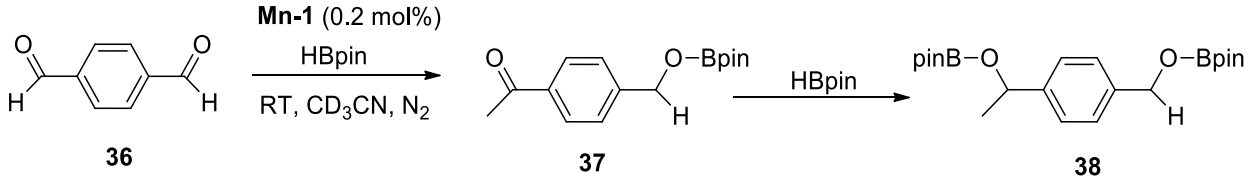

Scheme 9. Intramolecular chemoselective reactions catalyzed by **Mn-1**

6.2.4. Mechanistic investigations

The remarkable catalytic efficiency of **Mn-1** directed our attention towards the mechanistic understanding of hydroboration reactions. The stoichiometric reactions were first performed to identify the catalyst activation pathways. In a stoichiometric reaction between **Mn-1** and acetophenone in the absence of HBpin, no considerable changes in color and NMR spectra were observed. In comparison, an immediate and complete color change from green to dark/reddish brown was observed upon the addition of HBpin to a catalyst solution in CD_3CN, though the **Mn-1** signals were still present the ^{1}H NMR. A small, broad peak in ^{1}H NMR was observed at -21.9 ppm, tentatively assigned to a Mn-H species (35).[330] Also, new peaks appeared in ^{11}B NMR at 24.5 and 27.8 ppm, while the HBpin peak at 31.2 ppm mostly disappeared. In addition, the intensities of the catalyst peaks in ^{1}H NMR decreased over time and they completely disappeared (along with the -21.9 ppm peak) after adding additional HBpin. However, attempts to shed light

on the nature of boron and/or manganese containing species by ESI-MS and GC-MS were unsuccessful. When one equivalent of acetophenone was added to the 1:1 **Mn-1**/HBpin mixture, no hydroboration of acetophenone was observed even after 1 h, which suggested that the species generated from the 1:1 reaction of **Mn-1** and HBpin might not be active enough for hydroboration, and more HBpin was needed for catalytic turnover. Indeed, addition of the second equivalent of HBpin still showed no hydroboration and only after the third equivalent of HBpin did the characteristic peaks of acetophenone boronate ester (-C*H* at 5.18 and CH_3 at 1.45 ppm) start to appear. Conversely, adding one equivalent of HBpin to the 1:1 mixture of **Mn-1** and acetophenone changed the reaction color instantaneously to dark/reddish brown, but hydroboration was not observed. Additional HBpin was required for hydroboration of acetophenone to occur. The results strongly suggested that the catalyst is activated only after it interacts with the reducing agent, HBpin. These findings along with our previous studies collectively led us to assume that Mn(V) is reduced to a Mn(III) species by HBpin which further activates HBpin for hydroboration.

The effect of electronic factor of the carbonyl substrates on the rate of hydroboration was investigated by competition kinetics. A series of *para* substituted acetophenone derivatives, *p*-X-$C_6H_6COCH_3$ (X = OMe, NO_2, Cl, Br, CF_3) were paired with the parent acetophenone to compete for insufficient amount of HBpin. The relative reactivity of acetophenones was determined from the integrations of the corresponding benzylic protons of the hydroboration products in the ^{1}H NMR. The plot against the Hammett constants thus obtained shows a linear relationship with a positive slope (ρ = 0.95), in agreement with the observation that electron withdrawing groups accelerate the reaction in the *para* substituted acetophenone series.

To gain more insights into the catalyst activation process, we performed a set of control experiments with deuterated pinacolborane, DBpin.[331] In a competitive reaction between HBpin

and DBpin with acetophenone, both hydrogen and deuterium incorporated products were formed in a ratio of 70:30 according to the NMR analysis, which gives an H/D KIE of 2.3. GC/MS analysis of the isotopic distribution of hydroboration products yielded a similar KIE of 2.2. The observation also affirmed that HBpin is the only H source in these reactions. The modest KIE suggested that the B-H bond breaking is one of the slow steps during the catalytic conditions. Interestingly, in another competitive reaction of HBcat and DBpin with acetophenone (molar ratio 1:1:1), crossover products **41** and **31** were formed along with the expected hydroboration products **39** and **40** (Scheme 10). According to ^{1}H NMR analysis, **31** was observed, as judged by the appearance of 5.26 ppm peak assigned to the methine proton in **31**, from the beginning in the reaction along with **39**. The presence of crossover products were also confirmed by the GC/MS analysis of the isotopic distribution of the reaction products. These observations prompted us to explore if the reaction was reversible at any stage. A mixture of 1:1 HBcat and DBpin in the presence of 1 mol% **Mn-1** showed no scrambling between H and D. Addition of 1 equiv. of *p*-CF_3 acetophenone to a freshly generated boronate ester from acetophenone and HBpin (1:1 ratio) at standard catalytic conditions (0.5 mol% **Mn-1**) showed no further reaction, thus excluding the reversibility at the product formation stage during the reaction.

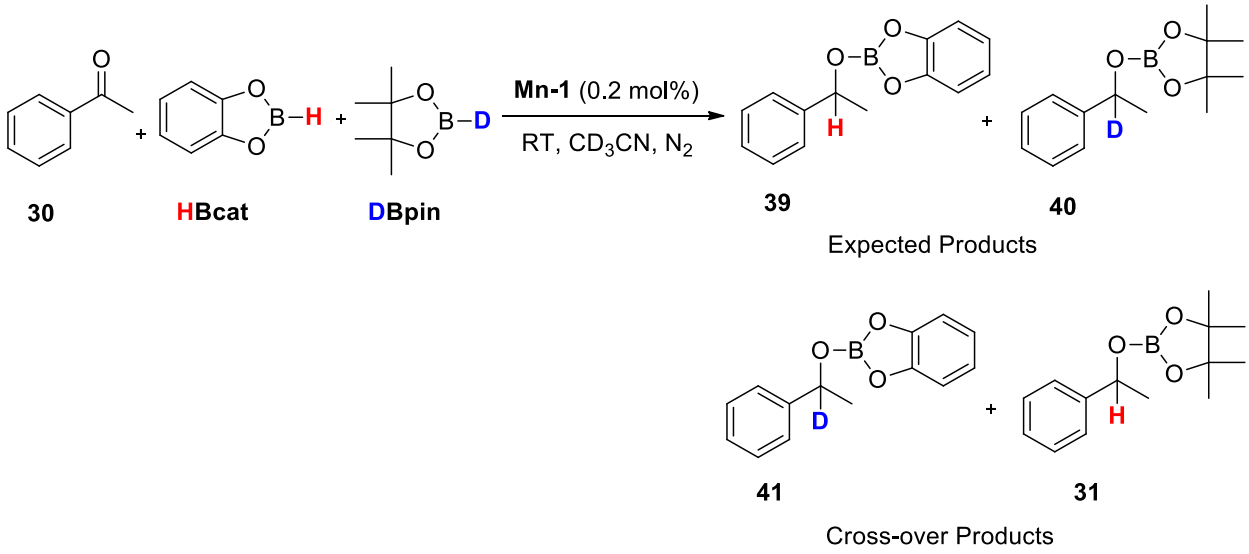

Scheme 10. A controlled competitive reaction between DBpin and HBcat with acetophenone

Based on these discoveries, we propose a borane-associated catalytic cycle for the hydroboration of carbonyl compounds (Scheme 11). We assume that initial coordination between HBpin and catalyst generates an active metal hydride species (L_nMn-H) (**42**) by releasing dehydroboronated compound and N_2, which is responsible for the effective hydroboration of carbonyls. The active 35 further coordinates with HBpin to form 36, which further coordination with carbonyl substrate to produce 37 and followed by H transfer to generate 38. Formation of 36 is also correlated with the observation of cross-over products in deuterium-labeled competitive studies. In a final step, a σ-metathesis of 38 regenerates the metal hydrido complex (35) and to provide the hydroboronated product, alkoxy boronate ester.[321,329,332]

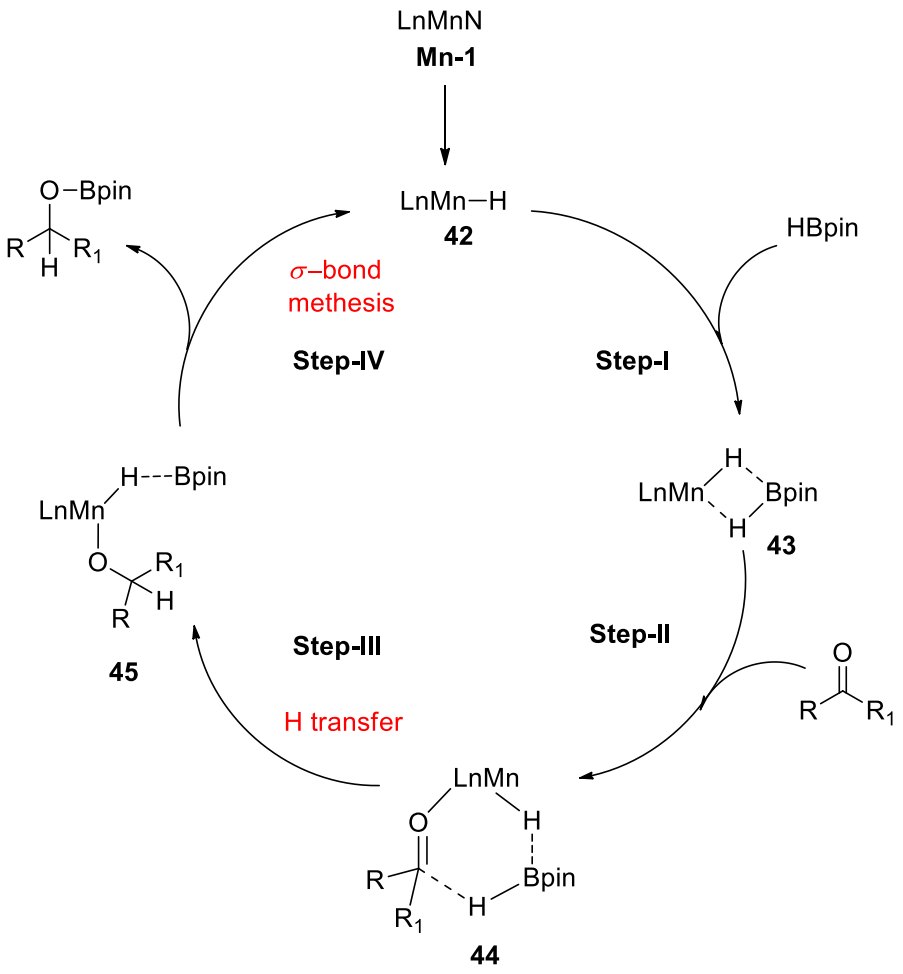

Scheme 11**.** Tentative mechanistic proposal for the **Mn-1** catalyzed hydroboration of carbonyls

6.3. Conclusions

In Conclusion, we have described that **Mn-1** could be employed as an excellent catalyst for the hydroboration of carbonyl compounds. The catalytic system features low catalyst loading, mild reaction conditions, a broad scope of substrates, good functional group compatibility, and excellent selectivity of aldehydes over ketones. Preliminary kinetic experiments indicate that B-H bond breaking is one of the slow steps in the reaction. In consideration of the controlled deuterium experiments and kinetic studies, a manganese reduced species, Mn-H, mediated tentative mechanism was proposed. Detailed mechanistic investigations and further catalytic activity exploration of MnN species will be focused on our future work.

6.4. Experimental section

All the chemicals were purchased from Sigma Aldrich. Deuterated solvents were purchased from the Cambridge Isotope Laboratories. Solvents were degasified and dried over molecular sieves (4 Å) overnight prior to use. Glassware was dried overnight prior to use. ^{1}H, ^{13}C, and ^{11}B NMR spectra were recorded on a Bruker AVANCE 500 NMR spectrometer in deuterated acetonitrile. Boron trifluoride diethyl etherate ($BF_3.OEt_2$) was used as the standard reference for ^{11}B NMR analysis. The purchased reagents which are packed under inert atmosphere were used as received and all other reagents were degasified by using standard Schlenk line technique. GC analyses were performed using a GC-MS (6890GC, 5975C) equipped with an autosampler (7386B series) and a split/splitless injector (Agilent Technologies, Santa Clara, CA, USA). Separations were accomplished using a 24.6 m long DB-5 capillary column, 0.25 mm internal diameter (I.D.) and 0.25 mm film thickness (J&W Scientific, Rancho Cordova, CA, USA) at a constant helium flowrate of 1.0 mL/min. Samples (1.0 μL) were injected into a single gooseneck splitless liner with glasswool in a pulse splitless injection mode for with 25 psi for 0.3 min, and solvent delay was set to 2.5 min. The temperature programs were evaluated to allow for an efficient separation of all analytes, solvents, and derivatization agents. The column temperature program started at 35 °C with a hold of 1 min, followed by the gradient of 20 °C/min to 320 °C and hold for 1 min. The MS data (total ion chromatogram, TIC) were acquired in the full scan mode (m/z of 35–850) at a scan rate of 1.84 scan/s using the electron ionization (EI) with an electron energy of 70 eV.

General procedure for the hydroboration of crabonyls. All the reactions were performed under nitrogen atmosphere in Glove Box using J-Young NMR tube. Calculated amount of catalyst, **Mn-1**, (0.002 to 1 mol%) was added to 0.35-0.4 mL of CD_3CN solution at room temperature. To this

was added, carbonyl substrate followed by hydroborane. The progress of the reaction was monitored by using ^{1}H, ^{13}C, and ^{11}B NMR.

NMR characterization data

Acetophenone hydroboration product: ^{1}H NMR (500 MHz, CD_3CN, 298 K, δ): 1.22 (m, 12H, 4C*H₃*), 1.49 (d, 3H, -C*H₃*), 5.26 (q, 1H, -OC*H*), 7.28 (m, 1H, -*Ph*), 7.38 (m, 4H, -*Ph*). ^{13}C {1H} NMR (125 MHz, CD_3CN, 298 K, δ): 25.33 (4C*H₃*), 27.08 (*C*H₃), 73.23 (O*C*H), 83.51 (-B-O*C*Hpin), 126.18, 128.08, 129.17, 145.65 (*Ph*). **Hydrolysis product (1-phenylethanol):** ^{1}H NMR (500 MHz, $CDCl_3$, 298 K, δ): 1.42 (d, 3H, C*H₃*), 4.84 (q, 1H, OC*H*), 7.18 (d, 2H, *Ph*), 7.20 (d, 3H, *Ph*)

Table 16. Entry 1, p-Chloroacetophenone hydroboration product: ^{1}H NMR (500 MHz, CD_3CN_3, 298 K, δ): 1.21 (m, 12H, 4C*H₃*), 1.43 (d, 3H, -C*H₃*), 5.20 (q, 1H, -OC*H*), 7.31 (m, 4H, -*Ph*). ^{11}B {^{1}H} NMR (99 MHz, CD_3CN, 298 K, δ): 25.40. **Hydrolysis product (1-(4-Chlorophenyl)ethanol):** ^{1}H NMR (500 MHz, $CDCl_3$, 298 K, δ): 1.40 (d, 3H, -C*H₃*), 4.89 (q, 1H, -OC*H*), 7.30 (m, 4H, -*Ph*)

Table 16. Entry 2, p-Bromoacetophenone hydroboration product: ^{1}H NMR (500 MHz, CD_3CN, 298 K, δ): 1.20 (m, 12H, 4C*H₃*), 1.43 (d, 3H, -C*H₃*), 5.16 (q, 1H, -OC*H*), 7.25 (m, 2H, -*Ph*), 7.46 (m, 2H, -*Ph*). ^{11}B {^{1}H} NMR (99 MHz, CD_3CN, 298 K, δ): 25.40. **Hydrolysis product (1-(4-Bromophenyl)ethanol):** ^{1}H NMR (500 MHz, $CDCl_3$, 298 K, δ): 1.42 (d, 3H, -C*H₃*), 4.72 (q, 1H, -OC*H*), 7.18 (m, 2H, -*Ph*), 7.42 (m, 2H, -*Ph*)

Table 16. Entry 3, p-Trifluoromethyl acetophenone hydroboration product: ^{1}H NMR (500 MHz, CD_3CN, 298 K, δ): 1.20 (m, 12H, 4C*H₃*), 1.47 (d, 3H, -C*H₃*), 5.29 (q, 1H, -OC*H*), 7.52 (m, 2H, -*Ph*), 7.64 (m, 2H, -*Ph*). ^{11}B {^{1}H} NMR (99 MHz, CD_3CN, 298 K, δ): 25.42. **Hydrolysis**

product (1-(4-Trifluoromethylphenyl)ethanol): ^{1}H NMR (500 MHz, $CDCl_3$, 298 K, δ): 1.51 (d, 3H, -C*H₃*), 4.88 (q, 1H, -OC*H*), 7.44 (m, 2H, -*Ph*), 7.57 (m, 2H, -*Ph*)

Table 16. Entry 4, p-Nitroacetophenone hydroboration product: ^{1}H NMR (500 MHz, CD_3CN, 298 K, δ): 1.21 (m, 12H, 4C*H₃*), 1.46 (d, 3H, C*H*$_3$), 5.30 (q, 1H, OC*H*), 7.55 (d, 2H, *Ph*), 8.16 (d, 2H, *Ph*). **Hydrolysis product (1-(4-Nitrorophenyl)ethanol):** ^{1}H NMR (500 MHz, $CDCl_3$, 298 K, δ): 1.49 (d, 3H, C*H*$_3$), 4.97 (q, 1H, OC*H*), 7.51 (d, 2H, *Ph*), 8.04 (d, 2H, *Ph*)

Table 16. Entry 5, p-Methylacetophenone hydroboration product: ^{1}H NMR (500 MHz, CD_3CN, 298 K, δ): 1.22 (m, 12H, 4C*H₃*), 1.47 (d, 3H, C*H*$_3$), 2.33 (s, 3H, C*H*$_3$), 5.22 (q, 1H, OC*H*), 7.16 (d, 2H, *Ph*), 7.26 (d, 2H, *Ph*). ^{11}B {^{1}H} NMR (99 MHz, CD_3CN, 298 K, δ): 24.49. **Hydrolysis product (1-(4-Methylphenyl)ethanol):** ^{1}H NMR (500 MHz, $CDCl_3$, 298 K, δ): 1.41 (d, 3H, C*H*$_3$), 2.25 (s, 3H, C*H*$_3$), 4.82 (q, 1H, OC*H*), 7.08 (d, 2H, *Ph*), 7.15 (d, 2H, *Ph*).

Table 16. Entry 6, p-Methoxyacetophenone hydroboration product: ^{1}H NMR (500 MHz, CD_3CN, 298 K, δ): 1.22 (m, 12H, 4C*H₃*), 1.45 (d, 3H, C*H*$_3$), 5.18 (q, 1H, OC*H*), 6.88 (d, 2H, *Ph*), 7.27 (d, 2H, *Ph*). ^{11}B {^{1}H} NMR (99 MHz, CD_3CN, 298 K, δ): 24.39. **Hydrolysis product (1-(4-Methoxyphenyl)ethanol):** ^{1}H NMR (500 MHz, $CDCl_3$, 298 K, δ): 1.50 (d, 3H, C*H*$_3$), 3.6 (s, 3H, C*H*$_3$), 4.87 (q, 1H, OC*H*), 6.88 (d, 2H, *Ph*), 7.27 (d, 2H, *Ph*)

Table 16. Entry 7, Cyclopropylphenylketone hydroboration product: ^{1}H NMR (500 MHz, CD_3CN, 298 K, δ): 0.40-0.50 (m, 4H, cyclopropyl 2C*H*$_2$), 1.21 (m, 1H, cyclopropyl C*H*), 1.23 (m, 12H, 4C*H₃*), 4.49 (m, 1H, OC*H*), 7.28 (m, 1H, *Ph*), 7.36 (m, 2H, *Ph*), 7.41 (m, 2H, *Ph*). **Hydrolysis product (α-Cyclopropylbenzylalcohol):** ^{1}H NMR (500 MHz, $CDCl_3$, 298 K, δ): 0.35-0.46 (m, 4H, cyclopropyl 2C*H*$_2$), 0.56 (m, 1H, cyclopropyl C*H*), 4.02 (m, 1H, OC*H*), 7.20 (m, 1H, *Ph*), 7.31 (m, 2H, *Ph*), 7.48 (m, 2H, *Ph*)

Table 16. Entry 8, Benzophenone hydroboration product: ^{1}H NMR (500 MHz, CD_3CN, 298 K, δ): 1.26 (m, 12H, 4C*H₃*), 6.30 (s, 1H, OC*H*), 7.31 (m, 2H, *Ph*), 7.39 (m, 4H, *Ph*), 7.48 (m, 4H, *Ph*). **Hydrolysis product (α-Phenylbenzenemethanol)**: ^{1}H NMR (500 MHz, $CDCl_3$, 298 K, δ): 2.37 (s, 1H, *OH*), 5.81 (s, 1H, OC*H*), 7.28 (m, 2H, *Ph*), 7.33 (m, 4H, *Ph*), 7.37 (m, 4H, *Ph*)

Table 16. Entry 9, 2-Pentanone hydroboration product: ^{1}H NMR (500 MHz, CD_3CN, 298 K, δ): 0.89 (m, 3H, CH_3), 1.13 (m, 2H, CH_2), 1.23 (m, 12H, 4CH_3), 1.35 (m, 3H, OCHCH_3), 1.43 (m, 2H, OCHCH_2), 4.11 (m, 1H, OC*H*)

Table 16. Entry 10, Cyclohexanone hydroboration product: ^{1}H NMR (500 MHz, CD_3CN, 298 K, δ): 1.19 (m, 12H, 4CH_3), 1.25 (m, 4H, CH_2), 1.49 (m, 2H, CH_2), 1.69 (m, 2H, CH_2), 1.78 (m, 2H, CH_2), 3.90 (m, 1H, OC*H*)

Table 16. Entry 11, 3-Cyclohexene hydroboration product: ^{1}H NMR (500 MHz, CD_3CN, 298 K, δ): 1.25 (m, 12H, 4CH_3), 1.65 (m, 2H, CH_2), 1.79 (m, 1H, C*H*), 1.91 (m, 1H, C*H*), 2.03 (m, 2H, CH_2), 4.58 (m, 1H, OC*H*), 5.73 (m, 1H, C*H*=CH), 5.88 (m, 1H, C*H*=CH). ^{11}B {^{1}H} NMR (99 MHz, CD_3CN, 298 K, δ): 25.17. **Hydrolysis product (3-Cyclohexene-1-methanol):** ^{1}H NMR (500 MHz, $CDCl_3$, 298 K, δ): 1.58-2.36 (m, 6H, 3CH_2), 4.45 (m, 1H, OC*H*), 5.62 (m, 1H, C*H*=CH), 5.71 (m, 1H, C*H*=CH)

Table 16. Entry 12, Benzylideneacetophenone hydroboration product: ^{1}H NMR (500 MHz, CD_3CN, 298 K, δ): 1.26 (m, 12H, 4CH_3), 5.81 (m, 1H, -OC*H*), 6.44 (m, 1H, -OCHC*H*=CH), 6.74 (m, 1H, -OCHCH=C*H*), 7.26-7.56 (m, 10H, *Ph*). ^{11}B {^{1}H} NMR (99 MHz, CD_3CN, 298 K, δ): 26.10. **Hydrolysis product (1,3-Diphenyl-2-propen-1-ol):** ^{1}H NMR (500 MHz, $CDCl_3$, 298 K, δ): 5.20 (m, 1H, -OC*H*), 6.35 (m, 1H, -OCHC*H*=CH), 6.68 (m, 1H, -OCHCH=C*H*), 7.18-7.46 (m, 10H, -*Ph*)

Table 16. Entry 13, 4-phenyl-3-butyne-2-one hydroboration product: ^{1}H NMR (500 MHz, CD_3CN, 298 K, δ): 1.24 (m, 12H, 4C*H₃*), 1.52 (d, 3H, -C*H₃*), 5.05 (q, 1H, -OC*H*), 7.35 (m, 3H, -*Ph*), 7.42 (m, 2H, -*Ph*). ^{13}C {1H} NMR (125 MHz, CD_3CN, 298 K, δ): 24.30 (4*C*H_3), 24.92 (4*C*H_3), 61.97 (-O*C*H), 83.87 (4° *C* of Bpin), 84.19 (-OCH*C*≡C), 90.89 (-OCHC≡*C*Ph), 129.43, 129.73, 132.32, 133.75 (*Ph*). ^{11}B {^{1}H} NMR (99 MHz, CD_3CN, 298 K, δ): 25.48. **Hydrolysis product (4-phenyl-3-butyne-2-ol):** ^{1}H NMR (500 MHz, $CDCl_3$, 298 K, δ): 1.46 (m, 3H, -C*H₃*), 4.84 (m, 1H, -OC*H*), 7.29 (m, 2H, -*Ph*), 7.31 (m, 3H, -*Ph*)

Table 17. Entry 1 & 3, Benzaldehyde hydroboration product: ^{1}H NMR (500 MHz, CD_3CN, 298 K, δ): 1.21 (m, 12H, 4C*H₃*), 4.85 (s, 2H, OC*H₂*), 6.95 (d, 2H, *Ph*), 7.31 (d, 2H, *Ph*). ^{13}C {1H} NMR (125 MHz, CD_3CN, 298 K, δ): 25.03 (4*C*H_3), 67.35 (O*C*H_2), 83.76 (B-O*C*Hpin), 127.68,128.37, 129.32, 140.51 (*Ph*). ^{11}B {^{1}H} NMR (99 MHz, CD_3CN, 298 K, δ): 24.05. **Hydrolysis product (Benzyl alcohol)** ^{1}H NMR (500 MHz, $CDCl_3$, 298 K, δ): 4.68 (s, 2H, OC*H₂*), 7.19 (m, 2H, *Ph*), 7.35-7.40 (m, 3H, *Ph*)

Table 17. Entry 2 & 4, p-Methoxybenzaldehyde decanal hydroboration product: ^{1}H NMR (500 MHz, CD_3CN, 298 K, δ): 1.26 (m, 12H, 4C*H₃*), 3.78 (s, 3H, OC*H₃*), 4.83 (s, 2H, OC*H₂*), 6.92 (d, 2H, *Ph*), 7.29 (d, 2H, *Ph*). **Hydrolysis product (p-Methoxybenzyl alcohol)** ^{1}H NMR (500 MHz, $CDCl_3$, 298 K, δ): 3.52 (s, 3H, OC*H₃*), 4.61 (s, 2H, OC*H₂*), 6.82 (m, 2H, *Ph*), 7.11 (m, 2H, *Ph*)

Table 17. Entry 5, p-Nitro benzaldehyde hydroboration product: ^{1}H NMR (500 MHz, CD_3CN, 298 K, δ): 1.23 (m, 12H, 4C*H₃*), 4.98 (s, 3H, OC*H*), 7.52 (d, 2H, *Ph*), 8.17 (d, 2H, *Ph*). **Hydrolysis product (p-Nitrobenzyl alcohol)** ^{1}H NMR (500 MHz, $CDCl_3$, 298 K, δ): 4.81 (s, 2H, OC*H₂*), 7.45 (m, 2H, *Ph*), 8.09 (m, 2H, *Ph*)

Table 17. Entry 6, p-Cyanobenzaldehyde hydroboration product: ^{1}H NMR (500 MHz, CD_3CN, 298 K, δ): 1.23 (m, 12H, 4C*H₃*), 4.93 (m, 2H, OC*H*$_2$), 7.46 (m, 2H, *Ph*), 7.69 (m, 2H, *Ph*). ^{13}C {1H} NMR (125 MHz, CD_3CN, 298 K, δ): 24.92 (4*C*H$_3$), 66.44 (O*C*H$_2$), 83.99 (B-O*C*Hpin), 111.76, 127.90, 133.16, 145.89 (*Ph*). **Hydrolysis product (p-Cyanobenzyl alcohol)** ^{1}H NMR (500 MHz, $CDCl_3$, 298 K, δ): 4.76 (s, 2H, OC*H*$_2$), 7.42 (m, 2H, *Ph*), 7.62 (m, 2H, *Ph*)

Table 17. Entry 7, p-Chlorobenzaldehyde hydroboration product: ^{1}H NMR (500 MHz, CD_3CN, 298 K, δ): 1.22 (m, 12H, 4C*H₃*), 4.96 (m, 2H, OC*H*$_2$), 7.45 (m, 2H, *Ph*), 7.62 (m, 2H, *Ph*). ^{11}B {^{1}H} NMR (99 MHz, CD_3CN, 298 K, δ): 24.92. **Hydrolysis product (p-Chlorobenzyl alcohol)** ^{1}H NMR (500 MHz, $CDCl_3$, 298 K, δ): 4.69 (s, 2H, OC*H*$_2$), 7.39 (m, 2H, *Ph*), 7.50 (m, 2H, *Ph*)

Table 17. Entry 8, p-Bromobenzaldehyde hydroboration product: ^{1}H NMR (500 MHz, CD_3CN, 298 K, δ): 1.23 (m, 12H, 4C*H₃*), 4.95 (m, 2H, OC*H*$_2$), 7.43 (m, 2H, *Ph*), 7.65 (m, 2H, *Ph*). ^{11}B {^{1}H} NMR (99 MHz, CD_3CN, 298K, δ): 24.95. **Hydrolysis product (p-Bromobenzyl alcohol)** ^{1}H NMR (500 MHz, $CDCl_3$, 298 K, δ): 4.55 (s, 2H, OC*H*$_2$), 7.22 (m, 2H, *Ph*), 7.37 (m, 2H, *Ph*)

Table 17. Entry 9, o-Bromo benzaldehyde decanal hydroboration product: ^{1}H NMR (500 MHz, CD_3CN, 298 K, δ): 1.24 (m, 12H, 4C*H₃*), 4.93 (s, 3H, OC*H*), 7.19 (m, 1H, *Ph*), 7.36 (m, 1H, *Ph*), 7.47 (m, 1H, *Ph*), 7.54 (d, 1H, *Ph*). **Hydrolysis product (o-Bromobenzyl alcohol)** ^{1}H NMR (500 MHz, $CDCl_3$, 298 K, δ): 4.72 (s, 2H, OC*H*$_2$), 7.11 (m, 1H, *Ph*), 7.28 (m, 1H, *Ph*), 7.41 (m, 1H, *Ph*), 7.48 (m, 1H, *Ph*)

Table 17. Entry 10, trans-3-Phenyl-2-propenal hydroboration product (Cinnamaldehyde): ^{1}H NMR (500 MHz, CD_3CN, 298 K, δ): 1.29 (m, 12H, 4C*H₃*), 4.65 (m, 2H, OC*H*$_2$), 6.34 (m, 1H, -C*H*=CHPh), 6.36 (m, 1H, -CH=C*H*Ph), 7.23-7.29 (m, 3H, *Ph*), 7.41 (m, 2H, *Ph*). ^{13}C {1H} NMR

(125 MHz, CD_3CN, 298 K, δ): 24.30 (4*C*H_3), 25.01 (4*C*H_3), 65.85 (-O*C*H_2), 83.57 (-O*C*H_2), 131.30 (*C*H=CHPh), 153.43 (CH=*C*HPh), 127.26,128.52, 128.50, 137.67 (*Ph*). ^{11}B {^{1}H} NMR (99 MHz, CD_3CN, 298 K, δ): 25.60. **Hydrolysis product (Cinnamyl alcohol)**: ^{1}H NMR (500 MHz, $CDCl_3$, 298 K, δ): 4.12 (s, 2H, OC*H*$_2$), 6.20 (m, 1H, -C*H*=CHPh), 6.34 (m, 1H, -CH=C*H*Ph), 7.01 (m, 2H, *Ph*), 7.08-7.17 (m, 3H, *Ph*)

Table 17. Entry 11, 3-Cyclohexenecarboxaldehyde hydroboration product: ^{1}H NMR (500 MHz, CD_3CN, 298 K, δ): 1.21 (m, 12H, 4C*H*$_3$), 1.27 (m, 4H, C*H*$_2$), 2.03 (m, 3H, C*H* & C*H*=C*H*), 3.67 (m, 2H, OC*H*$_2$), 5.64 (m, 2H, -OC*H*$_2$). ^{11}B {^{1}H} NMR (99 MHz, CD_3CN, 298 K, δ): 25.32. **Hydrolysis product (3-Cyclohexene-1-methanol)** ^{1}H NMR (500 MHz, $CDCl_3$, 298 K, δ): 1.25-2.52 (m, 6H, C*H*$_2$), 3.56 (m, 2H, OC*H*$_2$), 5.61 (m, 2H, C*H*=C*H*)

Table 17. Entry 12, 2-Formylpyridine hydroboration product: ^{1}H NMR (500 MHz, CD_3CN, 298 K, δ): 1.22 (m, 12H, 4C*H*$_3$), 4.92 (s, 2H, OC*H*$_2$), 7.38 (m, 1H, *pyridine*), 7.46 (m, 1H, *pyridine*), 7.87 (m, 1H, *pyridine*), 8.54 (m, 1H, *pyridine*). ^{13}C {1H} NMR (125 MHz, CD_3CN, 298 K, δ): 25.58 (4*C*H_3), 67.25 (-O*C*H_2), 82.19 (-B-O*C*pin), 121.17 (*pyridine*), 124.06 (*pyridine*), 139.49 (*pyridine*), 146.29 (*pyridine*), 149.99 (*pyridine*). ^{11}B {^{1}H} NMR (99 MHz, CD_3CN, 298 K, δ): 21.25. **Hydrolysis product (2-Pyridinemethanol)** ^{1}H NMR (500 MHz, $CDCl_3$, 298 K, δ): 4.78 (s, 2H, OC*H*$_2$), 7.31 (m, 1H, *pyridine*), 7.39 (m, 1H, *pyridine*), 7.81 (m, 1H, *pyridine*), 8.42 (m, 1H, *pyridine*)

Table 17. Entry 13, Furfural hydroboration product: ^{1}H NMR (500 MHz, CD_3CN, 298 K, δ): 1.26 (m, 12H, 4C*H*$_3$), 4.80 (s, 2H, OC*H*$_2$), 6.32-6.36 (m, 2H, *furan ring*), 7.48 (m, 1H, *furan ring*). **Hydrolysis product (2-Furanmethanol)** ^{1}H NMR (500 MHz, $CDCl_3$, 298 K, δ): 4.72 (s, 2H, OC*H*$_2$), 6.01 (m, 1H, *furan ring*), 6.32 (m, 1H, *furan ring*), 7.33 (m, 1H, *furan ring*)

Table 17. Entry 14, Thiophene-2-carboxaldehyde hydroboration product: ^{1}H NMR (500 MHz, CD_3CN, 298 K, δ): 1.29 (m, 12H, 4C*H₃*), 5.04 (s, 2H, OC*H*$_2$), 7.02-7.06 (m, 2H, *thiophene ring*), 7.36 (m, 1H, *thiophene ring*). **Hydrolysis product (2-Thiophenemethanol)** ^{1}H NMR (500 MHz, $CDCl_3$, 298 K, δ): 4.82 (s, 2H, OC*H*$_2$), 6.98 (m, 1H, *thiophene ring*), 7.01 (m, 1H, *thiophene ring*), 7.28 (m, 1H, *thiophene ring*)

Acetylbenzaldehyde hydroboration product: ^{1}H NMR (500 MHz, CD_3CN, 298 K, δ): **(Aldehyde group reduction only)** 1.24 (m, 12H, 4C*H₃*), 2.54 (m, 3H, unreacted C*H₃*), 4.94 (q, 1H, -OC*H*), 7.42 (m, 2H, -*Ph*), 7.93 (m, 2H, -*Ph*). ^{13}C {1H} NMR (125 MHz, $CDCl_3$, 298 K, δ): 24.30 (4*C*H$_3$), 27.36 (unreacted C*H₃*), 66.65 (-OC*H*$_2$), 84.12 (4° *C* of Bpin), 127.27, 129.25, 130.46, 145.57 (*Ph*), 129.15, 129.57, 133.96, 138.20 (unreacted *Ph*), 198.28 (unreacted CO of ketone group). (**After aldehyde and ketone groups reduction, 2nd equivalent of HBpin was added)** 1.20 (m, 24H, 4C*H₃*), 2.54 (m, 3H, (ketone) C*H₃*), 4.89 (m, 2H, (aldehyde) -OC*H*$_2$), 5.26 (m, 1H, (ketone) -OC*H*), 7.33 (m, 4H, -*Ph*). **Hydrolysis product (α-Methyl-1,4-benzenedimethanol)** ^{1}H NMR (500 MHz, $CDCl_3$, 298 K, δ): 1.43 (m, 3H, (ketone) C*H₃*), 4.96 (m, 2H, (aldehyde) -OC*H*$_2$), 5.23 (m, 1H, (ketone) -OC*H*), 7.25-7.32 (m, 4H, -*Ph*)

REFERENCES

1 Larranaga, A.; Lomora, M.; Sarasua, J. R.; Palivan, C. G.; Pandit, A. Polymer capsules as micro-/nanoreactors for therapeutic applications: Current strategies to control membrane permeability. *Prog. Mater. Sci.* **2017**, *90*, 325−357.

2 Peplow, M. The plastics revolution: how chemists are pushing polymers to new limits. *Nature* **2016**, *536*, 266−268.

3 Connor, E. F.; Lees, I.; MacLean, D. Polymers as drugs-Advances in therapeutic applications of polymer binding agents. *J. Polym. Sci., Part A: Polym. Chem*. **2017**, *55*, 3146−3157.

4 Vilela, C.; Sousa, A. F.; Fonseca, A. C.; Serra, A. C.; Coelho, J. F. J.; Freirea, C. S. R.; Silvestre. A. J. D. The quest for sustainable polyesters–insights into the future. *Polym. Chem*. **2014**, 5, 3119–3141.

5 Walther, G. High-performance polymers from nature: catalytic routes and processes for industry. *ChemSusChem* **2014**, *7*, 2081−2088.

6 Jambeck, J. R.; Geyer, R.; Wilcox, C.; Siegler, T. R.; Perryman, M.; Andrady, A.; Narayan, R.; Law, K. L. Plastic waste inputs from land into the ocean. *Science* **2015**, *347*, 768−771.

7 Cunliffe, D.; Pennadam, S.; Alexander, C. Synthetic and biological polymers-merging the interface. *Eur. Polym. J*. **2004**, *40*, 5−25.

8 Gö pferich, A. Mechanisms of polymer degradation and erosion. *Biomaterials* **1996**, *17*, 103−114.

9 Ragauskas, A. J.; Williams, C. K.; Davison, B. H.; Britovsek, G.; Cairney, J.; Eckert, C. A. The path forward for biofuels and biomaterial. *Science* **2006**, *311*, 484−489.

10 Moharamned, N.; Aghajani, M.; Atabi, F.; Azarkamand, S. Petrochemical supply chain's share in emission of greenhouse gases, case study: Shazand petrochemical complex. *Am. J. Environ. Sci*. **2013**, *9*, 334−342.

11 Intergovernmental Panel on Climate Change (IPCC). *Fourth Assessment Report: Climate Change; Cambridge University Press*: Cambridge, UK, 2007

12 Llevot, A.; Dannecker, P. K.; von Czapiewski, M.; Over, L. C.; Söyler, Z.; Meier, M. A. R. Renewability is not enough: recent advances in the sustainable synthesis of biomass-derived monomers and polymers. *Chem. - Eur. J.* **2016**, *22*, 11510−11521.

13 Kiely, D. E.; Chen, L.; Lin, T.-H. Hydroxylated nylons based on unprotected esterified D-glucaric acid by simple condensation reactions. *J. Am. Chem. Soc*. **1994**, *116*, 571−578.

14 Galbis, J. A.; de Gracia, M.; García-Martín, M. de Paz, V.; Galbis, E. Synthetic Polymers from Sugar-Based Monomers. *Chem. Rev*. **2016**, *116*, 1600−1636.

15 Gandini, A. Polymers from Renewable Resources: A challenge for the future of macromolecular materials. *Macromolecules* **2008**, *41*, 9491−9504.

16 Fenouillot, F.; Rousseau, A.; Colomines, G.; SaintLoup, R.; Pascault, J. P. Polymers from renewable 1,4:3,6-dianhydrohexitols (isosorbide, isomannide and isoidide): A review. *Prog. Polym. Sci*. **2010**, *35*, 578–622.

17 Rose, M.; Palkovits, R. Isosorbide as a Renewable Platform chemical for Versatile Applications—Quo Vadis?. *ChemSusChem* **2012**, *5*, 167–176.

18 Yokoe, M.; Aoi, M.; Okada, M. Biodegradable polymers based on renewable resources. IX. Synthesis and degradation behavior of polycarbonates based on 1,4:3,6-dianhydrohexitols and tartaric acid derivatives with pendant functional groups. *J. Polym. Sci., Part A: Polym. Chem.* **2005**, *43*, 3909−3919.

19 Brust, A.; Lichtenthaler, F. W.; Peters, S. C. R. Facile conversion of glycosyloxymethyl-furfural into γ-keto-carboxylic acid building blocks towards a sustainable chemical industry. Green Chem. ***2013***, *15*, 1368–1372.

20 Rinaldi, R.; Schuth, F. Design of solid catalysts for the conversion of biomass. *Energ. Environ. Sci*. **2009**, *2*, 610–626.

21 Zhao, L.; Zhang, L.; Wang, Z. Synthesis and degradable properties of cycloaliphatic epoxy resin from renewable biomass-based furfural. *RSC Adv.* **2015***, 5,* 95126−95132.

22 Li, C.; Zhang, Z.; Zhao, Z. K. Direct conversion of glucose and cellulose to 5-hydroxymethylfurfural in ionic liquid under microwave irradiation. *Tetrahedron Letters* **2009***, 50,* 5403−5405.

23 Putten, R. J.; van der Waal, J. C.; de Jong, E.; Rasrendra, C. B.; Heeres, H. J.; de Vries, J. G. Hydroxymethylfurfural, A Versatile Platform Chemical Made from Renewable Resources. *Chem Rev.* **2013***,* 113*,* 1499−597.

24 Holfinger, M. S.; Conner, A. H.; Holm, D. R.; Hill, C. G. Synthesis of Difurfuryl Diamines by the Acidic Condensation of Furfurylamine with Aldehydes and Their Mechanism of Formation. *J. Org Chem.* **1995***, 60,* 1595−1598.

25 Hu, F.; La Scala, J. J.; Sadler, J. M.; Palmese, G. R. Synthesis and Characterization of Thermosetting Furan-Based Epoxy Systems. *Macromolecules,* **2014**. 47. 3332−3342.

26 Saha, B.; Abu-Omar, M. M. Advances in 5-Hydroxymethylfurfural Production from Biomass in Biphasic Solvents. *Green Chem.* **2014**, *16,* 24−38.

27 Carniti, P.; Gervasini, A.; Biella, S.; Auroux, A. Niobic Acid and Niobium Phosphate as Highly Acidic Viable Catalysts in Aqueous Medium: Fructose Dehydration Reaction. *Catal. Today* **2006**, *118,* 373–378.

28 Tong, X.; Li, Y. Efficient and Selective Dehydration of Fructose to 5-Hydroxymethylfurfural Catalyzed by Brønsted-Acidic Ionic Liquids. *ChemSusChem* **2010**, *3*, 350–355.

29 Hu, F.; Yadav, S. K.; La Scala, J. J.; Sadler, J. M.; Palmese, G. R. Preparation and Characterization of Fully Furan-Based Renewable Thermosetting Epoxy-Amine Systems. *Macromolecular Chemistry and Physics.* **2015***, 216,* 1441–1446.

30 Tong, X.; Ma, Y.; Li, Y. Biomass into chemicals: Conversion of sugars to furan derivatives by catalytic processes. *Appl. Catal. A Gen*. **2010**, 385, 1–13.

31 Davis, S. E.; Houk, L. R.; Tamargo, E. C.; Datye, A. K.; Davis, R. J. Oxidation of 5-Hydroxymethylfurfural over Supported Pt, Pd and Au Catalysts. *Catal. Today* **2011**, *160*, 55–60.

32 Lipik, V. T.; Abadie, M. J. Process Optimization of Poly(E-caprolactone) Synthesis by Ring Opening Polymerization," *Iranian Polymer Journal,* **2010***, 19,* 885–893.

33 Fried, J. R. *Polymer Science and Technology*, 3 ed. Upper Saddle River, NJ: Pearson Education, Inc., 2014.

34 Chalid, M.; Heeres, H. J.; Broekhuis, A. A. Green Polymer Precursors from Biomass-Based Levulinic Acid. *Procedia Chemistry* **2012***, 4,* 260–267.

35 Bechthold, I.; Bretz, K.; Kabasci, S.; Kopitzky, R.; Springer, A. Succinic Acid: A New Platform Chemical for Biobased Polymers from Renewable Resources. *Chemical Engineering & Technology.* **2008***,* 31, 647–654.

36 Galbis, J. A.; García-Martín, M. G. *Sugars as monomers. In Monomers, polymers and composites from renewable resources*; Belgacem, M. N., Gandini, A., Eds.; Elsevier: Oxford. 2008; 89−114.

37 García-Martín, M. G.; Ruiz Perez, R.; Benito Herna ́ ndez, E.; ́ Espartero, J. L.; Muñ oz-Guerra, S.; Galbis, J. A. Carbohydrate-based polycarbonates. Synthesis, structure and biodegradation studies. *Macromolecules* **2005**, *38*, 8664−8670.

38 Sablong, R.; Duchateau, R.; Koning, C. E.; Wit, G. d.; Van Es, D.; Koelewijn, R.; Van Haveren, J. Incorporation of Isosorbide into Poly(butylene terephthalate) via Solid-State Polymerization. *Biomacromolecules* **2008**, *9*, 3090−3097.

39 Wu, J.; Eduard, P.; Jasinska-Walc, L.; Rozanski, A.; Noordover, B. A. J.; van Es, D. S.; Koning, C. E. Fully Isohexide-Based Polyesters: Synthesis, Characterization, and Structure−Properties Relations. *Macromolecules* **2013**, *46,* 384−394.

40 Jasinska, L.; Villani, M.; Wu, J.; Van Es, D.; Klop, E.; Rastogi, S.; Koning, C. E. Novel, Fully Biobased Semicrystalline Polyamides. *Macromolecules* **2011**, *44*, 3458−3466.

41 Corma, A.; Iborra, S.; Velty, A. Chemical Routes for the Transformation of Biomass into Chemicals. *Chem. Rev.* **2007,** 107, 2411–2502.

42 Zhang, Y.-H. P.; Lynd, L. R. Toward an Aggregated Understanding of Enzymatic Hydrolysis of Cellulose: Noncomplexed Cellulase Systems. *Biotechnol. Bioeng.* **2004,** 88, 797–824.

43 Cope, A. C.; Shen, T. Y. The Stereochemistry of 1,4: 3,6-Dianhydrohexitol Derivatives. *J. Am. Chem. Soc.* **1956,** 78, 3177–3182.

44 Thiem, J.; Bachmann, F. Synthesis and properties of polyamides derived from anhydro- and dianhydroalditols. *Makromol. Chem.* **1991,** 192, 2163–2182.

45 Thiem, J.; Lüders, H. Synthesis and properties of polyurethanes derived from diaminodianhydroalditols. *Makromol. Chem.* **1986,** 187, 2775–2785.

46 Ciampi, S.; Harper, J. B.; Gooding, J. J. Wet Chemical Routes to the Assembly of Organic Monolayers on Silicon Surfaces via the Formation of Si-C Bonds: Surface Preparation, Passivation and Functionalization. *Chem. Soc. Rev*. **2010**, 39, 2158−2183.

47 Trovitch, R. J. The Emergence of Manganese-Based Carbonyl Hydrosilylation Catalysts. *Acc. Chem. Res*. **2017**, *50*, 2842−2852.

48 Ojima, I.; Nihonyanagi, M.; Nagai, Y. Rhodium Complex Catalysed Hydrosilylation of Carbonyl Compounds. *J. Chem. Soc., Chem. Commun*. **1972**, 938–938.

49 Ojima, I.; Kogure, T.; Nihonyanagi; Nagai, Y. Reduction of Carbonyl Compounds with Various HydrosilaneRhodium(I) Complex Combinations. *Bull. Chem. Soc. Jpn*. **1972**, *45*, 3506–3506.

50 Chaudhary, S.K.; Hernandez, O. 4-Dimethylaminopyridine: An efficient and selective catalyst for the silylation of alcohols. *Tetrahedron Lett*. **1979**, *20*, 99–102.

51 Kim, S.; Chang, H. 1,1,3,3-Tetramethylguanidine: An Effective catalyst for the t-butyldimethylsilylation of alcohols. *Synth. Commun*. **1984**, *14*, 899–904.

52 Tuck, C. O.; Perez, E.; Horvath, I. T.; Sheldon, R. A.; Poliakoff,´ M. Valorization of Biomass: Deriving More Value from Waste. *Science* **2012**, *337*, 695−699.

53 Gandini, A.; Belgacem, M. N. Monomers, Polymers and Composites from Renewable Resources 2008.

54 Kamigaito, M.; Satoh, K.; Tang, C.; Ryu, C. Y. Sustainable Vinyl Polymers via Controlled Polymerization of Terpenes. *Sustainable Polymers from Biomass* **2017**, 55−90.

55 Kawakami, Y.; Li, Y. Approaches to polymers containing a siliconoxygen bond in the main chain. *Des. Monomers Polym*. **2000**, *3*, 399−419.

56 Ware, T.; Jennings, A. R.; Bassampour, Z. S.; Simon, D.; Son, D. Y.; Voit. W. Degradable, silyl ether thiol–ene networks. *RSC Adv*. **2014**, *4*, 39991–40002.

57 Moretto, H.-H.; Schulze, M.; Wagner, G. Silicones. In Ullmann's Encyclopedia of Industrial Chemistry; Wiley-VCH, Weinheim, Germany, 2005.

58 Lauter, U.; Kantor, S. W.; Schmidt-Rohr, K.; MacKnight, W. J. Vinyl Substituted Silphenylene Siloxane Copolymers: Novel High Temperature Elastomers. *Macromolecules* **1999**, *32*, 3426−3431.

59 Kawakita, T.; Oh, H.-S.; Moon, J.-Y.; Liu, Y.; Imae, I.; Kawakami, Y. Synthesis, Characterization and Thermal Properties of Phenylene-disiloxane Polymers Obtained from Catalytic Cross-dehydrocoupling Polymerization of bis(dimethylsilyl)benzene Isomers and Water. Polym. Int. **2001**, *50*, 1346−1351.

60 Li, Y.; Kawakami, Y. Catalytic Cross-dehydrocoupling Polymerization of 1,4-bis(dimethylsilyl)benzene with Water. A New Approach to Poly[(oxydimethylsilylene)-(1,4-phenylene)-(dimethylsilylene)]. *Macromolecules* **1999**, *32*, 3540−3542.

61 Li, Y.; Kawakami, Y. Efficient Synthesis of Poly(silyl ether)s by Pd/C and RhCl(PPh3)3-Catalyzed Cross-dehydrocoupling Polymerization of bis(hydrosilane)s with Diols. Macromolecules **1999**, *32*, 6871−6873.

62 Zhang, R.; Mark, J. E.; Pinhas, A. R. Dehydrocoupling Polymerization of Bis-silanes and Disilanols to Poly(silphenylenesiloxane) as Catalyzed by Rhodium Complexes. *Macromolecules* **2000**, *33*, 3508−3510.

63 Oishi, M.; Moon, J.-Y.; Janvikul, W.; Kawakami, Y. Synthesis of Poly(Methylphenylsiloxane) Rich in Syndiotacticity by Rh-Catalysed Stereoselective Cross-dehydrocoupling Polymerization of Optically Active 1,3-dimethyl-1,3-diphenyldisiloxane Derivatives. *Polym. Int*. **2001**, *50*, 135−143.

64 Zhai, X, -Y.; Hu, S, -B.; Shi, L.; Zhou, Y. G. Synthesis of Poly(silyl ethers) via Iridium-Catalyzed Dehydrocoupling Polymerization. *Organometallics* **2018**, *37*, 2342−2347.

65 Zhai, X. Y.; Wang, X. -Q.; Ding, Y. -X.; Zhou, Y. -G. Partially biobased polymers: The synthesis of polysilylethers via dehydrocoupling catalyzed by an anionic iridium complex. *Chinese Chem. Let.* **2019**. https://doi.org/10.1016/j.cclet.2019.07.017

66 Lichtenberg, C.; Viciu, L.; Adelhardt, M.; Sutter, J.; Meyer, K.; de Bruin, B.; Grîtzmacher, H. Low-Valent Iron(I) Amido Olefin Complexes as Promotors for Dehydrogenation Reaction. *Angew.Chem. Int. Ed*. **2015**, *54*, 5766–5771.

67 Cheng, C.; Watts, A.; Hillmyer, M. A.; Hartwig, J. F. Polysilylether: a Degradable Polymer from Biorenewable Feedstocks. *Angew. Chem., Int. Ed*. **2016**, *55*, 11872−11876.

68 Li, C.; Wang, L.; Wang, M.; Liu, B.; Liu, X.; Cui, D. Step-Growth Coordination Polymerization of 5-Hydroxymethyl Furfural with Dihydrosilanes: Synergistic Catalysis Using Heteroscopionate Zinc Hydride and B(C6F5)3. *Angew. Chem.* **2019**, *131*, 11556 –11560.

69 Li, Y.; Kawakami, Y. Synthesis and properties of polymers containing silphenylene moiety via catalytic cross-dehydrocoupling polymerization of 1,4-bis (dimethylsilyl) benzene. *Macromolecules* **1999**, *32*, 8768−8773.

70 Mabry, J. M.; Runyon, M. K.; Weber, W. P. Reversible Redox Cleavage/Coupling of Polystyrene with Disulfide or Thiol Groups Prepared by Atom Transfer Radical Polymerization. *Macromolecules* **2002**, *35*, 2207–2212.

71 Li, C.; Hua, X.; Mou, Z.; Liu, X.; Cui, D. Zinc-catalyzed hydrosilylation copolymerization of aromatic dialdehydes with diphenylsilane. *Macromol. Rapid Commun*. **2017**, *38*, 1700590.

72 Sample, C. S.; Lee, S. -H.; Bates, M. W.; Ren, J. M.; Lawrence, J.; Lensch, V.; Gerbec, J. A.; Bates, C. B.; Li, S.; Hawker, C. J. Metal-Free Synthesis of Poly(silyl ether)s under Ambient Conditions. Macromolecules **2019**, *525*, 1993–1999.

73 Chakraborty, S.; Bhattacharya, P.; Dai, H.; Guan, H. Nickel and Iron Pincer Complexes as Catalysts for the Reduction of Carbonyl Compounds. *Acc. Chem. Res*. **2015**, *48*, 1995–2003.

74 Gopalaiah, K. Chiral Iron Catalysts for Asymmetric Synthesis. *Chem. Rev*. **2013**, *113*, 3248–3296.

75 Dargusch, M. S.; Dehghan-Manshadi, A.; Shahbazi, M.; Venezuela, J.; Tran, X.; Song, J.; Liu, N.; Xu, C.; Ye, Q.; Wen, C. Exploring the Role of Manganese on the Microstructure, Mechanical Properties, Biodegradability, and Biocompatibility of Porous Iron Based Scaffolds. *ACS Biomater. Sci. Eng*. **2019**, *5*, 1686−1702.

76 Cotton, F. A.; Wilkinson, G. *Advanced Inorganic Chemistry*, 4th ed.; Wiley: Interscience, 1980; pp 736−737.

77 Katsuki, T. Some Recent Advances in Metallosalen Chemistry, **2003**, *3*, 281–297.

78 Liu, W.; Groves, J. T. Manganese Catalyzed C–H Halogenation. *Acc. Chem. Res*. **2015**, *48*, 1727–1735.

79 Zheng, J.; Elangovan, S.; Valyaev, D. A.; Brousses, R.; César, V.; Sortais, J. B.; Darcel, C.; Lugan, N.; Lavigne. G. Hydrosilylation of Aldehydes and Ketones Catalyzed by Half-Sandwich Manganese(I) N-Heterocyclic Carbene Complexes. *Adv. Synth. Catal*. **2014**, *356*, 1093–1097.

80 Trovitch, R. J. Comparing Well-Defined Manganese, Iron, Cobalt, and Nickel Ketone Hydrosilylation Catalysts. *Synlett* **2014**, *25*, 1638–1642.

81 Chidara, V. K.; Du, G. An Efficient Catalyst Based on Manganese Salen for Hydrosilylation of Carbonyl Compounds. *Organometallics* **2013**, *32*, 5034–5037.

82 Yiu, S.-M.; Lam, W. W. Y.; Ho, C.-M.; Lau. T.-C. Facile N···N Coupling of Manganese(V) Imido Species. *J. Am. Chem. Soc*. **2007**, *129*, 803−809.

83. Greene, T.W.; Wuts, P.G. M. *Protective Groups in Organic Synthesis*, 3rd ed.; John Wiley & Sons: New York, 1991.

84. Lalonde, M.; Chan. T. H. Use of Organosilicon Reagents as Protective Groups in Organic Synthesis. *Synthesis* **1985**, 817–845.

85. Pouget, E.; Tonnar, J.; Lucas, P.; Lacroix-Desmazes, P.; Ganachaud, F.; Boutevin. B. Well-Architectured Poly(dimethylsiloxane)-Containing Copolymers Obtained by Radical Chemistry. *Chem. Rev*. **2010**, *110*, 1233–1277.

86. Lazaro, G.; Fernandez-Alvarez, F. J.; Iglesias, M.; Horna, C.; Vispe, E.; Sancho, R.; Lahoz, F. J.; Iglesias, M.; Perez-Torrente, J. J.; Oro, L. A. Developments and Perspectives of Oxide-based Catalysts for the Oxygen Evolution Reaction. *Catal. Sci. Technol*. **2014**, *4*, 62–70.

87. Wondimagegn, T.; Ziegler. T. The Role of External Alkoxysilane Donors on Stereoselectivity and Molecular Weight in MgCl2-Supported Ziegler–Natta Propylene Polymerization: A Density Functional Theory Study. *J. Phys. Chem. C*. **2012**, *116*, 1027–1033.

88. Huh, S.; Wiench, J. W.; Trewyn, B. G.; Song, S.; Pruski, M.; Lin, V. S.-Y. Tuning of Particle Morphology and Pore Properties in Mesoporous Silicas with Multiple Organic Functional Groups. *Chem. Commun*. **2003**, 2364–2365.

89. Kuroda, K.; Shimojima, A. ; Kawahara, K. ; Wakabayashi, R. ; Tamura, Y. ; Asakura, Y. ; Kitahara, M. Control of Doping in Cu_2SnS_3 through Defects and Alloying. *Chem. Mater*. **2014**, *26*, 211–220.

90 Hoffmann, F.; Cornelius, M.; Morell, J.; Froba, M. Silica-based Mesoporous Organic-inorganic Hybrid Materials. *Angew. Chem., Int. Ed*. **2006**, *45*, 3216–325.

91. Cazacu, M.; Munteanu, G.; Racles, C.; Vlad, A.; Marcu. M. New ferrocene-containing structures: Poly(silyl ester)s. *J. Organomet. Chem*. **2006**, *691*, 3700–3707.

92. Wang, M.; Weinberg, J. M.; Wooley, K. L. Synthesis of Poly(silyl ester)s via AB Monomer Systems. *Macromolecules* **2000**, *33*, 734–742.

93. Patschinski, P.; Zhang, C.; Zipse. H. The Lewis Base-Catalyzed Silylation of Alcohols–A Mechanistic Analysis. *J. Org. Chem*. **2014**, *79*, 8348−8357.

94 Corey, E. J.; Venkateswarlu, A. Protection of hydroxyl groups as tert-butyldimethylsilyl derivatives. *J. Am. Chem. Soc.* **1972**, *94*, 6190–6191.

95 Lombardo, L. Diisopropylethylamine: An effective catalyst for the introduction of the t-butyldimethylsilyl group. Tetrahedron Lett. **1984**, *25*, 227–228

96. Corey, E. J.; Cho, H.; Rucker, C.; Hua. D. H. Studies with Trialkylsilyltriflates: New Syntheses and Applications. *Tetrahedron Lett*. **1981**, *22*, 3455-3458.

97. Mojtahed, M. M.; Abbasi, H.; Abaee, M. S. A Novel Efficient Method for the Silylation of Alcohols Using Hexamethyldisilazane in an Ionic Liquid. *Phosphorus, Sulfur, and Silicon* **2006**, *181,* 1541–1544.

98 Zareyee, D.; Asghari, R.; Khalilzadeh, M. A. Silylation of Alcohols and Phenols with Hexamethyldisilazane over Highly Reusable Propyl Sulfonic Acid Functionalized Nanostructured SBA-15. *Chin. J. Catal*. **2011**, *32*, 1864–1868.

99. Bedard, T. C.; Corey. J. Y. Conversion of Hydrosilanes to Alkoxysilanes Catalyzed by Cp2TiCl2/nBuLi. *J. Organomet. Chem*. **1992**, *428*, 315–333.

100. Peterson, E.; Khalimon, A. Y.; Simionescu, R.; Kuzmina, L. G.; Howard, J. A. K.; Nikonov, G. I. Diversity of Catalysis by an Imido-Hydrido Complex of Molybdenum. Mechanism of Carbonyl Hydrosilylation and Silane Alcoholysis. *J. Am. Chem. Soc*. **2009**, *131***,** 908–909.

101. Gregg, B. T.; Cutler, A. R. Manganese Carbonyl Bromide-Catalyzed Alcoholysis of the Monohydrosilane HSiMe2Ph. *Organometallics* **2002**, *13*, 1039–1043.

102. Bikard, Y.; Mezaache, R.; Weibel, J. M.; Benkouider, A.; Sirlin, C.; Pale, C, P. Diarylmethyl Ethers and Pd Salts or Complexes: A Perfect Combination for the Protection and Deprotection of Alcohols. *Tetrahedron* **2008***, 64*, 10224–10232.

103. Ito, H.; Takagi, K.; Miyahara, T.; Sawamura, M. Gold(I)−Phosphine Catalyst for the Highly Chemoselective Dehydrogenative Silylation of Alcohols. *Org. Lett.* **2005**, *7*, 3001–3004.

104. Ito, H.; Watanabe, A.; Sawamura, M. Versatile Dehydrogenative Alcohol Silylation Catalyzed by Cu(I)−Phosphine Complex. *Org. Lett*. **2005**, *7*, 1869–1871.

105. Gao, D.; Cui. C. N-Heterocyclic Carbene Organocatalysts for Dehydrogenative Coupling of Silanes and Hydroxyl Compounds. *Chem. Eur.* J. **2013**, *19*, 11143 –11147.

106. Blackwell, J. M.; Foster, K. L.; Beck, V. H.; Piers, W. E. B(C6F5)3-Catalyzed Silation of Alcohols: A Mild, General Method for Synthesis of Silyl Ethers. *J. Org. Chem*. **1999**, *64*, 4887–4892.

107 Gevorgyan, V.; Liu, J. X.; Rubin, M.; Benson, S.; Yamamoto, Y. A Novel Reduction of Alcohols and Ethers with A Hsiet3/Catalytic B(C6F5)3 System. Tetrahedron Lett. *1999*, **40**, 8919–8922.

108. Liu, G.-B.; Zhao, H.-Y.; Thiemann, T. Triphenylphosphine-Catalyzed Dehydrogenative Coupling Reaction of Carboxylic Acids with Silanes – A Convenient Method for the Preparation of Silyl Esters. *Adv. Synth. Catal*. **2007**, *349*, 807–811.

109. Chauhan, M. ; Chauhan, B. P. S. ; Boudjouk, P. An Efficient Pd-Catalyzed Route to Silyl Esters. *Org. Lett*. **2000**, *2*, 1027–1029.

110. Ojima, Y.; Yamaguchi, K.; Mizuno, N. An Efficient Solvent-Free Route to Silyl Esters and Silyl Ethers. *Adv. Synth. Catal*. **2009**, *351*, 1405–1411.

111 Lorenz, C.; Schubert, U. Conversion of Hydrosilanes to Silanols and Silyl Esters Catalyzed by [Ph3PCuH]6. *Inorg. Chem*. **1997**, *36*, 1258–1259.

112 Liu, G.-B.; Zhao, H.-Y.; Thiemann, T. Carboxylic Acids with Silanes—Convenient Methods for an Atom-Economical Preparation of Silyl Esters. *Synth. Commun*. **2007**, *37*, 2717–2727.

113 Catalysis without Precious Metals (Eds.: R. M. Bullock), Wiley-VCH: Weinheim, Germany, 2010.

114 Zell, T.; Milstein, D. Hydrogenation and Dehydrogenation Iron Pincer Catalysts Capable of Metal–Ligand Cooperation by Aromatization/Dearomatization. *Acc. Chem. Res*. **2015**, *48*, 1979–1994.

115. Mukhopadhyay, T. K.; Flores, M.; Groy, T. L.; Trovitch, R. J. A Highly Active Manganese Precatalyst for the Hydrosilylation of Ketones and Esters. *J. Am. Chem. Soc*. **2014**, *136,* 882−885.

116. Abbina, S.; Bian, S.; Oian, C.; Du, G. Scope and Mechanistic Studies of Catalytic Hydrosilylation with a High-Valent Nitridoruthenium(VI). *ACS Catal*. **2013**, *3*, 678–684.

117. Truong, T. V.; Kastl, E. A.; Du, G. Cationic Nitridoruthenium(VI) Catalyzed Hydrosilylation of Ketones and Aldehydes. *Tetrahedron Lett*. **2011**, *52*, 1670–1672.

118 Jimenez, M. V.; Perez-Torrente, J. J.; Bartolome, M. I.; Gierz, V.; Lahoz, F. J.; Oro, L. A. Rhodium(I) Complexes with Hemilabile N-Heterocyclic Carbenes: Efficient Alkyne Hydrosilylation Catalysts. *Organometallics* **2008**, *27*, 224–234.

119. Tondreau, A. M.; Atienza, C. C. H.; Weller, K. J.; Nye, S. A.; Lewis, K. M.; Delis, J. G. P.; Chirik, P. J. Iron Catalysts For Selective Anti-Markovnikov Alkene Hydrosilylation Using Tertiary Silanes. *Science* **2012**, **335**, 567–570.

120. Mitsudome, T.; Yamamoto, Y.; Noujima, A.; Mizugaki, T.; Jitsukawa, K.; Kaneda, K. Highly Efficient Etherification of Silanes by Using a Gold Nanoparticle Catalyst: Remarkable Effect of O2. *Chem. Eur. J*. **2013**, *19*, 14398–14402.

121 Petersen, N.; Raebiger, J. W.; Miller, J. S. J. [MnII(*t*Bu)4salen]2 and Its Reaction with TCNE. *Solid State Chem*. **2001**, *159*, 403–406

122 Khan, N. H.; Pandya, N.; Kumar, M.; Bera, P. K.; Kureshy, R. I.; Abdi, S. H. R.; Bajaj, H. C. Influence of chirality using Mn(iii) salen complexes on DNA binding and antioxidant activity. *Org. Biomol. Chem*. **2010**, *8*, 4297–4307.

123 Du Bois, J.; Hong, J.; Carreira, E. M.; Day, M. W. *J. Am. Chem. Soc*. **1996**, *118*, 915−916.

124 Huesing, N.; Raab, C.; Torma, V.; Roig, A.; Peterlik, H. Periodically mesostructured silica monoliths from diol-modified silanes. *Chem. Mater.* **2003,** *15,* 2690–2692.

125 Weber, W. P. Silicon Reagents for Organic Synthesis. Springer: Berlin, 1983; pp 21–39.

126 Hsiue, G.-H.; Wei, H.-F.; Shiao, S.-J.; Kuo, W.-J.; Sha, Y.-A. Chemical modification of dicyclopentadiene-based epoxy resins to improve compatibility and thermal properties. *Polym. Degrad. Stab.* **2001**, *73*, 309–318.

127 Ohshita, J.; Watanabe, T.; Kanaya, D.; Ohsaki, H.; Ishikawa, M. Polymeric organosilicon systems. 22. Synthesis and photochemical properties of poly[(disilanylene)oligophenylylenes] and poly[(silylene)biphenylylenes]. *Organometallics* **1994**, *13*, 5002–5012.

128 Feigl, A.; Bockholt, A.; Weis, J.; Rieger, B. Modern synthetic and application aspects of polysilanes: An underestimated class of materials? *Adv. Polym. Sci.* **2010**, *235*, 1–31.

129 Mazurek, M. H. Silicones. In *Comprehensive Organometallic Chemistry III*, Mingos, D. M. P.; Crabtree, R. H. Ed.; Elsevier: Amsterdam, **2007**; Vol. 3, pp 651–697.

130 Meng, Y.; Wei, Z.; Lu, Y. L.; Zhang, L. Q. Structure, morphology, and mechanical properties of polysiloxane elastomer composites prepared by in situ polymerization of zinc dimethacrylate. *eXPRESS Polym. Lett.* **2012**, *6*, 882–894.

131 Merker, R. L.; Scott, M. J. Preparation and properties of poly(tetramethyl-*p*-silphenylene-siloxane*). J. Polym. Sci., Part A* **1964**, *2*, 15–29.

132 Merker, R. L.; Scott, M. J.; Haberland, G. G. Random and block copolymers of poly(tetramethyl-*p*-silphenylene-siloxane) and polydimethylsiloxane. *J. Polym. Sci., Part A* **1964**, *2*, 31– 44.

133 Dorset, D.; McCourt, M. P. Direct phase determination for polymer fibre X-ray data—the structure of poly(tetramethyl-*p*-silphenylene siloxane). *Polymer* **1997**, *38*, 1985–1989.

134 Dunnavant, W. R.; Markle, R. A.; Sinclair, R. G.; Stickney, P. B.; Curry, J. E.; Byrd, J. D. *p*,*p*'-Biphenol-dianilinosilane condensation copolymers. *Macromolecules* **1968**, *1*, 249–254.

135 Nagasaki, Y.; Matsukura, F.; Masao, K.; Aoki, H.; Tokuda, T. New thermosensitive rubbery polymers. Synthesis of poly(siloxyethylene glycol) and its aqueous solution properties. *Macromolecules* **1996**, *29*, 5859–5863.

136 Martinez-Crespiera, S.; Ionescu, E.; Kleebe, H. Z.; Riedel, R. Pressureless synthesis of fully dense and crack-free SiOC bulk ceramics via photo-crosslinking and pyrolysis of a polysiloxane. *J. Eur. Ceram. Soc*. **2011**, *31*, 913–919.

137 Harshe, R.; Balan, C.; Riedel, R. Amorphous Si(Al)OC ceramic from polysiloxanes: bulk ceramic processing, crystallization behavior and applications. *J. Eur. Ceram. Soc*. **2004**, *24*, 3471–3482.

138 Ji, F.; Li, Y. L.; Feng, J. M.; Su, D.; Wen, Y. Y.; Feng, Y.; Hou, F. Electrochemical performance of graphene nanosheets and ceramic composites as anodes for lithium batteries. *J. Mater. Chem*. **2009**, *19*, 9063–9067.

139 Liu, X.; Xie, K.; Wang, J.; Zheng, C. M.; Pan, Y. Si/Si–O–C composite anode materials exhibiting good *C* rate performances prepared by a sol–gel method. *J. Mater. Chem.* **2012**, *22*, 19621–19624.

140 Graczyk-Zajac, M.; Wimmer, M.; Neumann, C.; Riedel, R. Lithium intercalation into SiCN/disordered carbon composite. Part 1: Influence of initial carbon porosity on cycling performance/capacity. *J. Solid State Electrochem*. **2015**, *19*, 2763–2769.

141 Lu, K.; Erb, D.; Liu, M. Thermal stability and electrical conductivity of carbon-enriched silicon oxycarbide. *J. Mater. Chem. C.* **2016**, *4*, 1829–1837.

142 Colombo, P.; Mera, G.; Riedel, R.; Soraru, G. D. Polymer-derived ceramics: 40 years of research and innovation in advanced ceramics. *J. Am. Ceram. Soc*. **2010**, *93*, 1805–1837.

143 Gregori, G.; Kleebe, H. J.; Blum, Y. D.; Babonneau, F. Evolution of C-rich SiOC ceramics: Part II. Characterization by high lateral resolution techniques: electron energy-loss spectroscopy, high-resolution TEM and energy-filtered TEM. *Int. J. Mater. Res*. **2006**, *97*, 710–720.

144 Sahmetlioglu, E.; Nguyen, H. T. H.; Nsengiyumva, O.; Göktürk, E.; Miller, S. A. Silicon acetal metathesis polymerization. *ACS Macro Lett*. **2016**, *5*, 466–470.

145 Miller, S. A. Sustainable polymers: Opportunities for the next decade. *ACS Macro Lett*. **2013**, *2*, 550–554.

146 Wang, M.; Zhang, Q.; Wooley, K. L. Silyl ether-coupled poly(ε-caprolactone)s with stepwise hydrolytic degradation profiles. *Biomacromolecules* **2001**, *2*, 1206–1213.

147 Drake, K.; Mukherjee, I.; Mirza, K.; Ji, H.-F.; Bradley, J.-C.; Wei, Y. Novel diacetylinic aryloxysilane polymers: a new thermally cross-linkable high temperature polymer system. *Macromolecules* **2013**, *46*, 4370–4377.

148 Yun, S. B.; Park, Y. T. Synthesis and properties of poly(carbomethyloctylsiloxane)s by melt copolymerization of bis(diethylamino)methyloctylsilane and aryldiol derivatives. *Bull. Korean Chem. Soc*. **2008**, *29*, 2373–2378.

149 Jung, I. K.; Park, T. T.; Melt copolymerization reactions between 1,3-bis((diethylamino) tetramethyldisiloxane and aryldiol derivatives. *Bull. Korean Chem. Soc*. **2011**, *32*, 1303–1309.

150 Jung, E, A.; Park, Y. T. Synthesis and photoelectronic properties of thermally stable poly[oxy(2,7-fluoren-9-onenylene)oxy(diorganosilylene)]s. *Bull. Korean Chem. Soc.* **2012**, *33*, 2031–2037.

151 Jung, E, A.; Park, Y. T. Synthesis and properties of poly[oxy(arylene)oxy-(tetramethyldisilylene)]s via melt copolymerization reaction. *Bull. Korean Chem. Soc*. **2013**, *34*, 1637–1642.

152 Liaw, D. J.; Liaw, B. Y. Synthesis and characterization of novel polyaryloxydiphenylsilane derived from 2,2′- dimethyl-biphenyl-4,4′-diol. *J. Polym. Sci., Part A: Polym. Chem.* **1999**, *37*, 4591–4595.

153 Issam, A. M.; Haris, M. Synthesis, characterization and optical properties of novel nonlinear polysilylether. *J. Inorg. Organomet. Polym.* **2009**, *19*, 454–458.

154 Nishikubo, T.; Kameyama, A.; Hayashi, N. A novel synthesis of poly(silyl ether)s by addition reactions of diepoxide with dichlorosilane compounds. *Polym. J.* **1993**, *25*, 1003–1005.

155 Liaw, D. -J. Synthesis of poly(silyl ether) by the addition reaction of bisphenol-s diglycidyl ether and dichlorodiphenylsilane. *Polymer* **1997**, *38*, 5217–5219.

156 Nishikubo, T.; Kameyama, A.; Kimura, Y.; Fukuyo, K. Novel synthesis of poly(silyl ethers) by the addition reaction of bis(epoxides) with dichlorosilanes or bis(chlorosilanes). *Macromolecules* **1995**, *28*, 4361–4365.

157 Nishikubo, T.; Kameyama, A.; Kimura, Y.; Nakamura, T. New synthesis of poly(silyl ether) and poly(germyl ether) by addition reactions of bisepoxides with dimethyldiphenoxysilane and dimethyldiphenoxygermane. *Macromolecules* **1996**, *29*, 5529–5534.

158 An Introductory Guide to the Safe Handling of Chlorosilanes. https://www.dowcorning.com/content/publishedlit/01-4012-01.pdf. Accessed January 25, 2017.

159 Dunnavant, W. R.; Markle, R. A.; Stickney, P. B.; Curry, J. E.; Byrd, J. D. Synthesis of polyaryloxysilanes by melt-polymerizing dianilino- and diphenoxysilanes with aromatic diols. *J. Polym. Sci., Part A: Polym. Chem*. **1967**, *5*, 707–724.

160 Padmanabon, M.; Kakimoto, M.; Imai, Y. Synthesis and characterization of new photosensitive poly (oxyaryleneoxydisilane)s from 1,2-bis (diethylamino) tetramethyldisilane and various bisphenols. *J. Polym. Sci., Part A: Polym. Chem*. **1990**, *28*, 2997–3005.

161 Henglei, F. A.; Schmulder, P. Über polyacetale des formaldehyds mit methylsilanolen. *Makromol. Chem*. **1954**, *13*, 53–70.

162 Imai, Y. J. Synthesis of new functional silicon-based condensation polymers. *Macroml. Sci. Chem. A*. **1991**, *28*, 1115–1135.

163 Li, Y.; Seino, M.; Kawakami, Y. Asymmetric synthesis of optically active poly(silyl ether)s having reactive Si−H groups by stereoselective cross-dehydrocoupling polymerization of bis(silane)s with diols. *Macromolecules* **2000**, *33,* 5311–5314.

164 Paulasaari, J. K.; Weber, W. P. Ruthenium-catalyzed hydrosilation copolymerization of aromatic α,ω-diketones with 1,3-tetramethyldisiloxane. *Macromolecules* **1998**, *31,* 7105–7107.

165 Mabry, J. M.; Paulasaari, J. K.; Weber, W. P. Synthesis of poly(silyl ethers) by Ru-catalyzed hydrosilylation. *Polymer* **2000**, *41*, 4423–4428.

166 Mabry, M. J.; Runyon, M. K.; Weber, W. P. Synthesis of copoly[arylene-1,2-dioxy/oligodimethylsiloxanylene]s by Ruthenium-catalyzed dehydrogenative silylation copolymerization of *o*-quinones with *α,ω*-dihydridooligodimethylsiloxanes. *Macromolecules* **2001**, *34,* 7264–7268.

167 Lázaro, G.; Fernández-Alvarez, F. J.; Iglesias, M.; Horna, C.; Vispe, E.; Sancho, R.; Lahoz, F. J.; Iglesias, M.; Pérez-Torrente, J. J.; Oro, L. A. Heterogeneous catalysts based on supported Rh–NHC complexes: synthesis of high molecular weight poly(silyl ether)s by catalytic hydrosilylation. *Catal. Sci. Technol*. **2014**, *4*, 62–70.

168 Lázaro, G.; Iglesias, M.; Fernández-Alvarez, F. J.; Sanz Miguel, P. J.; Pérez-Torrente, J. J.; Oro, L. A. Synthesis of poly(silyl ether)s by Rhodium(I)–NHC catalyzed hydrosilylation: Homogeneous versus heterogeneous catalysis. *ChemCatChem* **2013**, *5*, 1133–1141.

169 Purkayastha, A.; Baruah, J. B. Silicon–oxygen bonding on diphenylsilane through palladium(ii)-catalysed reactions. *Appl. Organometal. Chem*. **2000**, *14*, 477–483.

170 Cella, J.; Rubinsztajn, S. Preparation of polyaryloxysilanes and polyaryloxysiloxanes by B(C6F5)3 catalyzed polyetherification of dihydrosilanes and bis-phenols. *Macromolecules* **2008**, *41*, 6965–6971.

171 Zhao, M.; Xie, W.; Cui, C. Cesium carbonate catalyzed chemoselective hydrosilylation of aldehydes and ketones under solvent-free conditions. *Chem. Eur. J*. **2014**, *20*, 9259–9262.

172 Lichtenberg, C.; Adelhardt, M.; Wörle, M.; Büttner, T.; Meyer, K.; Grützmacher, H. Mono- and dinuclear neutral and cationic iron (II) compounds supported by an amidinato-diolefin ligand: characterization and catalytic application. *Organometallics* **2015**, *34*, 3079–3089.

173 Du, G.; Abu-Omar, M. M. Oxo and imido complexes of rhenium and molybdenum in catalytic reductions. *Cur. Org. Chem*. **2008**, *12*, 1185–1198.

174 Du. G.; Fanwick, P. E.; Abu-Omar, M. M. mechanistic insight into hydrosilylation reactions catalyzed by high valent Re≡X (X = O, NAr, or N) complexes: The silane (SiH) does not add across the metal−ligand multiple bond. *J. Am. Chem. Soc*. **2007**, *129*, 5180–5187.

175 Vijjamarri, S.; Chidara, V. K.; Rousova, J.; Du, G. Dehydrogenative coupling of alcohols and carboxylic acids with hydrosilanes catalyzed by a salen–Mn(V) complex. *Catal. Sci. Technol.* **2016**, *6*, 3886–3892.

176 Abbina, S.; Du, G. Zinc-catalyzed highly isoselective ring opening polymerization of *rac*-lactide. *ACS Macro Lett*. **2014**, *3*, 689–692.

177 Bian, S.; Pagan, C.; Andrianova, A. A.; Du, G. Synthesis of polycarbonates and poly(ether carbonate)s directly from carbon dioxide and diols promoted by a Cs2CO3/CH2Cl2 system. *ACS Omega* **2016**, *1*, 1049–1057.

178 Abbina, S.; Chidara, V. K.; Bian, S.; Ugrinov, A.; Du, G. Synthesis of chiral *C*2-symmetric bimetallic zinc complexes of amido-oxazolinates and their application in copolymerization of CO2 and cyclohexene oxide. *ChemistrySelect* **2016**, *1,* 3175–3183.

179 Bryan, Z. J.; Hall, A. O.; Zhao, C. T.; Chen, J.; McNeil, A. C. Limitations of using small molecules to identify catalyst-transfer polycondensation reactions. *ACS Macro Lett*. **2016**, *5*, 69–72.

180 Jenekhe, S. A. The Special Issue on Organic Electronics. *Chem. Mater*. **2004**, *16*, 4381.

181 Brook, M. A. *Silicon in Organic, Organometallic, and Polymer Chemistry*, John Wiley & Sons: New York, 2000.

182 Chen, J.; Cao, Y. Silole-containing polymers: chemistry and optoelectronic properties. *Macromol. Rapid Commun*. **2007**, *28*, 1714–1742.

183 Mukherjee, D.; Thompson, R. R.; Ellern, A.; Sadow, A. D. Coordinatively saturated tris(oxazolinyl)borato zinc hydride-catalyzed cross dehydrocoupling of silanes and alcohols. *ACS Catal*. **2011**, *1*, 698–702.

184 Luo, X. L.; Crabtree, R. H. Homogeneous catalysis of silane alcoholysis via nucleophilic attack by the alcohol on an Ir(η2-HSiR3) intermediate catalyzed by [IrH2S2(PPh3)2]SbF6 (S = solvent). *J. Am. Chem. Soc*. **1989**, *111*, 2527–2535.

185 Wang, Y.-Z.; Deng, X.-X.; Li, L.; Li, Z.-L.; Du, F.-S.; Li, Z.-C. One-pot synthesis of polyamides with various functional side groups via Passerini reaction. *Polym. Chem.* **2013**, *4*, 444–448.

186 Schubert, U.; Ackermann, K.; Worle, B. A Long silicon-hydrogen bond or a short silicon-hydrogen nonbond? Neutron-diffraction study of (*η*5-CH3C5H4)(CO)2(H)MnSiF(C6H5)2. *J. Am. Chem. Soc*. **1982**, *104*, 7378–7380.

187 Corey, E. J. Reactions of hydrosilanes with transition metal complexes. *Chem. Rev.* **2016**, *116*, 11291–11435.

188 Scherer, W.; Eickerling, G.; Tafipolsky, M.; McGrady, G. S.; Sirsch, P.; Chatterton, N. P. Elucidation of the bonding in Mn(η2-SiH) complexes by charge density analysis and *T*1 NMR measurements: asymmetric oxidative addition and anomeric effects at silicon. *Chem. Commun.* **2006**, 2986–2988.

189 McGrady, G. S.; Sirsch, P.; Chatterton, N. P.; Ostermann, A.; Gatti, C.; Altmannshofer, S.; Herz, V.; Eickerling, G.; Scherer, W. Nature of the bonding in metal-silane *σ*-complexes. *Inorg. Chem.* **2009**, *48*, 1588–1598.

190 Sun, J.; Lu. R. S.; Bau, R.; Yang, G. K. Oxidative addition of silanes to cyclopentadienylbis(phosphine)carbonylmanganese. Fluxional behavior of manganese silyl hydride complexes. *Organometallics* **1994**, *13*, 1317–1325.

191 Cavanaugh, M. D.; Gregg, B. T.; Cutler, A. R. Manganese carbonyl complexes as catalysts for the hydrosilation of ketones: Comparison with RhCl(PPh3)3. *Organometallics* **1996**, *15*, 2764–2769.

192. Weissermel, K. Raw Material-Polymer Interrelationships-Today and Tomorrow. *Angew. Chem. Int. Ed*. **1980**, *19*, 79–87.

193. Fernando, S.; Adhikari, S.; Chandrapal, C.; Murali. N. Biorefineries: Current Status, Challenges, and Future Direction. *Energy Fuels* **2006**, *20*, 1727–1737.

194. Van der Ploeg, F. Natural resources: curse or blessing. *J. Econ. Lit*. **2011**, *49*, 366–420.

195. El-Chichakli, B.; von Braun, J.; Lang, C.; Barben, D.; Philp. J. Policy: Five cornerstones of a global bioeconomy. *Nature News* **2016**, *535*, 221–223.

196. Zhu, Y.; Romain, C.; Williams, C. K. Sustainable polymers from renewable resources. *Nature* **2016**, *540*, 354–362.

197. Cui, M, -S.; Deng, J.; Li, X, -L.; Fu, Y. Production of 4-hydroxymethylfurfural from derivatives of biomass derived glycerol for chemicals and polymers. *ACS Sustainable Chem. Eng*. **2016**, *4*, 1707−1714.

198. Leitner, W.; Klankermayer, J.; Pischinger, S.; Pitsch, H.; Kohse-Hçinghaus, K. Advanced biofuels and beyond: chemistry solutions for propulsion and production. *Angew. Chem. Int. Ed*. **2017**, *56*, 5412–5452.

199. Kashin, A. S.; Galkin, K. I.; Khokhlova, E. A.; Ananikov, V. P. Direct observation of self-organized water-containing structures in the liquid phase and their influence on 5-(hydroxymethyl)furfural formation in ionic liquids. *Angew. Chem. Int. Ed.* **2016**, *55*, 2161–2166.

200. Hazra, C. K; Gandhamsetty, N.; Park, S.; Chang, S. Borane catalysed ring opening and closing cascades of furans leading to silicon functionalized synthetic intermediates. *Nature Commun.* **2016**, *7*, 13431–13440.

201. Xia, H.; Xu, S.; Yan, X.; Zuo, X. High yield synthesis of 5-hydroxymethylfurfural from cellulose using FePO4 as the catalyst. *Fuel Process. Technol*. **2016**, *152*, 140–146.

202. Bohre, A.; Dutta, S.; Saha, B.; Abu-Omar, M. M. Upgrading furfurals to drop-in biofuels: An overview. *ACS Sustainable Chem. Eng*. **2015**, *3*, 1263–1277.

203. West, R. M.; Liu, Z. Y.; Peter, M.; Dumesic, J. A. Liquid alkanes with targeted molecular weights from biomass-derived carbohydrates. *ChemSusChem* **2008**, *1*, 417−424.

204. Datrika, R.; Kallam, S. R.; Khobare, S. R.; Gajare, V. S. Kommi, M.; Mohan, H. R. Vidavalur, S.; Pratap, T. V. Stereoselective synthesis of (R)-(–) and (S)-(+)-phoracantholide I from (R)-(+)-γ-valerolactone. *Tetrahedron: Asymmetry* **2016**, *27*, 603–607.

205. Koh, P. F.; Loh, T. P. Synthesis of biologically active natural products, aspergillides A and B, entirely from biomass derived platform chemicals. *Green Chem*. **2015**, *17*, 3746–3750.

206. Yao, S.; Wang, X.; Jiang, Y.; Wu, F.; Chen, X.; Mu, X. One step conversion of biomass derived 5-hydroxymethylfurfural to 1,2,6-hexanetriol over Ni−Co−Al mixed oxide catalysts under mild conditions. *ACS Sustainable Chem. Eng*. **2014**, *2*, 173−180.

207. Sousa, A. F.; Vilela, C.; Fonseca, A. C.; Matos, M.; Freire, C. S. R.; Gruter, G.-J. M.; Coelho, J. F. J.; Silvestre, A. J. D. Biobased polyesters and other polymers from 2,5-furandicarboxylic acid: a tribute to furan excellency. *Polym. Chem*. **2015**, *6*, 5961−5983.

208. Rücker, C.; Kümmerer, K. Environmental chemistry of organosiloxanes. Ch*em. Rev.* **2015,** 11*5,* 466–524.

209. Kocienski, P. *Protecting Groups*, 3rd ed.; Thieme: Stuttgart, 2003.

210. Uhrich, K. E.; Cannizzaro, S. M.; Langer, R. S.; Shakesheff, K. M. Polymeric systems for controlled drug release. *Chem. Rev.* **1999**, 99, 3181–3198.

211. Shen, C.; Oh, W. –S.; Williams, J. R. Effect of post-silanization drying on the bond strength of composite to ceramic. *J. Prosthet Dent*. **2004**, 91, 453–458.

212. Oberhammer, H.; Boggs, J. E. Importance of (p-d) π Bonding in the Siloxane Bond. *J. Am. Chem. Soc.* **1980**, *102*, 7241–7244.

213. Nye, S. A.; Swint, S. A. Synthesis and properties of polyoxyarylenesiloxanes. J. Polym. Sci., Part A: *Polym. Chem*. **1994**, *32*, 131−138.

214. Lázaro, G.; Fernández-Alvarez, F. J.; Iglesias, M.; Horna, C.; Vispe, E.; Sancho, R.; Lahoz, F. J.; Iglesias, M.; Pérez-Torrente, J. J.; Oro, L. A. Heterogeneous catalysts based on supported Rh−NHC complexes: synthesis of high molecular weight poly(silyl ether)s by catalytic hydrosilylation. *Catal. Sci. Technol*. **2014**, *4*, 62−70.

215. Drynda, A.; Hassel, T.; Wilhelm, F.; Peuster, M. In vitro and in vivo corrosion properties of new iron–manganese alloys designed for cardiovascular applications. *J. Biomed. Mater. Res*. **2015**, *103*. 649–660.

216. Vijjamarri, S.; Chidara, V. K.; Du, G. Versatile manganese catalysis for the synthesis of poly(silylether)s from diols and dicarbonyls with hydrosilanes. *ACS Omega* **2017**, *2*, 582–591.

217. Abbina, S.; Chidara, V. K.; Du, G. Ring Opening Copolymerization of Styrene Oxide and Cyclic Anhydrides Using Highly Effective Zinc Amido-Oxazolinate Catalysts. *ChemCatChem* **2017**, *9*, 1343–1348.

218. Musau, R. M.; Munavu, R. M., The preparation of 5-hydroxymethyl-2-furaldehyde (HMF) from D-fructose in the presence of DMSO. *Biomass* **1987,** *13*, 67–74.

219. Timko, J. M.; Cram, D. J., Furanyl unit in host compounds. *J. Am. Chem. Soc.* **1974,** *96*, 7159–7160.

220. Cottier, L.; Descotes, G.; Soro, Y., Heteromacrocycles from Ring-Closing Metathesis of Unsaturated Furanic Ethers. *Synth. Commun.* **2003,** *33*, 4285–4295.

221. Amarasekara, A. S.; Green, D.; McMillan, E., Efficient oxidation of 5-hydroxymethylfurfural to 2,5-diformylfuran using Mn(III)–salen catalysts. *Catal. Commun.* **2008,** *9*, 286–288.

222. Rapeyko, A.; Arias, K. S.; Climent, M. J.; Corma, A.; Iborra, S., Polymers from biomass: one pot two-step synthesis of furilydenepropanenitrile derivatives with MIL-100(Fe) catalyst. *Catal. Sci. & Tech.* **2017,** *7*, 3008–3016.

223. Han, X.; Li, C.; Liu, X.; Xia, Q.; Wang, Y., Selective oxidation of 5-hydroxymethylfurfural to 2,5-furandicarboxylic acid over MnOx-CeO2 composite catalysts. *Green Chem.* **2017,** *19*, 996–1004.

224. Fang, R.; Luque, R.; Li, Y., Efficient one-pot fructose to DFF conversion using sulfonated magnetically separable MOF-derived Fe3O4 (111) catalysts. *Green Chem.* **2017,** *19*, 647–655.

225. Amarasekara, A. S.; H. Nguyen, L.; Okorie, N. C.; M. Jamal, S., A two-step efficient preparation of a renewable dicarboxylic acid monomer 5,5'-[oxybis(methylene)]bis[2-furancarboxylic acid] from d-fructose and its application in polyester synthesis. *Green Chem.* **2017,** *19*, 1570–1575.

226. Zheng, R. X, Xu, X. D.; Tian, Z.;Yang, J. S. Chemical constituents from the fruits of hippophae rhamnoides *Nat Prod Res*. **2009**, *23*, 1451−1456.

227. Zeng, C.; Seino, H.; Ren, J.; Hatanaka, K.; Yoshie, N. Bio-based furan polymers with self-healing ability. *Macromolecules* **2013**, *46*, 1794−1802.

228. Hernandez, N.; Williams, R. C.; Cochran, E. W. The battle for the 'green' polymer: different approaches for biopolymer synthesis: bioadvantaged vs. bioreplacement. Organic Biomolecular Chemistry. *Org. Biomol. Chem.* **2014**, *12*, 2834–2849.

229. Daya, D.; Day. G. Climate change, fossil fuel prices and depletion: The rationale for a falling export tax. *Economic Modelling* **2017**, *63*, 153–160.

230. Mecking, S. Nature or petrochemistry? – Biologically degradable materials. *Angew. Chem. Int. Ed***. 2004**, *43*, 1078–1085.

231. Gandini, A.; Lacerda, T. M.; Carvalho, A. J. F.; Trovatti, E. Progress of polymers from renewable resources: furans, vegetable oils, and polysaccharides. *Chem. Rev.* **2016**, *116*, 1637–1669.

232. Lillie, L. M.; Tolman, W. B.; Reineke. T. M. Structure/property relationships in copolymers comprising renewable isosorbide, glucarodilactone, and 2,5-bis(hydroxymethyl)furan subunits. *Polym. Chem*. **2017**, *8*, 3746–3754.

233 Werpy, T. A.; Holladay, J. E.; White, J. F. PNNL-14808, Pacific Northwest National Laboratory, Richland, WA, **2004**, pp. 1−63.

234. Delidovich, I.; Hausoul, P. J. C.; Deng, L.; Pfützenreuter, R.; Rose, M.; Palkovits, R. Alternative Monomers Based on Lignocellulose and Their Use for Polymer Production. *Chem. Rev*. **2016**, *116*, 1540–1599.

235 Söylera, Z.; Meier, M. A. R. Sustainable functionalization of cellulose and starch with diallyl carbonate in ionic liquids. *Green Chem*. **2017**, *19*, 3899– 3907.

236 Zakharova, E.; Martínez de Ilarduya, A.; León, S.; Muñoz-Guerra, S. Sugar-based bicyclic monomers for aliphatic polyesters: a comparative appraisal of acetalized alditols and isosorbide. Designed Monomers and Polymers. *Des. Monomers Polym.* **2017**, *20,* 157– 166.

237. Wan, J.; Zhao, J.; Gan, B.; Li, C.; Molina-Aldareguia, J.; Zhao, Y.; Pan, Y. -T.; Wang, D-Y. Ultrastiff Biobased Epoxy Resin with High Tg and Low Permittivity: From Synthesis to Properties. *ACS Sustainable Chem. Eng*. **2016**, *4*, 2869–2880.

238. Nair, L. S.; Laurencin, C. T. Biodegradable polymers as biomaterials. *Prog. Polym. Sci*. **2007**, *32*, 762−798.

239. Heller, J.; Barr, J.; Ng, S.; Abdellauoi, K.; Gurny. R. Poly(ortho esters): synthesis, characterization, properties and uses. *Adv. Drug Deliv. Rev*. **2002**, *54*, 1015−1039.

240. Langer, R.; Tirrell, D.A. Designing materials for biology and medicine. *Nature* **2004**, *428*, 487–492.

241. Tian, H.; Tang, Z.; Zhuang, X.; Chen.; X.; Jing.; X. Biodegradable synthetic polymers: Preparation, functionalization and biomedical application. *Prog Polym Sci*. **2012,** *37*, 237–280.

242. Braun, D.; Bergmann, M. Bergmann, M. 1,4:3,6-Dianhydrohexite als Bausteine für Polymere. *Adv. Synth. Catal*. **1992**, *334*, 298–310.

243. Stoss, P.; Hemmer, R. 1,4:3,6-dianhydrohexitols. *Adv. Carbohydr. Chem. Biochem*. **1991**, *49*, 93−173.

244. Rajput, B. S.; Gaikwad, S. R.; Menona, S. K.; Chikkali, S. H. Sustainable polyacetals from isohexides. *Green Chem*. **2014**, *16*, 3810–3818.

245. Kieber, R. J.; Silvera, S. A.; Kennemur, J. G. Stereochemical effects on the mechanical and viscoelastic properties of renewable polyurethanes derived from isohexides and hydroxymethylfurfural. *Polym. Chem*. **2017**, *8*, 4822–4829.

246. Lavilla, C.; Alla, A.; de Ilarduya, A. M.; Muñoz-Guerra, S. High Tg Bio-Based Aliphatic Polyesters from Bicyclic d-Mannitol. *Biomacromolecules* **2013**, *14,* 781–793.

247. Mauldin, T. C.; Zammarano, M.; Gilman, J. W.; Shieldsc, J. R.; Boday, D. J. Synthesis and characterization of isosorbide-based polyphosphonates as biobased flame-retardants. *Polym. Chem*. **2014**, *5*, 5139–5146.

248. Bachmann, F.; Reimer, J.; Ruppenstein, M.; Thiem, J. Synthesis of a novel starch-derived AB-type polyurethane. *Macromol. Rapid Commun*. **1998**, *19,* 21–26.

249. Janvier, M.; Moebs-Sanchez, S.; Popowycz, F. Biosourced Ligands from Isosorbide for the Ethylation of Aldehydes or Alkynylation of Imines. *Eur. J. Org. Chem*. **2016**, 2308–2318.

250. Phan, D. -N.; Lee, H.; Choi, D.; Kang, C. -Y.; Im, S. S. Kim, I. S. Recent Advances in Nanoporous Membranes for Water Purification. *Nanomaterials* **2018**, *8,* 56–65.

251. Ji, X.; Wang, Z.; Yan, J.; Wang, Z. Partially bio-based polyimides from isohexide-derived diamines. *Polymer* **2015**, *74,* 38–45.

252. Ji, X.; Yan, J.; Liu, X.; Wang, Z. Wang, Z. Synthesis and properties of polyimides derived from bis(4-aminophenyl)isohexides. *High Perform. Polym.* **2017**, *29,* 197–204.

253. Jasinska-Walc, L.; Dudenko, D.; Rozanski, A.; Thiyagarajan, S.; Sowinski, P.; van Es, D.; Shu, J.; Hansen, M. R.; Koning, C. E. Structure and Molecular Dynamics in Renewable Polyamides from Dideoxy–Diamino Isohexide. *Macromolecules* **2012**, *45*, 5653–5666.

254. Philip, B.; Sreekumar, K. Optically active poly(ester-amide)s: Synthesis and characterization. *Polym. Int*. **2001**, *50,* 1318–1323.

255. Ji, X.; Wang, Z.; Wang, Z.; Yan, J. Bio-Based Poly(Ether Imide)s from Isohexide-Derived Isomeric Dianhydrides. *Polymers* **2017**, *9,* 569–584.

256. Gallagher, J. J.; Hillmyer, M. A.; Reineke, T. M. Isosorbide-based Polymethacrylates. *ACS Sustainable Chem. Eng*. **2015**, *3,* 662−667.

257. Kim, H, -J.; Kang, M, -S.; Knowles, J. C.; Gong, M. -S. Synthesis of highly elastic biocompatible polyurethanes based on bio-based isosorbide and poly(tetramethylene glycol) and their properties. *J. Biomater. Appl*. **2014**, *29,* 454–464.

258. Ma, C.; Fe, X.; Cheng, W.; Tan, X.; Su, Q.; Zhang, S. Tailoring Molecular Weight of Bioderived Polycarbonates via Bifunctional Ionic Liquids Catalysts under Metal-Free Conditions. *ACS Sustainable Chem. Eng*. **2018**, *6*, 2684–2693.

259. Vendamme, R.; Eevers. W. Sticky Degradable Bioelastomers. *Chem. Mater*. **2017**, *29,* 5353–5363.

260. Gomurashvili, Z.; Kricheldorf. H, R.; Katsarava, R. Amino acid based bioanalogous polymers: Synthesis and study of new (polyester amide)s composed of hydrophobic α-amino acids and dianhydrohexitoles. *J. Macromol. Sci, Part A*. **2000**, *37,* 215–227.

261. Okada, M.; Yamada, M.; Yokoe, M.; Aoi, K. Biodegradable Polymers Based on Renewable Resources. V. Synthesis and Biodegradation Behavior of Poly(ester amide)s Composed of 1,4:3,6-Dianhydro-D-glucitol, Amino Acid, and Aliphatic Dicarboxylic Acid Units. *J. Appl. Polym. Sci*. **2001**, *81,* 2721-2734.

262. Vijjamarri, S.; Streed, S.; Serum, E, M.; Sibi, M, P.; Du, G. *ACS Sustainable Chem. Eng*. **2018**, *6*, 2491–2497.

263. Anbu, N.; Dhakshinamoorthy, A. Cu3(BTC)2 catalyzed dehydrogenative coupling of dimethylphenylsilane with phenol and homocoupling of dimethylphenylsilane to disiloxane. *J. Colloid Interf. Sci.* **2017**, *490,* 430–435.

264. Chauvier, C.; Godou, T.; Cantat, T. Silylation of O–H bonds by catalytic dehydrogenative and decarboxylative coupling of alcohols with silyl formats. *Chem. Commun*. **2017**, *53,* 11697–11700.

265. Harinath, A.; Bhattacharjee, A. J.; Anga, A. S.; Panda, T. K. Dehydrogenative Coupling of Hydrosilanes and Alcohols by Alkali Metal Catalysts for Facile Synthesis of Silyl Ethers. *Aust. J. Chem*. **2016**, *70,* 724–730.

266. Kricheldorf, H. R.; Behnken, G.; Sell, M. Influence of Isosorbide on Glass-Transition Temperature and Crystallinity of Poly(butylene terephthalate). *Macromol. Sci. Chem*. **2007**, *44*, 679–684.

267. Wu, J.; Eduard, P.; Thiyagarajan, S. Noordover, B. A. J.; van Es, D. S.; Koning, C. E. Semi-aromatic polyesters based on a carbohydrate-derived rigid diol for engineering plastics. *ChemSusChem* **2015**, *8*, 67–72.

268. Gustini, L.; Lavilla, C.; de Ilarduya, A. M.; Muñoz-Guerra, S.; Koning, C. E. Isohexide and Sorbitol-Derived, Enzymatically Synthesized Renewable Polyesters with Enhanced Tg. *Biomacromolecules* **2016**, *17*, 3404–3416.

269 Kawakami, Y.; Li, Y.; Liu, Y.; Seino, M.; Pakjamsai, C.; Oishi, M.; Cho, Y. H.; Imae, I. Control of molecular weight, stereochemistry and higher order structure of siloxane-containing polymers and their functional design. *Macromol. Res.* **2004**, *12*, 156–171.

270. Minegishi, S.; Ito, M.; Kameyama, A.; Nishikubo, T. Synthesis of poly(silyl ether)s containing pendant chloromethyl groups by the polyaddition of bis(oxetane)s with dichlorosilanes. *J. Polym. Sci. Part A*. **2000**, *38*, 2254–2259.

271. Wu, W.-X.; Qu, L.; Liu, B.-Y.; Zhang, W.-W.; Wang, N.; Yu, X.-Q. Lipase-catalyzed synthesis of acid-degradable poly(β-thioether ester) and poly(β-thioether ester-co-lactone) copolymers. *Polymer* **2015**, *59*, 187–193.

272. Ortmann, P.; Heckler, I.; Mecking, S. Physical properties and hydrolytic degradability of polyethylene-like polyacetals and polycarbonates. *Green Chem.* **2014**, *16*, 1816–1827.

273. Pemba, A. G.; Flores, J. A.; Miller, S. A. Acetal metathesis polymerization (AMP): A method for synthesizing biorenewable polyacetals. *Green Chem.* **2013**, *15*, 325–329.

274. Paramonov, S. E.; Bachelder, E. M.; Beaudette, T. T.; Standley, S. M.; Lee, C. C.; Dashe, J.; Frechet, J. M. J. PREVARTICLENEXT Journal Logo Fully Acid-Degradable Biocompatible Polyacetal Microparticles for Drug Delivery. *Bioconjugate Chem.* **2008**, *19*, 911–919.

275. Parrott, M.C.; Luft, J. C.; Byrne, J. D.; Fain, J. H.; Napier, M. E.; DeSimone, J. M. Tunable Bifunctional Silyl Ether Cross-Linkers for the Design of Acid-Sensitive Biomaterials. *J. Am. Chem. Soc*. **2010**, *132*, 17928–17932.

276 Fürstner, A. Catalysis for Total Synthesis: A Personal Account. *Angew. Chem., Int. Ed*. **2014**, *53*, 8587–8598.

277 Fyfe, J. W. B.; Watson, A. J. B. Recent Developments in Organoboron Chemistry: Old Dogs, New Tricks. *Inside Chem*. **2017**, *3*. 31–55.

278 Zhang, J.; Xie, Z. Synthesis, Structure, and Reactivity of 13- and 14-Vertex Carboranes. *Acc. Chem. Res*. **2014**, *47*, 1623–1633.

279 Shenvi, R. A.; O'Malley, D. P.; Baran, P. S. Chemoselectivity: The Mother of Invention in Total Synthesis. *Acc. Chem. Res*. **2009**, *42*, 530–541.

280 Cho, B. T. Recent Development and Improvement for Boron Hydride-Based Catalytic Asymmetric Reduction of Unsymmetrical Ketones. *Chem. Soc. Rev*. **2009**, 38, 443−452.

281 Miyaura, N. Hydroboration, Diboration, Silylboration, and Stannylboration. In Catalytic Heterofunctionalization; Wiley-VCH Verlag GmbH: Weinheim, 2001; pp 1−45.

282 Magano, J.; Dunetz, J. R. Large-Scale Carbonyl Reductions in the Pharmaceutical Industry. *Org. Process Res. Dev*. **2012**, *16*, 1156−1184.

283 Geier, S.J.; Vogels, C.M.; Westcott, S.A.; Current Developments in the Catalyzed Hydroboration Reaction. *ACS Symp. Ser*. **2016**, *1236*, 209−225.

284 Shin, W. K.; Kim, H.; Jaladi, A. K.; An, D, K. Catalytic Hydroboration of Aldehydes and Ketones with Sodium Hydride: Application to Chemoselective Reduction of Aldehydes Over Ketones. *Tetrahedron*, **2018**, *74*, 6310−6315.

285 Shegavia, M. L.; Bose, S. K. Recent advances in the catalytic hydroboration of carbonyl compounds. *Catal. Sci. Technol*. **2019**, *9*, 3307−3336.

286 Khalimon, A. Y.; Farha, P.; Kuzmina, L. G.; Nikonov, G. I. Catalytic Hydroboration by an Imido-Hydrido Complex of Mo(IV). *Chem. Commun*. **2012**, *48*, 455−457.

287 Kaithal, A.; Chatterjee, B.; Gunanathan, C. Ruthenium Catalyzed Selective Hydroboration of Carbonyl Compounds. *Org. Lett*. **2015**, *17*, 4790−4793.

288 Newland, R. J.; Lynam, J. M.; Mansell, S. M. Small Bite-Angle 2-Phosphinophosphinine Ligands Enable Rhodium-Catalysed Hydroboration of Carbonyls. *Chem. Commun.* **2018**, *54*, 5482−5485.

289 King, A. E.; Chantal, S.; Stieber, E.; Henson, N. J.; Kozimor, S. A.; Scott, B. L.; Smythe, N. C.; Sutton, A. D.; Gordon, J. C. Ni(bpy)(cod): A Convenient Entryway into the Efficient Hydroboration of Ketones, Aldehydes, and Imines. *Eur. J. Inorg. Chem.* **2016**, 1635–1640.

290 Zeng, H.; Wu, J.; Li, S.; Hui, C.; Ta, A.; Cheng, S. -Y.; Zheng, S.; Zhang, G. Copper(II)-Catalyzed Selective Hydroboration of Ketones and Aldehydes. *Org. Lett*. **2019**, *21*, 401−406.

291 Lummis, P. A.; Momeni, M. R.; Lui, M. W.; McDonald, R.; Ferguson, M. J.; Miskolzie, M.; Brown, A.; Rivard, E. Accessing Zinc Monohydride Cations through Coordinative Interactions. *Angew. Chem., Int. Ed*. **2014**, *53*, 9347−9351.

292 Zhu, Z.; Wu, X.; Xu, X.; Wu, Z.; Xue, M.; Yao, Y.; Shen, Q.; Bao, X. n-Butyllithium Catalyzed Selective Hydroboration of Aldehydes and Ketones. *J. Org. Chem*. **2018**, *83*, 10677−10683.

293 Mukherjee, D.; Shirase, S.; Spaniol, T. P.; Mashima, K.; Okuda, J. Magnesium Hydridotriphenylboronate $[Mg(thf)_6][HBPh_3]_2$: A Versatile Hydroboration Catalyst. *Chem. Commun*. **2016**, *52*, 13155−13158.

294 Osseili, H.; Mukherjee, D.; Beckerle, K.; Spaniol, T. P.; Okuda, J. Me6TREN-Supported Alkali Metal Hydridotriphenylboronates $[(L)M][HBPh_3]$ (M = Li, Na, K): Synthesis, Structure, and Reactivity. *Organometallics* **2017**, *36*, 3029−3034.

295 Yadav, S.; Pahar, S.; Sen, S. S. Benz-Amidinato Calcium Iodide Catalyzed Aldehyde and Ketone Hydroboration with Unprecedented Functional Group Tolerance. *Chem. Commun*. **2017**, *53*, 4562−4564.

296 Yang, Z.; Zhong, M.; Ma, X.; De, S.; Anusha, C.; Parameswaran, P.; Roesky, H. W. An Aluminum Hydride That Functions like a Transition-Metal Catalyst. *Angew. Chem., Int. Ed*. **2015**, *54*, 10225−10229.

297 Jakhar, V. K.; Barman, M. K.; Nembenna, S. Aluminum Monohydride Catalyzed Selective Hydroboration of Carbonyl Compounds. *Org. Lett*. **2016**, *18*, 4710−4713.

298 Blake, A. J.; Cunningham, A.; Ford, A.; Teat, S. J.; Woodward, S. Enantioselective Reduction of Prochiral Ketones by Catecholborane Catalysed by Chiral Group 13 Complexes. *Chem. - Eur. J*. **2000**, *6*, 3586−3594.

299 Wu, Y.; Shan, C.; Sun, Y.; Chen, P.; Ying, J.; Zhu, J.; Liu, L.; Zhao, Y. Main Group Metal–Ligand Cooperation of N-Heterocyclic Germylene: An Efficient Catalyst for Hydroboration of Carbonyl Compounds. *Chem. Commun*. **2016**, *52*, 13799−13802.

300 Sharma, M. K.; Ansari, M.; Mahawar, P.; Rajaramanb, G.; Nagendran, S. Expanding the Limits of Catalysts with Low-Valent Main-Group Elements for the Hydroboration of Aldehydes and Ketones Using [L†Sn(II)][OTf] (L†=aminotroponate; OTf = triflate). *Dalton Trans*. **2019**, *48*, 664–672.

301 Chong, C. C.; Hirao, H.; Kinjo, R. Metal-Free σ-Bond Metathesis in 1,3,2-Diazaphospholene-Catalyzed Hydroboration of Carbonyl Compounds. *Angew. Chem., Int. Ed*. **2015**, *54*, 190−194.

302 Weidner, V. L.; Barger, C. J.; Delferro, M.; Lohr, T. L.; Marks, T. J. Rapid, Mild, and Selective Ketone and Aldehyde Hydroboration/Reduction Mediated by a Simple Lanthanide Catalyst. *ACS Catal*. **2017**, *7*, 1244–1247.

303 Wang, W.; Shen, X.; Zhao, F.; Jiang, H.; Yao, W.; Pullarkat, S. A.; Xu, L.; Ma, M. Ytterbium-Catalyzed Hydroboration of Aldehydes and Ketones. *J. Org. Chem*. **2018**, *83*, 69–74.

304 Chen, S.; Yan, Xue, M.; Hong, Y.; Yao, Y.; Shen, Q. Tris(cyclopentadienyl)lanthanide Complexes as Catalysts for Hydroboration Reaction toward Aldehydes and Ketones. *Org. Lett*. **2017**, *19*, 3382–3385.

305 Chakraborty, S.; Guan, H. First-Row Transition Metal Catalyzed Reduction of Carbonyl Functionalities: A Mechanistic Perspective. *Dalton Trans*. **2010**, *39*, 7427–7436.

306 Su, B.; Cao, Z. -C.; Shi, Z. -J. Exploration of Earth-Abundant Transition Metals (Fe, Co, and Ni) as Catalysts in Unreactive Chemical Bond Activations. *Acc. Chem. Res*. **2015**, *48*, 886–896.

307 Miao, J.; Ge, H. Recent Advances in First-Row-Transition Metal Catalyzed Dehydrogenative Coupling of C(sp3)–H Bonds. *Eur. J. Org. Chem*. **2015**, 7859–7868.

308 Sarvary, I.; Almqvist, F.; Frejd, T. Asymmetric Reduction of Ketones with Catecholborane Using 2,6-BODOL Complexes of Titanium(IV) as Catalysts. *Chem. - Eur. J*. **2001**, *7*, 2158−2166.

309 Oluyadi, A. A.; Ma, S.; Muhoro, C. N. Titanocene (II)-Catalyzed Hydroboration of Carbonyl Compounds. *Organometallics* **2013**, *32*, 70−78.

310 Das, U. K.; Higman, C. S.; Gabidullin, B.; Hein, J. E.; Baker, R. T. Efficient and Selective Iron-Complex-Catalyzed Hydroboration of Aldehydes. *ACS Catal*. **2018**, *8*, 1076−1081.

311 Baishya, A.; Baruah, S.; Geetharani, K. Efficient Hydroboration of Carbonyls by an Iron (II) Amide Catalyst. *Dalton Trans*. **2018**, *47*, 9231−9236.

312 Zhang, G.; Zeng, H.; Wu, J.; Yin, Z.; Zheng, S.; Fettinger, J. C. Highly Selective Hydroboration of Alkenes, Ketones and Aldehydes Catalyzed by a Well-Defined Manganese Complex. *Angew. Chem*. **2016**, *55*, 14369−14372.

313 Chong, C. C.; Kinjo, R. Catalytic Hydroboration of Carbonyl Derivatives, Imines, and Carbon Dioxide. *ACS Catal*. **2015**, *5*, 3238−3259.

314 Elangovan, S.; Topf, C.; Fischer, S.; Jiao, H.; Spannenberg, A.; Baumann, W.; Ludwig, R.; Junge, K.; Beller, M. Selective Catalytic Hydrogenations of Nitriles, Ketones, and Aldehydes by Well-Defined Manganese Pincer Complexes. *J. Am. Chem. Soc*. **2016**, *138*, 8809–8814.

315 Papa, V.; Cabrero-Antonino, J. R.; Alberico, E.; Spannenberg, A.; Junge, K.; Junge, H.; Beller, M. Efficient and Selective Hydrogenation of Amides to Alcohols and Amines Using a Well-Defined Manganese–PNN Pincer Complex. *Chem. Sci*. **2017**, *8*, 3576–3585.

316 Widegren, M. B.; Harkness, G. J.; Slawin, A. M. Z.; Cordes, D. B.; Clarke, M. L. *Angew. Chem. Int. Ed*. **2017**, *56*, 1–5.

317 Yu, X. -Q.; Huang, J. -S.; Zhou, X. -G.; Che, C. -M. Amidation of Saturated C−H Bonds Catalyzed by Electron-Deficient Ruthenium and Manganese Porphyrins. A Highly Catalytic Nitrogen Atom Transfer Process. *Org. Lett*. **2000**, *21*, 2233–2236.

318 Wang, D.; Loose, F.; Chirik, P. J.; Knowles, R. R.; N–H Bond Formation in a Manganese(V) Nitride Yields Ammonia by Light-Driven Proton-Coupled Electron Transfer. *J. Am. Chem. Soc*.**2019**, *141*, 4795–4799.

319 Srinivasan, K.; Michaud, P.; Kochi, J. K. Epoxidation of Olefins with Cationic (salen) Manganese (III) Complexes. The Modulation of Catalytic Activity by Substituents. *J. Am. Chem. Soc*.**1986**, *108*, 2309–2320.

320 Antonangelo, A. R.; Bezzu, C. G.; McKeown, M. B.; Nakagak, S.; Highly Active Manganese Porphyrin-Based Microporous Network Polymers for Selective Oxidation Reactions. *J. Catals* **2019**, *369*. 133–142.

321 Vasilenko, V.; Blasius, C. K.; Gade, L. H. One-Pot Sequential Kinetic Profiling of a Highly Reactive Manganese Catalyst for Ketone Hydroboration: Leveraging σ-Bond Metathesis via Alkoxide Exchange Steps. *J. Am. Chem. Soc*. **2018**, *140*, 9244−9254.

322 Erken, C.; Kaithal, A.; Sen, S.; Weyhermüller, T.; Hölscher, M. Werlé, C.; Leitner, W. Manganese-Catalyzed Hydroboration of Carbon Dioxide and Other Challenging Carbonyl Groups. *Nat. Commun.* **2018**, 9, 4521–4528.

323 Schramm, V. L.; Wedler, F. C. Manganese in Metabolism and Enzyme Function, Academic Press, 1986.

324 Kaim, W.; Schwederski, B.; Klein, A. Bioinorganic Chemistry: Inorganic Elements in the Chemstry of Life, 2013.

325 Rittle, J.; Green, M. T. Cytochrome P450 Compound I: Capture, Characterization, and C-H Bond Activation Kinetics. *Science* **2010**, *330*, 933–937.

326 Vijjamarri, S.; Hull, M.; Du, G.; Renewable Isohexides-Based Hydrolytically Degradable Poly(silylethers) with High Thermal Stability. *ChemSusChem* **2018**, *11*, 2881–2888.

327 Nöth, H.; Wrackmeyer, B. *Nuclear Magnetic Resonance Spectroscopy of Boron Compounds*; Springer-Verlag: Berlin, 1978.

328 Yang, D.; Tanner, D. D. Mechanism of the reduction of ketones by trialkylsilane. Hydride transfer, SET-hydrogen atom abstraction, or free radical addition. *J. Org. Chem.* **1986***, 51,* 2267−2270.

329 Tamang, S. R.; Findlater. M. Iron Catalyzed Hydroboration of Aldehydes and Ketones. *J. Org. Chem*. **2017**, *82*, 12857−12862.

330 Qi, X.; Zheng, T.; Zhou, J.; Dong, Y.; Zuo, X.; Li, X.; Sun, H.; Fuhr, O.; Fenske, D. Magnesium-Catalysed Hydroboration of Aldehydes and Ketones. *Organometallics* **2019**, *38*, 268−277.

331 Lessard, S.; Peng, F.; Hall, D.G. α-Hydroxyalkyl Heterocycles via Chiral Allylic Boronates: Pd-Catalyzed Borylation Leading to a Formal Enantioselective Isomerization of Allylic Ether and Amine. *J. Am. Chem. Soc*. **2009**, *131*, 9612−9613.

332 Vasilenko, V.; Blasius, C. K.; Wadepohl, H.; Gade, L. H. Mechanism-Based Enantiodivergence in Manganese Reduction Catalysis: A Chiral Pincer Complex for the Highly Enantioselective Hydroboration of Ketones. *Angew. Chem. Int. Ed*. **2017**, *56*, 8393–8397.